DESIGN AND ANALYSIS OF GROUND STATIONS FOR PACSAT APPLICATIONS

by

Kenneth Eugene Neumeister

Thesis submitted to the Faculty of the
Virginia Polytechnic Institute and State University
in partial fulfillment of the requirements for
the degree of

MASTER OF SCIENCE

in

Electrical Engineering

APPROVED:

Timothy Pratt, Chairman

Charles W. Bostian

Fred J. Ricci

October 1990

Blacksburg, VA

LD
5655
V855
1990
N484
C.2

DESIGN AND ANALYSIS OF GROUND STATIONS FOR PACSAT APPLICATIONS

by

Kenneth Eugene Neumeister
Committee Chairman: Timothy Pratt
Electrical Engineering

(ABSTRACT)

Engineering problems involving the development of cheap, easy-to-use, and effective packet communications terminals for connectivity to low-earth-orbit satellites (PACSATs) are addressed.

Two prototype terminals were developed: a base station for maximum duration connectivity to the satellite, and a smaller station for portability and low cost. Commercially available systems for related amateur radio uses were integrated for these prototypes. The prototypes illustrated areas for further development before widespread use of PACSATs can be realized.

To better understand some of the issues for PACSATs, two analyses were developed. The first analysis approach characterizes PACSAT orbits so that tradeoffs are readily identified and quantified. Results from an analysis of one PACSAT orbit indicate conflicting needs for the two terminal types.

The second analysis approach addresses issues involving the use of an increasingly popular method for transmitting 9600 baud FSK which combines the spectral efficiency of premodulation pulse shaping with the simplicity of using FM discriminators for demodulation. The spectrum of the transmitted signal is studied and the performance of the demodulator is compared to that of an appropriate coherent receiver. Doppler shifts on the channel is particularly important for PACSAT communications. An analysis approach that addresses the mistuning problem is presented. Results of this analysis identify changes that would better suit the needs of PACSAT terminals.

Acknowledgements

This thesis presents results related to the Satellite Communication Laboratory's VITA project in which I was a research assistant. Through the duration of this research, I have benefited greatly from the many comments and suggestions from the graduate students, associates, and professors who work in the Lab and particularly those who worked on the project.

Including my graduate studies in general, I wish to thank Tim Pratt for allowing me to take on challenging assignments for each semester of my graduate education at Virginia Tech. The most valuable lessons that I learned in graduate school came from those challenges.

Contents

Figures

Tables

Chapter 1

Introduction

VITA, Volunteers in Technical Assistance, is a nonprofit organization that provides technical assistance worldwide, and especially to developing nations and areas of recent natural disasters. VITA is developing a communications network to improve their communications to their volunteers as well as provide organizations in developing nations with low-cost communications access to information available at VITA headquarters and other areas. This network integrates packet communications and a computer bulletin-board system (BBS) with a low-earth-orbit (LEO) satellite into a LEO packet store and forward system called PACSAT.

Although LEO store and forward satellites have been around for some time, PACSAT is unique because it is a commercial, general purpose system based on technologies and techniques developed by amateur radio experimenters over the past decade. The amateur radio community has developed techniques of packet communications for

terrestrial networks and satellite communications for long distance voice or Morse code (CW) communications. During the past few years, there have been a number of experiments that integrated the two.[1] The most recent experiments are included in the recent launch of six Oscar (Orbiting Satellite Carrying Amateur Radio) microsats. One of these microsats is the UoSAT3 (UO-14) with the PACSAT Communications Experiment (PCE) onboard, which is the the test bed for VITA's PACSAT concept. UoSAT3 was developed by the University of Surrey's Surrey Satellite Technology Limited (SST) which is also developing VITA's PACSAT satellite.

Virginia Tech in cooperation with the University of Virginia has developed communications ground stations for VITA to use with the PCE. These ground stations also serve as prototype ground stations for VITA's PACSAT. Some of Virginia Tech's contributions to the development and analysis of the ground station hardware and system are the subject of this thesis.

The following sections provide an overview of the technologies and techniques for the PACSAT concept and an overview of the contents of this thesis.

1.1 Amateur Satellites

There is a considerable amount of amateur radio interest in communications using satellites. With the launch of the six microsats in January, 1990, there is a total of 19 Oscar satellites. In addition, a number of amateur radio satellites have been launched by the USSR and by Japan. Even some shuttle missions and Mir (USSR's space station) missions have included amateur radio activities. Still other satellites, such as weather satellites, have attracted interest in simply receiving the satellites' data or telemetry. This interest has led to a considerable amount of development of ground stations for satellite communications. A good description of the extent of amateur radio interest in satellites and a good history of Oscar is presented in The Satellite Experimenter's Handbook.[2]

Perhaps the most popular satellites for amateur use are the Oscar Phase 3 satellites, Oscar 10 and 13. These satellites are in highly elliptical orbits with very high apogees. As a result, by operating transponders on these satellites, a radio amateur operator can communicate over very long ranges. However, in order to operate these satellites, specialized equipment is required. Due to the popularity of this type of communications, much of the

required equipment is available commercially and is relatively inexpensive.

Figure 1 shows a block diagram for a typical Oscar Phase 3 ground station. Due to the long ranges involved, the station requires a high gain antenna. Circular polarization is used on the satellite to avoid problems with Faraday rotation; however, the sense of the polarization should be switchable since the satellite may deliver opposite-sensed polarized signals at the ground station. A mast-mounted preamp is used primarily to overcome the cable losses between the antenna and the radio. The motion of the satellite in the sky dictates the use of rotors for antenna pointing in both the azimuth and elevation directions. The transceiver must be able to handle weak signals and be able to tune out the doppler shift from the satellite motion. For voice operation, the control of the rotors and tuning is often done manually with the aid of some satellite schedule information.

Due to the availability of Oscar Phase 3 equipment, it can be conveniently incorporated into PACSAT ground stations. Unlike the Oscar Phase 3 satellites, PACSAT transmits linear polarization of uncertain orientation. The Oscar type antennas are still useful because the polarization loss is a constant 3 dB; however, there is no requirement for switching the polarization sense. Also,

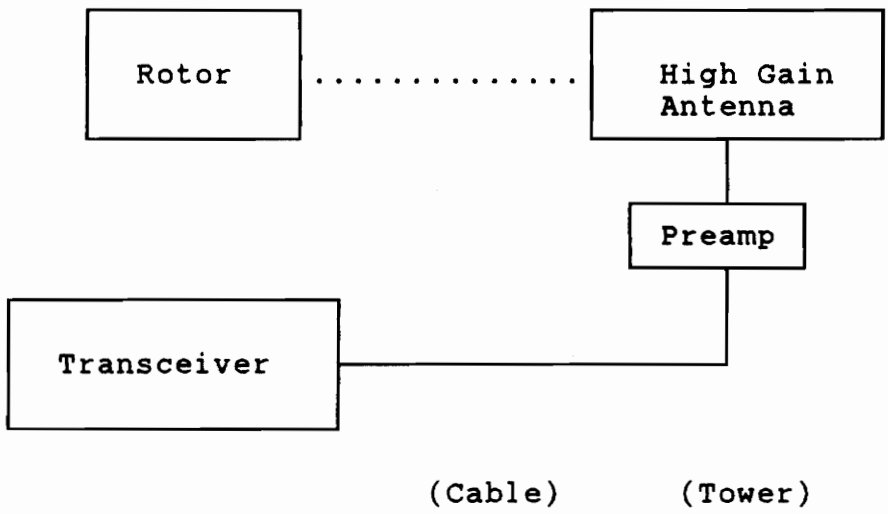

Existing:

- VHF/UHF "Mode J" Transceivers
- Orbit Prediction Software
- Amateur LEO Satellites

New Work:

- 9600 Baud for LEO Satellites
- Automation for Radio and Antennas
- Appropriate Orbit Prediction Software

Figure 1: Typical Oscar Phase 3 Ground Station

PACSAT ground stations must have the doppler tuning and rotor position under computer control for automation.

1.2 Amateur Packet Radio

With the proliferation of personal computers during the 198Øs, amateur radio operators began developing techniques to use radio communications for communication between their computers. These efforts culminated in the introduction of a standard for packet radio communications: AX.25. There are several ARRL (American Radio Relay League) publications that provide good descriptions of this protocol, its operation, and its history. A particularly good introduction to amateur packet radio is Your Gateway to Packet Radio.[3]

Packet communications was originally developed for communications between terminals and mainframe computers. This type of communications is characterized by a demand for a short burst of high speed communication separated by long periods of silence. The concept of organizing the information into packets (or groups of packets) is well suited for the bursty nature of this type of communications. These packets will also contain control

information which typically includes source, destination, sequence numbering, and error control.

Due to the many commercial uses for packet communications, there arose several protocol standards. One popular standard is the X.25 recommendation of the CCITT, the International Telegraph and Telephone Consultative Committee. This standard provides a packet interface between a data-terminal equipment (DTE) which is the data source or sink, and a data-communication equipment (DCE) which is part of the network. The X.25 standard includes a link layer standard known as LAPB (Balanced Link Access Procedures), which is a subset of the HDLC (High-level Data Link Control) protocols.[4]

1.2.1 A Short Overview of AX.25

The AX.25 standard is a modification of the HDLC used in X.25. The distinguishing feature of this modification is that it allows identification of source and destination fields with FCC allocated call-signs. Such identifications are known throughout any AX.25 network; this is different from X.25 which assigns logical addresses only at the interface between the DTE and the DCE. As a result, there is no distinction between a DCE

and a DTE in AX.25 and in the AX.25 protocol all nodes are referred to as DXEs. Furthermore, since there was a lack of network protocols or even the call setup protocols of X.25 in AX.25, AX.25 allows for intermediate destinations to be identified in each frame. These intermediate destinations allow the use of packet repeaters (digipeaters) but their implementation was only meant to be temporary until higher level protocols were developed.[5]

Figure 2 outlines some of the differences between HDLC and AX.25. The primary differences are in the definition of the address field, the use of the control field, and the reservation by AX.25 of the first byte of the information field for protocol identification (PID). The PID was reserved for future use by higher level (layer 3) protocols.

The frames of the two protocols are compared in Figure 2a. The frame, or packet, is bracketed by a pair of flags of 7E in hexadecimal which is a unique word within the protocol: An octet (sequence of 8 bits) consisting of 7E is always a flag occurring outside of the data fields within the packet. The address field contains source and destination information for both protocols but this field is larger for AX.25 since it must contain the source and destination call signs coded one call sign character per octet. Also, AX.25 allows for several

a) Field Comparison of HDLC and AX.25

Frame:

Flag	Address	Control	Information	FCS	Flag

HDLC: Øx7E 8 bits 8 bits n octets 16 bits Øx7E

AX.25: Øx7E 7N octets 8 bits n octets 16 bits Øx7E

(N > 2 for digipeat, n limited to 256 for AX.25)

b) Control Field Definitions

	HDLC								AX.25							
bit:	Ø	1	2	3	4	5	6	7	Ø	1	2	3	4	5	6	7
I-Frame:	Ø	-N(S)--			P	--N(R)-			Ø	-N(S)--			P	--N(R)-		
S-Frame:	1	Ø	S	S	P	--N(R)-			1	Ø	S	S	P	--N(R)-		
U-Frame:	1	1	M	M	P	M	M	M	1	1	M	M	P	M	M	M
UI-Frame:	----	NOT DEFINED ----							1	1	Ø	Ø	P	Ø	Ø	Ø

In both: N(R), N(S), P, S, and M bits operate the same way.

Figure 2: A Comparison of HDLC and AX.25

intermediate nodes to be identified as digipeaters so that the total address field can contain up to ten addresses or a total of 70 octets compared to one octet for HDLC. The FCS, frame check sequence, is a 16 bit cyclic redundancy code[6] that is used to detect if any errors occurred within the frame.

The control field in both protocols consists of an octet coded as shown in Figure 2b. AX.25 uses the same error recovery method as HDLC uses. Once a pair of nodes are connected, a sliding window flow control is used where the maximum window length is seven frames. The sliding window protocol is implemented through the control fields for I-Frames (which contain an information field) and S-Frames (supervisory frames which do not contain an information field). When an error is detected, the sending node retransmits the frame in error and all of the frames transmitted afterwards: this mode of operation is also called GO-BACK-N. When the maximum number of frames in a window is transmitted, the transmitting node stops transmitting until one of the frames is acknowledged. When a frame is acknowledged, the transmitting station assumes that all of the previous frames were also received and the window is adjusted to begin with the first frame that has not yet been acknowledged. The sliding window

flow control protocol is controlled by the N(S), N(R), S, and P subfields in the control field.

There is also a mode in both protocols that allows the transmission of control information before a connection exists (e.g., for when a request for connection is sent). This control information is sent in U-Frames. AX.25 expands the definition of the U-Frame to come up with a UI-Frame which allows information to be sent without establishing a connection. This mode is of some value to send beacon messages and was used for preliminary testing of the UoSAT3/PACSAT.

Due to the popularity of the AX.25 protocol, several manufacturers began developing TNCs which perform all of the AX.25 functions. A TNC, terminal node controller, consists of a packet assembler/disassembler for AX.25 and a FSK modem. These TNCs are fairly inexpensive and they greatly simplify the setup of a packet radio station. A block diagram for typical packet radio station for terrestrial use is shown in Figure 3. The TNC greatly simplifies the integration with just about any computer and radio.

Until recently these TNCs operated primarily at 1200 baud for VHF operation and used the Bell 202 modem standard. (For HF, 300 baud from the Bell 103 standard is popular.)[7] These modem standards were originally designed

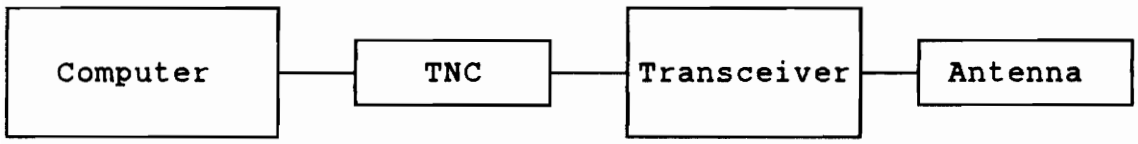

Existing:

- Terminal Emulation Software
- AX.25 TNC
- Transceivers

New Work: (Related to use of 9600 baud)

- Direct Modulation of FSK
- Efficient Protocols
- TNC Suitability

Figure 3: A Typical Terrestrial Packet Radio Station

for voice-grade telephone networks and their signals were provided to the radio as audio (mike) signals. This approach is referred to as AFSK, audio-frequency shift keying. Recently, a new approach to modems was developed to directly modulate the RF carrier. This approach allows 9600 baud communications within the same FM voice channel that was used to transmit 1200 baud AFSK. This modulation was selected for the PACSAT satellite.[8] It has some important features and it will be discussed in more detail in a later chapter. The primary disadvantage of this modulation compared to the earlier modulations is that it will only work with certain FM transceivers (generally, the more expensive base stations) and in most cases it requires a modification of the radio's hardware.

1.3 PACSAT BBS Protocol

The bulletin board system (BBS) aspect of PACSAT has its origins in the need for communications between personal computers which have proliferated in the past decade. Amateur packet radio operators have incorporated and improved the BBS concept for packet radio use. However, the basic BBS concept allows a user to enter, edit, browse, and retrieve messages through a remote

computer. Such a manual interface makes the BBS accessible but inefficient. Due to the limited visibility time available for a PACSAT, the PACSAT BBS system needs automation through a new set of protocols that are efficient for both the ground station and the satellite. When operational, these protocols should allow communications with PACSAT to occur without the presence of an operator.

New protocols for the BBS function are being developed by the University of Surrey and Virginia Tech for VITA's PACSAT. The primary protocol is a file transfer protocol which provides the functions normally associated with a BBS. Details of this protocol will be presented in future documentation of the PACSAT program.

1.4 Station Control Software

A lot of personal computer software has been developed for various amateur radio applications. In particular, software programs written for satellite tracking, for real-time control of rotors and radio tuning, and for terminal emulation are available. Satellite tracking software generally computes satellite position from the known ephemeris of the satellite.

Software for real-time control of the rotors and tuners operates in background so as not to interfere with the communications tasks. By using the software that has already been developed, considerable savings in time and development costs can be achieved.

1.5 PACSAT Ground Station Development

PACSAT ground stations combine features of both amateur satellite ground stations and terrestrial packet stations. The ground stations will also include new software for BBS protocols and station control.

1.5.1 Ground Station Requirements

In this project, VITA desired two different types of ground stations for PACSAT: a base station and a portable station. The two stations represent the extremes of a continuum of potential applications; however, both ground stations will be operated by relatively untrained operators. The communications and tracking aspects of the ground stations need to be automated and simple to use interfaces are also desired.

The base station may be required to handle a considerable amount of traffic and thus it should be able to communicate as efficiently as practical. For design purposes, the goal for the base station is to provide continuous communications to the satellite whenever it is more than ten degrees above the horizon. However, for PACSAT operation the requirements are better stated in terms of throughput. The minimum daily throughput of the base station will be sixteen A4 pages of uncompressed text (about 70 Kbytes). Such a requirement should be easily met if the above design goal is met.

The communications demand on the portable station is considerably less, but the portable station should be less expensive, more portable, and able to operate on batteries which may be recharged from solar energy. A daily throughput requirement of four A4 pages (17.5 KBytes) is reasonable for the portable station.

1.5.2 Development Project

At the beginning of the Fall semester in 1989, VITA awarded a contract to Virginia Tech to develop and to build a base station and a portable station for the PCE (PACSAT Communication Experiment). The commonwealth of

Virginia's Center for Innovative Technology (CIT) also contributed substantial funding for this project.

The contract involved collaboration between Virginia Tech's Satellite Communications Laboratory in Blacksburg, Virginia Tech's Northern Virginia Graduate Center (NVGC), the University of Virginia's Communications Systems Laboratory (through a subcontract from Virginia Tech), and Defense Systems Incorporated (DSI). The contract effort was divided among the groups as follows:

1. The Satellite Communications group, under Timothy Pratt's direction, developed the radios and antennas for the ground stations and coordinated the activities of the other groups.

2. The NVGC, under Fred . Ricci's direction, managed the development of software and the selection of computers for the ground stations.

3. The University of Virginia's Communications System Laboratory (U.Va.), under Steven G. Wilson's direction, developed the TNCs and modems.

4. And DSI agreed to test the portable ground station.

There was considerable background work accomplished prior to the award of the contract. Basic goals and

ground station concepts are described in a thesis by James Polaha.[9] Polaha's thesis also describes some orbital analyses and an analysis of a link budget relevant to PACSAT.

The development approaches for the two stations were slightly different. For both stations, the approach was to use commercially available products where ever possible. By using readily available parts, the stations development would be expedited and the stations would be easily replicated. The base station would combine features of high quality Oscar ground stations with terrestrial ground stations. Because the features of Oscar operation tend to be heavy, costly, and have large power drains, the portable station development attempts alternative approaches to satellite communications by using and modifying inexpensive equipment developed for terrestrial links.

A further constraint on development was to make the two stations similar with respect to software so that the portable station would use a subset of the software developed for the base station. This constraint attempts to avoid writing unique software for each station. Because the portable station will almost necessarily have a less capable computer than what can be used for the base

station, this constraint limits what can be done for base station software, at least for this project.

At the time that this contract began, there were many new products being introduced that may be useful for PACSAT operation. There are even more reports of products that are being developed. Due to the time constraints on the contract, the design of the stations are based on products that were available in December, 1989, when we began to buy the parts.

1.6 Accomplishments and Overview

System descriptions of the two PACSAT ground stations are provided in Chapter 2. This chapter presents detailed descriptions of the ground stations developed under this project. While the base station follows the standard approach outlined in the amateur literature, there were a number of unexpected problems that had to be solved to make the station work properly. After trying to meet PACSAT specific requirements, some of the problems identified (such as some limitations of the TNCs) will require new technology development by the manufacturers.

The design of the portable station takes a significant departure from the design of the base station

in order to obtain portability while maintaining a throughput capability. The portable station uses a much less expensive approach for the transceiver and a simple antenna system. Part of the portable station design relies on a demodulator developed by UVa; however, more specific information on their contributions are documented in their reports.[10]

1.6.1 Ground Station Analyses

In addition to the system development of the ground stations, some analysis has been carried out for the PACSAT orbit and the PACSAT modulation method.

Understanding the PACSAT orbital effects from a ground station perspective is important for the system design since it may identify properties which can be exploited to reduce the cost of the portable station, in particular. Results of an analysis of the PACSAT orbit are detailed in Chapter 3. The analytic approach taken is more comprehensive but less computationally intensive than the analysis presented in Polaha's Thesis.

The modulation method used for PACSAT is 9600 baud continuous-phase FSK (CPFSK) which is generated by direct FM modulation of the carrier with a shaped bipolar

waveform for zero ISI. Demodulation is accomplished by sampling the output of a FM discriminator at the points of maximum deviation. This approach is significantly different from the standard approaches described in most communications theory texts. Furthermore, due to the advantages of simple modulation and demodulation as well as its good spectral efficiency, this approach is becoming popular for commercial applications as well as in amateur radio. Thus, an analysis of this modulation and demodulation method is useful to determine how well it works and how it may be improved. A discussion of this modulation and an analysis is presented in Chapter 4.

Chapter 2

Ground Stations

2.1 Base Station

A prototype base station was assembled at Virginia Tech to verify the operation of the ground station system before integration of the parts with VITA's existing base station. The prototype consisted of several commercially available components. Most of the selected components were readily compatible in terms of hardware, which made integration relatively simple.

A block diagram of the PACSAT prototype base station is presented in Figure 4. The station consists of a PC-compatible computer, an AX.25 terminal node controller (TNC), a 9600 baud modem, a tracker interface card, a computer-controlled rotor controller, an azimuth and elevation rotor combination, a dual band (VHF/UHF) transceiver, a UHF preamp, and an Oscar-type antenna system. Not shown on the diagram are the power supply,

special interface cables, transceiver modifications, antenna tower and support, and the transient protection on the cabling that goes to the antenna.

The system-concept goal is to produce a completely automated base station. The computer should be able to compute accurately the satellite pass information including time of pass, duration of pass, and track history of look angles and tuning. During a pass the computer will operate the special PACSAT file transfer protocol and provide the look angles and tuning information for the hardware. The tracker provides the hardware and software interfaces between the computer and the tuner or rotor. The TNCs are separate special-purpose computers dedicated to the operation of the AX.25 link between the satellite and the ground station. The modem is actually a waveform generator that provides signals to directly modulate the FM transmitter, samples the received demodulated signal, and provides a TTL-compatible, digital data output.

The transceiver should be able to do the following: transmit on the 2-meter band, receive weak signals on the 70-cm band, handle 9600 baud signals with little distortion, and provide for computer control of tuning with sufficiently small tuning step sizes to counter the effects of doppler shift. A 70-cm band preamp located

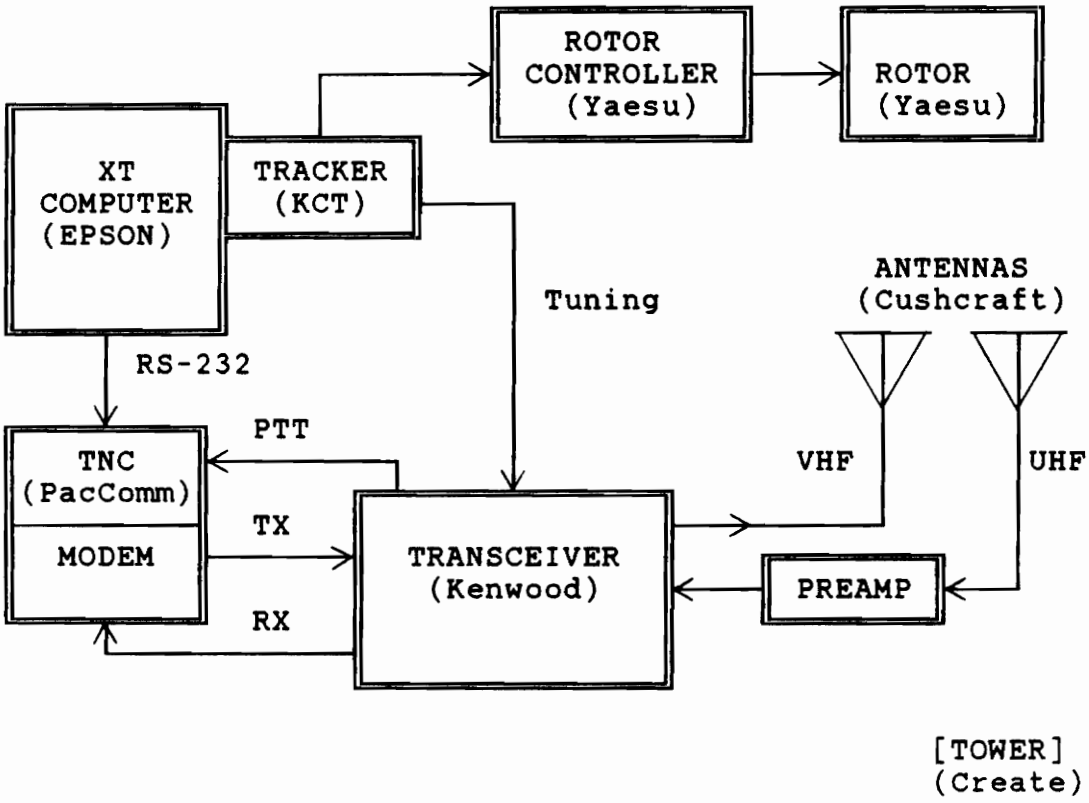

Figure 4: Base Station Block Diagram

close to the receiving antenna is useful to overcome the loss of the cable between the antenna and the transceiver. The antenna system is a readily available Oscar antenna set which provides reasonable gain and is circularly polarized to counter fading due to Faraday rotation of the linear polarization of the satellite. The rotor and its controller should be able to handle the load of the antenna and have provisions for computer control. The system also includes transient protection on the power line to the computer and all cabling to the antenna, rotors, and preamp.

2.1.1 Computer

The prototype base station computer is anEpson Equity-1+ computer which is PC-compatible (i.e., it has an 8088 processor). This particular model runs at a clock speed of 10 MHz. Its processing capabilities approximate those of a portable computer. The Epson includes a coprocessor in order to speed up the tracking programs for a more impressive display, but the basic operation of the station should not require a coprocessor. The computer is a desktop model with expansion slots and an EGA screen. We recommend using EGA (or better) graphics screen because

of the higher quality and the fact that some software packages (such as Instant-Track) do not support the older CGA screens. However, the operation of a base station does not require a graphics screen. The computer includes a 20 MB hard disk drive, which is required for the base station for the operation of the security software and which is convenient to store all of the software required for the base station.

This PC-compatible computer had two advantages for this contract. First of all, it is inexpensive. The above computer was bought on state contract for less than $1400. Buying a computer on state contract also allowed us to avoid a lengthy bidding procedure. Secondly, the resulting base station software should be transportable to the popular and relatively inexpensive portable computers which have 8088 processors.

2.1.2 Tracker

There are two steps to the tracking problem for the base station. The first step involves computing the position and doppler shifts of the signal from the satellite during the pass. The second step is to control the rotor and transceiver during a pass.

The base station uses the software and hardware package called Kansas City Tracker (KCT) from Grace Communications to interface to the rotor and the transceiver. We are not aware of any alternative packages. Although the package requires some effort to install, it includes direct interfacing with the specific models of transceiver and rotor that we have selected. Once installed, the tracker works fairly well although the software lacks a good user interface.

There are several shortcomings of this tracking package, probably because it is not yet completely debugged. The first problem to surface was a programming bug that caused the computer to crash at the end of some passes. This problem was corrected by a new version of the software.

Another problem involves the automatic tuning part of the software. To do automatic tuning, the software uses a table of frequencies which corresponds to the doppler shift of a reference frequency for the current pass. The software derives the doppler scale factor and then scales the uplink and downlink frequencies appropriately. In addition, the software interpolates the table entries in order to tune in the specified step size. The overall result is that the tuner is very computationally intensive. Since interrupts are masked during the tuning

computations, the tuner prevents the computer from reading data from the asynchronous RS-232 line to the TNC. Missing data from this link are irretrievably lost and probably undetectable. Inexplicably, the tuning software uses a lot of computer time even when the table is empty. While the KCT approach may be useful in order to be compatible with all the possible radios and applications, it is unnecessarily complex for this application. All that the base station needs is for the computer to output the current entry of a table of doppler shifted uplink and downlink frequencies to the radio.

The current version of the KCT software does not tune the Kenwood transceiver uplink frequency in the right direction. In other words, it adds the doppler instead of subtracting it. This appears to be yet another software bug. The uplink frequency should not require tuning (the satellite receiver was designed to accept doppler shifted signals); therefore, the current approach is not to use the uplink tuning feature until the KCT software can be replaced.

For the computation problem, we have evaluated two software packages from AMSAT. The most promising package was Instant-Track, but although this software gives impressive graphics and a good user interface, it neither supports transceiver tuning nor off-line operation through

the Kansas City Tracker. Without further development, Instant-track is only good for certain demonstrations. Quicktrack is a more mature package that does provide direct loading of the Kansas-City tracker tables and it allows file dumps of pass data. However, Quicktrack has a poor user interface.

These tracking programs provide more functions than are needed for a PACSAT ground station, especially a portable ground station. The added features of real time map displays, multi-satellite tracking, and mutual visibility schedules take up a lot of memory and are irrelevant for PACSAT operation. A simple tracking program that gives just the information required is recommended. Such a tracking program should be cheap compared to the $200 per copy for Instant-Track that AMSAT quoted for commercial applications.

2.1.3 TNC/Modem

The prototype base station uses a PacComm Micropower-2 TNC and a NB-96 9600 baud modem board. The boards were purchased separately and assembled at Virginia Tech. The assembly is straightforward and PacComm instructions are reasonably clear. The Micropower-2 TNC

is a separate unit that communicates to the PC via a RS-232 link. The 9600 baud modem connects on top of the TNC and the combination fits snugly in the Micropower-2 enclosure.

The RS-232 link is the weak link in the entire PACSAT communications system. The problem is that RS-232 is an asynchronous link that has no means for error recovery or for detection of missing bytes. Errors may occur from noise on the line but they are more likely to occur when the computer is too busy to service the port before a received byte is overwritten by a new byte. This problem cannot be solved by using a TNC that interfaces directly to the computer bus since the communication between the computer and the TNC is still asynchronous and follows the RS-232 standard. A new generation of TNCs should have a synchronous communications link to the host computer in order to avoid this problem. Unfortunately, RS-232 is the standard serial communications port for personal computers, especially for portable computers and older desktop models. Another alternative is to run all of the AX.25 software in the computer, but the 9600 baud protocol would require a very fast computer. The recommended solution for the near term is to run the link between the computer and the TNC at a low enough rate so that errors

are avoided. For the prototype base station, that rate is 4800 baud instead of the preferred rate of 19200 baud.

Back-to-back TNC tests at the University of Virginia Communication Systems Laboratory verified that the TNCs can communicate at 9600 baud. Communications through a radio link using two transceivers in separate rooms at Virginia Tech was verified next. Large files have been transferred over the radio link using various protocols (such as ASCII, Kermit, and XMODEM) on top of the AX.25. Not all protocols are compatible with AX.25, particularly those that use block sizes larger than the AX.25 packet length.

Large files have been transferred using the ASCII protocol with an effective data transfer rate of about 3500 bits per second (calculated as the ratio of the number of bits in the file to the amount of time required to send it). The file contained about 5300 bytes and was transferred in about 12 seconds. This is an equivalent of a dense (or unpacked) page of data; thus, for example, the time required for the transfer of 4 pages of data would be about one minute.

Procomm-plus has been used for communications software during laboratory tests. The communications software for the actual communications to the satellite will be discussed in a later section.

Recently, Kantronics introduced a new TNC (the Data Engine) based on a 10 MHz V40 processor (80286 compatible). Compared to the 4 MHz Z80 used in most other TNCs, including PacComm's, this new TNC should be a major improvement. Kantronics claims a throughput of 7200 bits per second when running packet at 9600 baud. The TNC still uses a RS-232 interface to the computer but since it uses an AT compatible processor and it has a lot of memory, customizing its software should be relatively simple, and standard personal computer compilers may be used. Unfortunately, this TNC was introduced too late for this project.

2.1.4 Transceiver

The transceiver selected for the base station is the Kenwood TS-790A dual band transceiver. Its features includes dual band operation with satellite communications capabilities. The transceiver has a serial port for computer control of tuning at increments of 100 Hz. The transmitting unit has the capability of transmitting up to 45 watts which is more than is required. Operation at its minimum power output (about 4 watts) should be adequate for PACSAT.

Although the radio caters to satellite users, it is not designed to handle 9600 baud signals. Furthermore, the radio requires some modification to operate out of the amateur bands.

The modification for reception of 428.01 MHz is simply the removal of programming diode D29 on the controller board. The controller board is the vertically mounted board behind the front panel and it is accessible by removing the top and bottom covers.

Transmitting on 148.56 MHz requires bypassing the internal controller altogether. For protection, the Kenwood was modified to transmit out-of-band for only the TNC. The connection to the TNC is through a 13 pin DIN connector at the rear of the unit. The modification involves isolating the PTT line from the TNC (pin 13 on the 13 pin connector) by cutting the trace beyond the first feedthrough from the connector. This trace is accessible on the bottom of the IF board. A jumper wire connects the trace from pin 13 of the connector to the wire marked TXS on connector CN48 of the IF board. The wires are spliced so that the PTT of the microphone will still cause transmission when the transceiver is tuned in the amateur band. If the transceiver is to transmit only for packet, then the TXS wire can be removed from connector CN48.

The modification required to operate at 9600 baud involves bringing the transmit signal from the TNC directly to the varactor for FM modulation and taking the TNC receive signal directly from the discriminator circuit. These signals are then buffered by an additional circuit to protect the IF board circuitry. The buffers are a pair of simple unity-gain op-amps on a small printed wiring board that will fit on a spot in the transceiver intended for an option that is not used for PACSAT operation. The input to the buffer for the varactor can be a sum of the TNC signal with the signal that originally went to the varactor so that the other features of the radio are still available. However, changing the driving circuit for the varactor requires that the modulator be retuned, which is accomplished by adjusting the trimmer capacitor by the varactor diode for exactly 10.695 MHz oscillation. The modulator circuit oscillates only while the transceiver is transmitting; therefore, the transmitter antenna ports should be properly loaded prior to tuning the circuit.

Under the control of the computer, the transceiver can tune out the doppler shift on both the uplink and the downlink. Fine tuning is desired to reduce the distortion caused by the narrow bandwidth IF filter when doppler shift is present. The transceiver can be tuned in 20 Hz

steps directly through its synthesized VFO; however, 2Ø Hz steps requires very frequent retuning commands during a pass. Since the synthesizer is changed for each step, bit errors are likely during the transient period when the synthesizer locks onto the new frequency. The retuning commands will occur asynchronously with the data transfer and thus should be made to occur infrequently if the retuning interferes with the signal quality. The current approach is to use 1ØØ Hz steps which appears to be a good compromise.

2.1.5 Preamp

A preamplifier mounted at the antenna mast is required for the base station to counter the loss in the long cable run between the antenna and the transceiver. An Advanced Receiver Research GaAs FET preamp was initially selected for the base station. Since this preamplifier does not include transmitter protection, some precautions must be used to avoid transmitting on UHF while the preamp is connected. However, this preamp failed after a few weeks of operation. Upon inspection, it was found that the preamp circuitry does not include protection diodes. Also, the original preamp did not have

a good dc path to ground to bleed off excess static electricity built up on the elements.

Even with protected diodes and with good grounding, the preamps still may fail occasionally. The development of a self-test that would include the preamp is desirable, especially for the automated versions of the ground stations.

The GaAs FET preamps typically have noise figures of about Ø.8 dB and gains of about 16 dB at the UHF frequencies.

2.1.6 Antenna System

The prototype ground station being assembled at Virginia Tech uses a Cushcraft AOP-1 Oscar Type antenna system that has separate Yagi Antennas for UHF and VHF. The circular polarization of these antennas will reduce the fading due to Faraday rotation caused by propagation through the ionosphere. However, the fading will not be completely eliminated because this setup uses a metallic cross boom which will cause the antenna to be somewhat elliptically polarized. Since the satellite is transmitting with linear polarization, there will be a constant 3 dB loss even if the antenna were perfectly

circular polarized. Figure 5 shows the possible fading for antennas with varying degrees of ellipticity. The epsilon factor is the arccotangent of the axial ratio for the polarization of the wave: 45° for circular, Ø° for linear. Note that when Faraday rotation is present, the motion of the satellite will most likely cause the rotation to change with time and thus the tau axis of the figure may be proportional to time.

The antenna is mounted on the roof of Whittemore Hall just behind the antenna range. The antenna is mounted on a tower so that the crossboom is about 12 feet above the roof. As a result, the antenna has very good visibility to the horizon in all directions except for the patch in the North that is blocked by the penthouse.

The antenna system uses crossed-yagis with 1Ø element-pairs for a gain of about 12 dB over a dipole. On the transmit side, there is 1ØØ feet of RG-8 (with foam dielectric) connected to a coax lightning arrestor and then to 15 feet of RG-58. At VHF, the cable to the transmit antenna should have about 3 dB of loss which is comparable to the loss at VITA headquarters. On the receive side, there is a similar arrangement except that a preamp is inserted between the RG-8 and the lightning arrestor. There will be about 2 dB of loss before the preamp and about 5 dB of loss after the preamp.

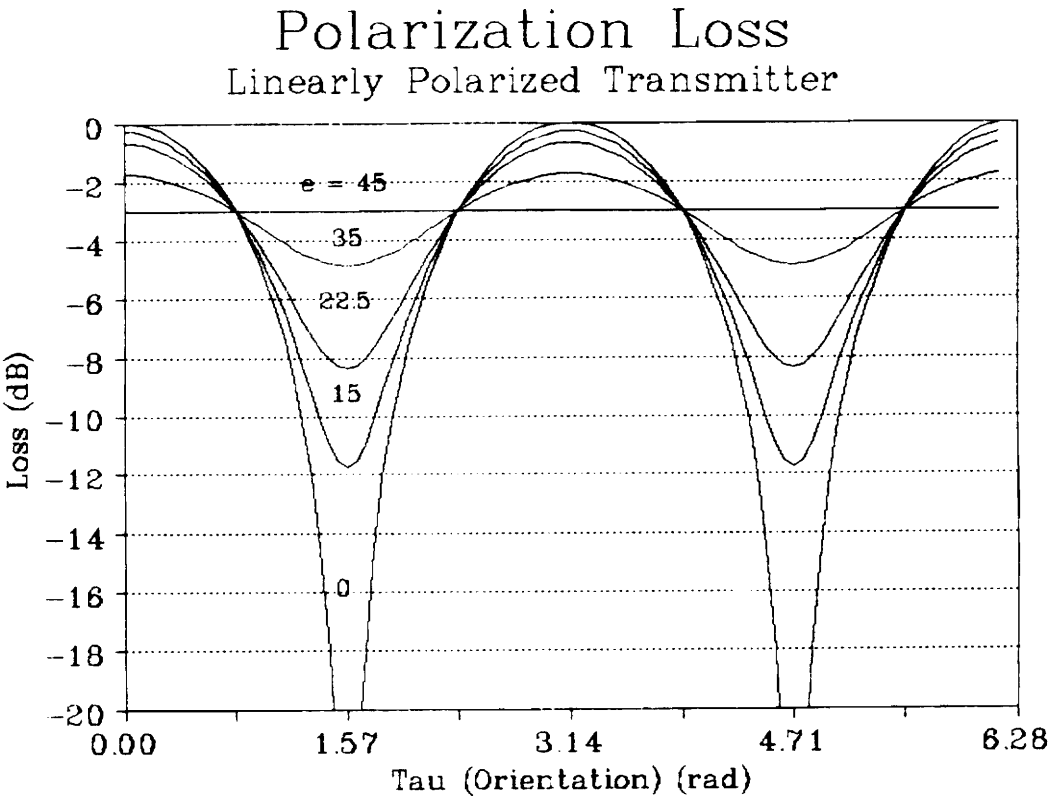

- Polarization mismatch loss for linearly polarized sending antenna and various polarizations for receiving antennas
- Tau is orientation mismatch in radians
- e (epsilon) is ArcCot(Axial Ratio) of polarization ellipse of receiving antenna

Figure 5: Fading Effect for Elliptically Polarized Antennas

For convenience, UHF connectors were used on the cables; however, these connectors are not recommended for these frequencies since they do not match the cable impedance and they are not weatherproof. The exposed connectors were sealed with butyl to provide weatherproofing. For reliability and performance, the UHF connectors should be replaced with type N connectors.

2.1.7 Rotor and Controller

The prototype base station uses the Yaesu G5400B rotor set. This combination azimuth and elevation rotor set should be more than sufficient to allow continuous tracking for most passes. The elevation rotor covers all elevation angles from 0° to 180° and the azimuth rotor covers all azimuth angles from 0° to 360°. The primary disadvantage of these rotors is that the azimuth rotor cannot rotate beyond 360° and thus a satellite pass that crosses south of the ground station will require the antenna to rotate all the way around the long way (which results in a loss of communications for up to a minute or so). The primary advantage of these rotors is that they are readily interfaced with the Kansas City Tracker. Although the Kansas City Tracker may be made to operate

with other rotors, it very readily interfaces with the Yaesu rotors.

2.2 Portable Station

Figure 6 shows the block diagram for the portable station. The portable station will consist of a computer, an external TNC, an antenna system, a transceiver system, and a power supply. The software for the portable station should be the same as for the base station except that it will not need Kansas City Tracker.

The operation of the portable station is similar to the base station except that control is simplified. The antennas do not require active tracking and the transceiver does not require tuning during a pass.

2.2.1 Computer

The computer is the Toshiba T-1200HB, a portable computer. Portable computers based on the 80C88 processor are available from many sources and a hard disk drive is probably required for operation and for storage of the software. A coprocessor is not included and it is assumed

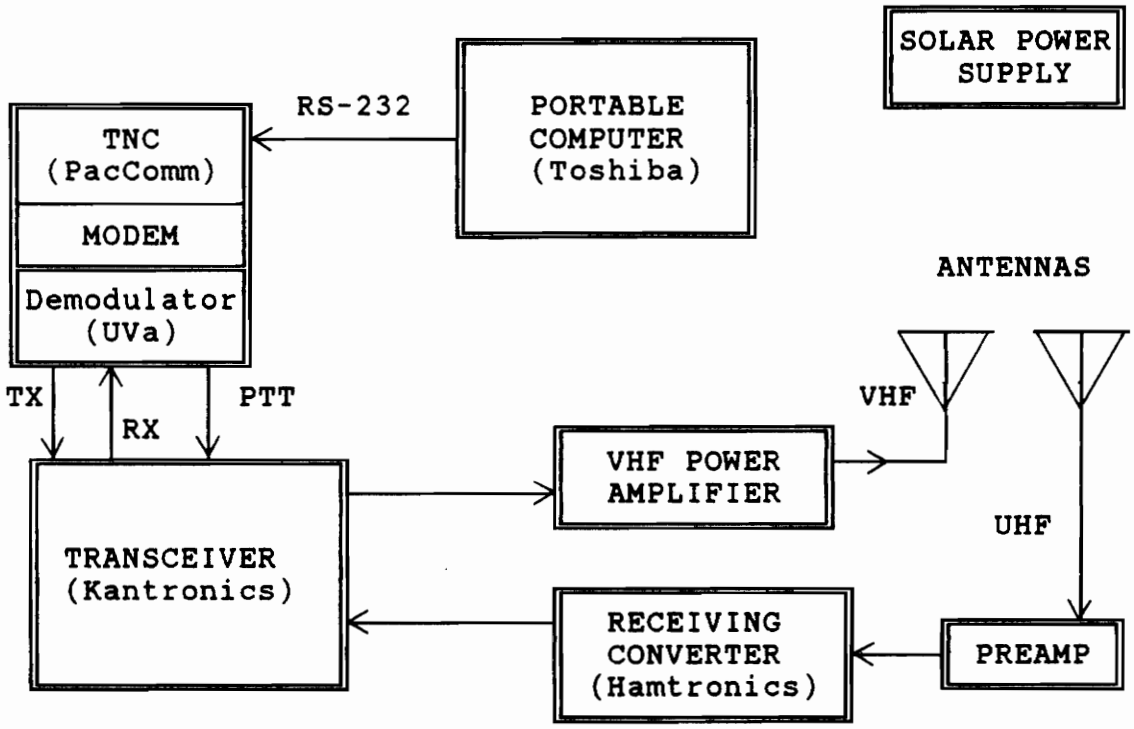

Figure 6: Portable Station Block Diagram

that the operator is willing to wait the additional time required to compute the pass information. A printer is highly desirable to print pass information and files that are received.

2.2.2 TNC/Modem

The TNC/modem is an external unit that is the heart of the portable station. This unit, developed by UVA, includes a small TNC and a modem for 9600 baud. In addition, it includes a PLL discriminator circuit that can receive signals shifted beyond the worst case doppler shifts expected from the satellite. The PLL ciruit provides automatic tuning of the received signal, and thus simplies the system and reduces the overall cost. This circuit allows the use of a simple fixed tuned transceiver, which is less much expensive than the tunable types.

The TNC uses a RS-232 interface to the computer, but this interface is less of a problem since the portable computer is dedicated to the communications task during the pass.

2.2.3 Antennas

There are a number of alternatives for the portable terminal antenna. For portability, mobile whip antennas appear promising. These antennas are lightweight and simple and with a suitable ground plane, they can have gains of up to 8 dB over isotropic. The disadvantage of these antennas is that the pattern is concentrated too close to the horizon. Because the antennas are vertically polarized, there will be fading due to Faraday rotation and satellite attitude. The fading can impact system performance since the system uses different bands for the uplink and downlink which will result in uncorrelated fading on the two bands. For example, there may be fading on the uplink when the downlink is open, but efficient operation of AX.25 will require both directions to be open simultaneously.

An alternative approach is to use a circularly polarized antenna but these antennas are more complex and less portable than the whips. Fading for the portable circularly polarized antenna is reduced but not eliminated since the circular polarization is usually only for a small range of angles.

2.2.4 Transceiver

The portable station transceiver is a modified Kantronics DVR2-2 dual channel "data-ready" transceiver. This transceiver is fixed tuned by selection of crystals. It is ready for 9600 baud communications since buffered access to the varactor and discriminator is provided through the external connector.

Figure 7 shows a block diagram of the modified Kantronics transceiver. In the unmodified transceiver, the transmit and receive circuits in the DVR2-2 follow separate paths, which are then combined through a T/R switch at the antenna port. For the portable ground station, the receive and transmit paths are separated so that the receive signal can come from a UHF to VHF down-converter and the transmit signal can go to an external amplifier.

With the addition of the external receiver converter (from Hamtronics) and a demodulation circuit being developed by the University of Virginia, this receiver will be low cost, lightweight, and small. However, an omnidirectional antenna may not provide sufficient gain for reception of a majority of satellite passes. An external power amplifier may be necessary for transmitting to the satellite.

a) TRANSMITTER

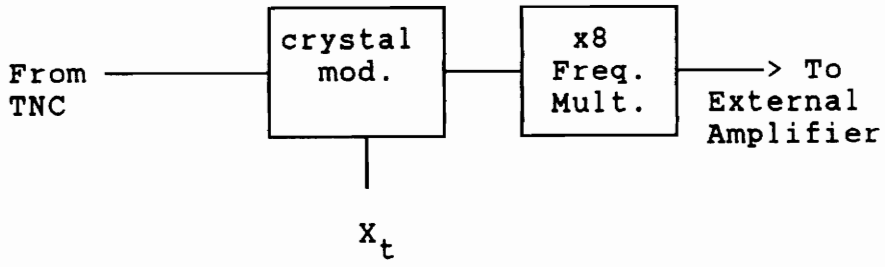

Crystal Frequency:

$$X_t = F_t / 8$$

b) RECEIVER

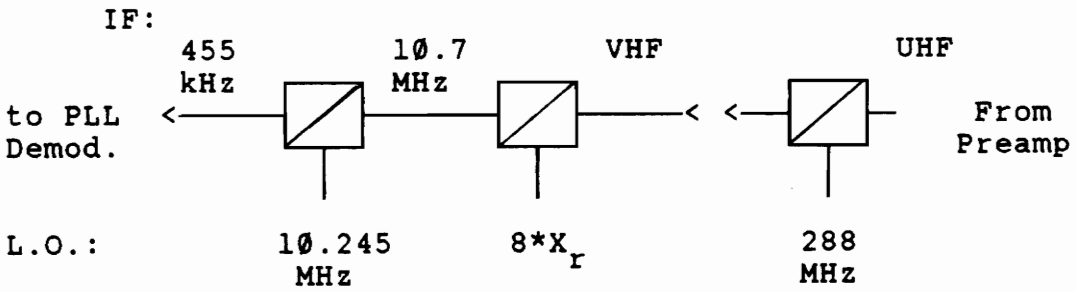

Crystal Frequency:

$$X_r = (F_r - 298.7\ \text{MHz})/8$$

Figure 7: Portable Transceiver Block Diagram and Frequency Plan

The frequency plan for the transceiver is determined by the desired operating frequencies and the architecture of the transceiver. For the transmit side, the output of a modulated crystal oscillator goes through a times-eight frequency multiplier to generate the desired transmit frequency. Thus the transmit crystal frequency is the the transmit frequency divided by eight. For the receive side, there is a down-conversion by 288 MHz to get to the VHF band and then another down-conversion to get to a 10.7 MHz IF. The second down-conversion frequency is determined by eight times the receive crystal frequency. Thus the receive crystal frequency is one eighth of the difference between the received frequency and 298.7 MHz.

2.2.5 Power Supply

The power supply requirements for a portable station depend on the usage of the station. Assuming that the communications part of the portable station operates only during a single satellite pass each day and that the computer will operate less than an hour each day, a portable solar power supply and battery may be used. Portable solar supplies generally provide less than 10 watts in full sunlight. The solar panels investigated for

this project deliver ten watts in full sunlight. Allowing for varying weather conditions, the average effective time of full sunlight is at least 2 hours during winter months and perhaps 5 hours during summer. Using the winter estimate, such a solar panel should deliver at least 20 watt-hours per day, or 1.66 amp-hour for a 12 volt battery.

Assuming that the communication equipment draws less than 5 amps during transmit and less than one amp during receive, the solar supply should be able to provide enough power to transmit for 10 minutes and receive for 50 minutes each day. Note that a typical portable ground station requirement may be four pages a day, which should require less than a minute of transmit time.

Since the computer may operate for longer periods of time, it may need a separate solar power supply.

Operating with smaller panels is attractive for very small data throughput requirements, especially if the station does not need to communicate every day. For the stations with a higher throughput requirements, a solar panel of 25 watts or more may be required. Such a panel is transportable in a vehicle such as a car, but it would be too heavy and bulky to check as baggage on an airline. The panel would have to be set up outside in a semipermanent arrangement.

2.3 Link Budgets

PACSAT ground station design will be driven by some overall throughput requirements (e.g., four pages of text per day for the portable station). However, the relationship between throughput and the link budget is complicated by the satellite motion. For a simple verification and comparison of the ground station designs, a link budget for a specific static case can be analyzed. In the following sections, link budgets are presented for when the satellite is at 10° in elevation. This case is representative of a worst case since the satellite is further away as the elevation angle decreases and operation below 10° elevation may not be necessary.

The following results serve to verify the ground station designs, but the budgets may lead to overly conservative designs since dynamic effects of the orbit or the actual throughput requirements are not addressed. In order to address the these issues of PACSAT ground station design, the link budget analysis should not only say how much margin exists for the link but also how long and how often the link signal will be above the required power level. An approach to addressing these dynamic effects is presented in chapter 3.

2.3.1 Margins

For packet communications, the link bit error rate does not translate to end-to-end bit error rates because of the provisions for error detection and packet retransmission. Instead, the link bit error rate will determine the efficiency of the link since higher bit error rates lead to more retransmissions. However, packet protocols offer considerable design flexibility to tradeoff bit error rate requirements with efficiency. For examples, two extreme applications of the AX.25 protocols are considered.

A very efficient point-to-point link will transmit packets back-to-back and use the GO-BACK-N error recovery approach with the ability of going back seven frames (packets). In such a case, the maximum packet size will be used for the best efficiency. A bit error in this design is costly since it may cause up to seven packets to be retransmitted. A design approach for this link may be to make bit errors rare within a set of seven frames of maximum size. Assuming that the desired probability of bit error within such a set is Ø.1, then there will be one bit error in seventy frames of 274 octets each (i.e., one bit error in 153440 bits). The required link bit error

rate would have to be 6.5E-6, which requires a link $E_b/N_\emptyset$ of about 13 dB for ideal (orthogonal) FSK.[11]

An alternative design could use a STOP-AND-WAIT approach whereby short packets are transmitted one at a time. (In such a system, efficiency can be regained by effective multiple access techniques.) Here, the design criterion could be to make bit errors rare within a small packet. Assuming that the probability of a bit error within a packet of 146 octets is Ø.1, then the required link bit error rate would be 8.6E-5 or about the value used in the U.Va. report[12]: an $E_b/N_\emptyset$ of 11.5 dB.

The following link budgets compute the margin for a required bit error rate of $1\emptyset^{-4}$ as suggested in the U.Va report. Since the receivers will not use coherent detection, an additional implementation margin of 5 dB is included. This margin corresponds to the measurements presented in the U.Va. report. The minimum level of $E_b/N_\emptyset$ for the following budgets is therefore 16.5 dB.

2.3.2 Uplink Budgets

The uplink power budgets are summarized in Tables 1 and 2. The tables are organized into three parts which are described in the following sections. The first part

accounts for the signal power gains (or losses) from the transmitter output to the first preamplifier of the receiver input. The second part accounts for the noise present in the receiver at the satellite. And the last part gives a summary of the budget with respect to the minimum signal identified in the previous section. The final margin is in addition to the 1Ø dB margin preallocated for the uncertainties concerning the nonthermal noise sources within the satellite's antenna pattern. As shown in the tables, both stations have reasonable link margins which result primarily from the relatively low losses for operation at VHF.

2.3.2.1 Link Budget Entries for Signal Power

The signal power available at the receiver is determined by the transmitter, the antenna arrangements, and the overall path loss. The path loss and satellite antennas are necessarily fixed quantities and the ground station design varies by the choice of transmitter and ground antenna. The cable loss for the ground station is unavoidable since the transmitter will generally be located at a considerable distance from the antenna; however, cable losses are manageable for VHF operation.

Table 1: Uplink Power Budget for a Base Station

Description	Value	dB
SIGNAL:		
Transmit Power (W)	4	6.02
Transmit Freq. (MHz)	148	
Cable:		
Type	RG-58	
Loss/ft (dB/100ft)	6	
Length (ft)	15	
Loss (total)	0.9	-0.90
Type	RG-8 (Foam)	
Loss/ft (dB/100ft)	3	
Length (ft)	100	
Loss (Total)	3	-3.00
Ant. Polarization	Circular	
Loss (dB)	3	-3.00
Add'l Margin (dB)	1	-1.00
Ant. Type	10 El. X-Yagi	
Gain (dbi)	14.4	14.40
Sat. Alt. (km)	800	
Min. El. angle (deg)	10	
Max. Range (km)	2367	
Path Loss	4.64E-15	-143.33
Sat. Ant. Type	Vert. Mono/GP	
Gain (min)	2	2
Total (W)	1.32E-13	-128.81
NOISE:		
Boltzman's k	1.38E-23	
Ant. Temp. (K)	290	
Sat. Cable Loss	negligible	
Bandwidth (Hz)	20000	
Excess Noise	10	10.00
Total Noise (W)	8.004E-16	-150.97

C/N	1.64E+02	22.16
Bit Rate (bps)	9600	
Eb/N0	3.42E+02	25.34
Min Eb/N0 (1E-4 ber)		16.50
Margin (dB)		8.84

The first entry is the transmitter power which is set by the capabilities of the systems. For the base station, minimum power is desired due to the high duty cycle that may be required. The minimum power output from the Kenwood transceiver is about 4 watts. For the portable station an external 20 watt amplifier is used.

Cable loss for VHF (at 148 MHz) is estimated from published charts.[13] The base station uses 100 feet of RG-8 with foam dielectric (estimated at 3 dB per 100 feet) and 15 feet of RG-58 (estimated at 6 dB per 100 feet). The portable station uses 65 feet of RG-58 for a loss of about 3.9 dB. Due to the power demand from the portable station's 20 watt amplifier, it would be desirable to use shorter cable, higher quality cable, and/or high gain antennas to reduce the transmit power requirement. However, the current portable station design is a good compromise when other factors such as weight, cost, size, and ruggedness are considered.

Polarization loss for the base station includes the constant 3 dB loss for using circular polarization antenna for a linearly polarized wave. An extra 1 dB margin is added for fading that may result from the antenna not being perfectly circular. Fading in excess of 1 dB is expected to be rare because the antenna should track the satellite, keeping it near the center of the beam. For

Table 2: Uplink Power Budget for a Portable Station

Description	Value	dB
SIGNAL:		
Transmit Power (W)	2Ø	13.Ø1
Transmit Freq. (MHz)	148	
Cable:		
Type	RG-58	
Loss/ft (dB/1ØØft)	6	
Length (ft)	65	
Loss (total)	3.9	-3.9Ø
Ant. Polarization	Vertical	
Loss (dB)	Ø	Ø.ØØ
Add'l Margin (dB)	6	-6.ØØ
Ant. Type	Vertical Whip	
Gain (dbi)	4	4.ØØ
Sat. Alt. (km)	8ØØ	
Min. El. angle (deg)	1Ø	
Max. Range (km)	2367	
Path Loss	4.64E-15	-143.33
Sat. Ant. Type	Vert. Mono/GP	
Gain (min)	2	2
Total (W)	3.78E-14	-134.22
NOISE:		
Boltzman's k	1.38E-23	
Ant. Temp. (K)	29Ø	
Sat. Cable Loss	negligible	
Bandwidth (Hz)	2ØØØØ	
Excess Noise	1Ø	1Ø.ØØ
Total Noise (W)	8.ØØ4E-16	-15Ø.97
C/N	4.73E+Ø1	16.75
Bit Rate (bps)	96ØØ	
Eb/NØ	9.85E+Ø1	19.93
Min Eb/NØ (1E-4 ber)		16.5Ø
Margin (dB)		3.43

the portable station, 6 dB of fading margin is allowed for mismatched orientations. If Faraday rotation is present, then the polarization orientation of the received signal at the satellite should be evenly distributed so that fading in excess of 6 dB should occur for less than 20% of the time. In the absence of Faraday rotation, there will be no loss since both antennas will be vertically polarized.

Antenna gain for the base station is typically 12.25 dBd (14.4 dBi) for a 10 element Yagi array. The portable station uses a 5/8 wavelength monopole which should give about 4 dBi of gain if it is suitably mounted on good ground plane and at a good height above the ground.[14]

Path loss is computed for the range to the satellite when the satellite is 10° above the horizon. For a 800 kilometer altitude satellite, the range is 2366 kilometers.

The satellite uses vertical monopole antennas. It is expected to provide at least 2 dB gain in the direction of the ground station when the satellite is 10° above the horizon. Assuming that the satellite is stabilized, the satellite antenna pattern will have a null below the satellite and the gain will increase for ground stations loacated closer to the horizon seen by the satellite.

2.3.2.2 Uplink Noise Calculation

The noise power is computed assuming that the satellite receiver uses a 20 kHz bandwidth filter to accept worst case doppler from the ground station. Also, since a substantial part of the antenna pattern will see a warm Earth with nonthermal natural and manmade noise sources, the effective noise temperature is estimated to be 10 dB over the standard 273K. The received noise power is a function of the satellite design and thus is fixed for all ground station designs. There is an assumption that the satellite has insignificant cable losses and that a preamp with a negligible noise figure is used.

2.3.2.3 Uplink Margin Calculation

The signal to noise ratio (C/N) is simply the ratio of the received signal power to the received noise power. However, for digital signals, E_b/N_0 is a more relevant quantity. E_b/N_0 is scaled from C/N by the ratio of bandwidth over the bit rate. The margin for the links are computed by comparing the estimated E_b/N_0 with the minimum E_b/N_0 required (16.5 dB) for the desired link bit error rate of 10^{-4}.

The result of this budget indicates considerable margin for both stations. (These margins are 8.8 dB for the base station and 3.4 dB for the portable station and do not include the 1Ø dB margin already allowed for excess noise.) The excess margin for the base station can help overcome even more noise or higher fading resulting from antenna imperfections. For the portable station, the margin can be used to reduce the transmit power in order to reduce current drain from the battery.

2.3.3 Downlink Budgets

The link budgets for the downlinks of the base station and the portable station are presented in Tables 3 and 4. The downlink is disadvantaged with respect to the uplink due both to the losses from the higher frequency involved (UHF instead of VHF), and to the limited transmit power available from the satellite.

2.3.3.1 Received Signal Power

The satellite transmitter power is limited both by the prime power available from its solar panels and

Table 3: Downlink Power Budget: Base Station

Description	Value	dB
SIGNAL:		
Transmit Power (W)	1.5	1.76
Transmit Freq. (MHz)	428	
Sat. Ant. Type	Vert. Mono/GP	
Gain (min)	2	2.ØØ
Sat. Alt. (km)	8ØØ	
Min. El. angle (deg)	1Ø	
Max. Range (km)	2367	
Path Loss	5.55E-16	-152.55
Cable:		
Type	RG-58	
Loss/ft (dB/1ØØft)	12	
Length (ft)	15	
Loss (total)	1.8	-1.8Ø
Ant. Polarization	Circular	
Loss (dB)	3	-3.ØØ
Add'l Margin (dB)	1	-1.ØØ
Ant. Type	1Ø El. X-Yagi	
Gain (dbi)	14.4	14.4Ø
Total (W)	9.56E-15	-14Ø.19
NOISE:		
Boltzman's k	1.38E-23	
Ant. Temp. (K)	44	
Preamp NF (dB)	Ø.8Ø	
Bandwidth (Hz)	15ØØØ	
System Temp @Preamp	186.13	
Total Noise (W)	3.85E-17	-164.14
C/N	2.48E+Ø2	23.95
Bit Rate (bps)	96ØØ	
Eb/NØ	3.88E+Ø2	25.89
Min Eb/NØ (1E-4 ber)		16.5Ø
Margin (dB)		9.39

storage batteries, and by its operation. The UoSAT3 satellite transmits continuously in order to maximize the life of the output power transistors. As a result, continuous transmission power is estimated to be about 1.5 watts. When communicating with the portable station, the satellite can be set up to transmit temporarily at about 5 watts, but, due to the additional power drain required, this mode may not be feasible for a large number of portable stations spread over the Earth. In any case, the portable station will have to communicate the need for more transmit power while the satellite is in its normal mode of transmitting with the lower power. For the portable station budget, it is assumed that the satellite will transmit at the higher power when needed although the operational details to make this happen have not yet been worked out.

The antenna gains, polarization losses, and path losses follow the same general assumptions as for the uplink. The only difference is that the losses increase as a result of operating at the higher frequency. (However, it should be noted that the higher frequency allows smaller antennas to be used for the required gain and the effects of Faraday rotation and nonthermal noise sources decrease with the increased frequency. Therefore,

Table 4: Downlink Power Budget: Portable Station

Description	Value	dB
SIGNAL:		
Transmit Power (W)	5	6.99
Transmit Freq. (MHz)	428	
Sat. Ant. Type	Vert. Mono/GP	
Gain (min)	2	2.00
Sat. Alt. (km)	800	
Min. El. angle (deg)	10	
Max. Range (km)	2367	
Path Loss	5.55E-16	-152.55
Cable:		
Type	RG-58	
Loss/ft (dB/100ft)	12	
Length (ft)	15	
Loss (total)	1.8	-1.80
Ant. Polarization	Vertical	
Loss (dB)	0	0.00
Add'l Margin (dB)	6	-6.00
Ant. Type	Vertical Whip	
Gain (dbi)	4	4.00
Total (W)	1.83E-15	-147.36
NOISE:		
Boltzman's k	1.38E-23	
Ant. Temp. (K)	200	
Preamp NF (dB)	0.80	
Bandwidth (Hz)	15000	
System Temp @Preamp	289.19	
Total Noise (W)	5.99E-17	-162.23
C/N	3.06E+01	14.86
Bit Rate (bps)	9600	
Eb/N0	4.79E+01	16.80
Min Eb/N0 (1E-4 ber)		16.50
Margin (dB)		0.30

some design benefits will not show up in link budget comparisons.)

Cable losses for the two stations is 1.8 dB from 15 feet of RG-58 between the antenna and the preamp. The preamp gain is considered high enough so that any additional losses or noise sources after the preamp can be ignored.

2.3.3.2 Downlink Noise Calculation

GaAs FET preamps are assumed for this budget; however, bipolar FET preamps may prove to be more rugged and reliable. Bipolar preamps have noise figures of about 1.2 dB whereas GaAs FET have Ø.8 dB NF.

The receiver has a bandwidth of about 15 kHz. A computation of system noise temperature measured at the preamp gives a result of about 186K for the base station and 29ØK for the portable station. Natural sky noise is included, but noise due to interference is not. The experience of operating the prototype base station for a couple of months at our location in Blacksburg indicates that the noise is low, but when interference is present, as happens occasionally, the downlink is lost.

Interference is particularly a problem for the downlink because the source can be very near the receiving antenna.

Since the portable station antenna has a pattern that is directed toward the horizon, the antenna noise will include a substantial amount of a warm Earth. The portable station antenna temperature is an estimate based on the assumption that 2/3 of the antenna aperture sees 29ØK Earth and the rest sees 44K sky.

2.3.3.3 Downlink Margin

The budgets indicate a fair margin of 9.4 dB for the base station and a weak margin of Ø.3 dB for the portable station. The base station margin is useful for overcoming excess noise. Experience from operating the prototype base station indicates that data can be received from satellite down to when the satellite is just above the horizon -- a situation in which which there is increased noise and more path loss than in the evaluated case.

The poor margin for the for the portable station is exacerbated by the fact that the evaluation is less certain. For example, the antenna gain may be considerably less than expected unless the mobile whip is

mounted on a good ground plane at a reasonable height (perhaps more than ten feet high).

By using less lossy cables, an antenna with less noise and more gain, and a better receiver implementation, the portable station margin can be improved substantially. However, these may not be necessary if the margin is acceptable when the satellite is at higher elevation angles and an acceptable margin is available for enough time to transmit the required amount of data. Thus the portable station design may be acceptable as is, but an alternative to a static link budget is required to validate the design. Chapter 3 discusses an alternative approach that more appropriately analyzes the capabilities of the portable station.

Chapter 3

PACSAT Orbit Characteristics

An understanding of the orbital characteristics from the perspective of the ground station is important for the system design of the ground station. The orbital characteristics relevant to a communications link include satellite position, motion, and attitude. These characteristics lead to path loss, look-angle variations, doppler shift, and polarization loss. Although identifying worst case conditions is fairly straight forward, information on the time variations and the relative frequency of occurrence of the effects is important. For the base station, such information can distinguish common effects from rare ones. For the portable station, this information can be used to exploit certain effects in order to produce a simpler ground station.

Most satellite communications texts concentrate on the problem of communicating to geostationary satellites. The results for geostationary satellites are fairly static

which simplifies the analysis considerably. These same techniques may be used to obtain results for specific cases, e.g., worst case.[15]

To obtain the dynamic effects of the orbit, the specific relations were re-evaluated over a number of intervals of several possible orbits. There are two approaches to do this type of analysis. The easiest approach is to obtain a tracking program (such as Quicktrack or Instant Track), and then produce plots or collect statistics of the desired effect over several passes. The disadvantages of this approach is that it requires a lot of computations and may miss important effects that occur with different initial conditions. The other approach involves a geometric study of the orbit to identify the possible orbits by a few parameters followed by a study of the statistics of those parameters. This approach provides a more complete understanding of the orbit and requires less computer time for the computation. This chapter presents results for the UoSAT3/PACSAT orbit with the latter type of analysis.

3.1 Analysis Background

The equations for satellite motion and position relative to a ground station are available from several sources including most satellite communications texts. A particularly good source that gives a good explanation of how to work with the equations and geometry is The Satellite Experimenter's Handbook.[16] In addition, the CRC Standard Mathematical Tables provides a good summary of the spherical trigonometry equations that are required for the satellite geometry.[17]

A satellite orbit is usually described by a set of parameters which is the satellite's ephemeris. Typically, this set includes satellite altitude, inclination, and eccentricity which define the shape of the orbit. Other parameters such as mean anomaly, argument of perigee, epoch time, and decay are important when the position of a specific satellite must be known for a specific time. This analysis concentrates on the general geometry of the orbit and thus the second set of parameters are not needed. Furthermore, because PACSATs are generally LEO satellites, the orbits are approximately circular.[18]

In addition to the satellite elements, four other parameters are required to identify a particular pass. For this analysis, the two important parameters are ground

station latitude and the earth-centered angle (PsiØ) between the satellite and the ground station at the time when the satellite is closest to the ground station. Time is measured relative to this time of closest approach. The other parameters place the orbital plane relative to the equator and differentiate between easterly and westerly passes. These latter parameters produce secondary effects and are ignored in the following results.

The definition of PsiØ is illustrated in Figure 8. Figure 8a shows a spherical view of the globe. Psi is the great circle arc from the ground station to the subsatellite point. PsiØ is the minimum value of that arc for that orbit. Psi is measured as the Earth-centered angle between the two surface points as shown in Figure 8.

The analysis takes the following steps. Time histories (trajectories) of each communications-related parameter (such as look angles) are recorded for various representative values of PsiØ. Then a simulation is run to measure the relative frequencies of the possible PsiØ results. The representative PsiØ values of the first step sample the possible range of PsiØ at equal intervals. This sampling eases the application of the PsiØ distribution information from the second step. The

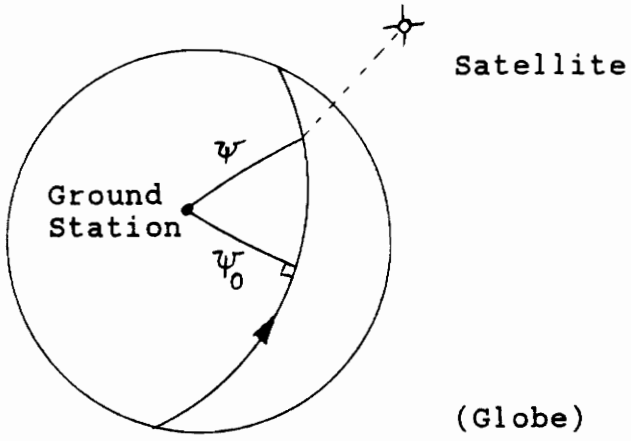

a) Psi and Psi∅ are Great Circle Arc Distances Between Ground Stations and Satellites

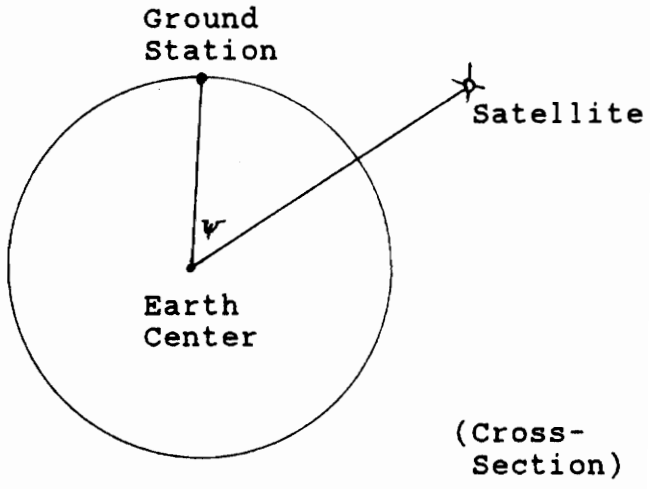

b) Psi is Earth Centered Angle Between Ground Station and Satellite

Figure 8: Definition of Psi∅

equations used in both steps of this analysis are presented in Appendix A.

The following results apply to the UoSAT3 satellite with an altitude of 800 kilometers and an inclination of 98.75°. VITA's PACSAT satellite will not necessarily have the same orbit. In fact, this orbit may not be the best orbit for VITA. For example, if most of the communications is with developing nations near the equator, then an equatorial orbit (with a relocated base station) would be a better choice than a polar orbit because the ground stations will have satellite visibility on every orbit.

3.2 Trajectories of Communication Link Properties

The dynamics of certain communications link parameters such as look angles, path losses, and doppler shifts are discussed in the following sections. The results are presented as collections of time history plots for individual passes. The specific parameters are completely determined by the relative positions of the satellite and the ground station as shown in Appendix section A-4. The relative positions of the satellite and the ground station are affected by both the orbital motion

and the Earth's rotation as presented in Appendix sections A-2 and A-3. While the motion from the Earth's rotation is primarily a property of the latitude of the ground station, the satellite motion, relative to the ground station, is primarily determined by the angular separation, PsiØ. Appendix section A-1 shows how the orbit may be determined for a specific PsiØ.

The overall result is that the time histories of the communications parameters are largely determined by PsiØ and ground station latitude. These time histories are referred to as trajectories in this thesis in order to emphasize the fact that they are deterministic.

The plots in the following sections present trajectories for a series of PsiØ angles. Due to the dependence of the trajectories on PsiØ, trajectories for intermediate values of PsiØ can be interpolated from the plotted trajectories. Likewise, the probability of occurrence of a range of trajectories can be inferred from the probability of occurrence of the corresponding range of PsiØ.

It should be noted that the trajectories are also dependent on two other parameters which determine the horizontal direction to the satellite. These secondary parameters are presented in the appendix but they are

ignored in the followed sections because their effects are small.

3.2.1 Look angles

The path of a satellite as it moves across the sky can be represented by the look angles in elevation and azimuth. Look angles to LEO satellites change more quickly than for most other types of orbits.

Figure 9 shows a typical set of look angle trajectories for a ground station near the equator. In this figure, the satellite path is plotted as elevation vs. azimuth. The path of the satellite is easy to visualize from this plot. The tic marks indicate time increments of 2Ø seconds. The higher density of tic marks near the horizon indicates that the satellite moves more slowly near the horizon and that the satellite spends most of each pass near the horizon. Near the equator, the satellite will pass nearly due east or due west at the point of closest approach for each pass.

The effect of the ground station being in higher latitudes is demonstrated in Figures 1Ø and 11. In the higher latitudes the satellite will pass more toward the

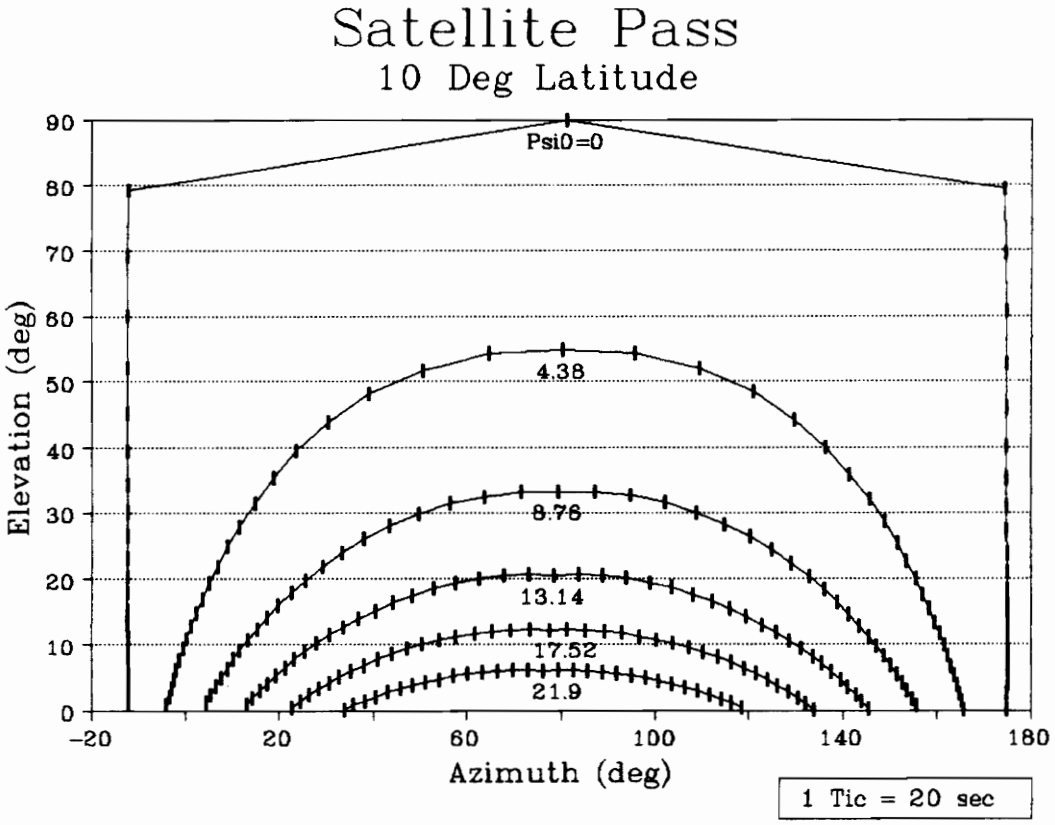

- Look Angles From Ground Station to Satellite
- Ground Station at 1Ø° N Latitude
- Trajectories For PsiØ at Equal Intervals of 4.38°
- Satellite Spends Most of the Time in Lower Elevations

Figure 9: Elevation vs. Azimuth from Ground Station at 1Ø° Latitude to Satellite for Various PsiØ

north (in the northern hemisphere) for the low elevation passes.

For VITA's PACSAT, Figure 9 is representative of the likely locations for the portable station, while Figure 1Ø is representative of the base station in Arlington and the prototype base station in Blacksburg.

3.2.1.1 Elevation Angles

Figure 12 shows typical plots of elevation trajectories with an explicit time axis. These plots are for a station near the equator, but they do not change significantly for higher latitudes. An important observation here is that few satellite passes will have high elevation angles and those that do will spend only a little time at the high elevation angles. This effect is exploited by the portable station. By concentrating its antenna pattern near the horizon, the portable station can both achieve some gain and have an omnidirectional pattern without losing too much of the communications window.

Because the rate of change of look angles is greatest at the peak of high passes, the rotors for the base station's high gain antennas may not be able to keep up. This figure indicates that a loss of communications

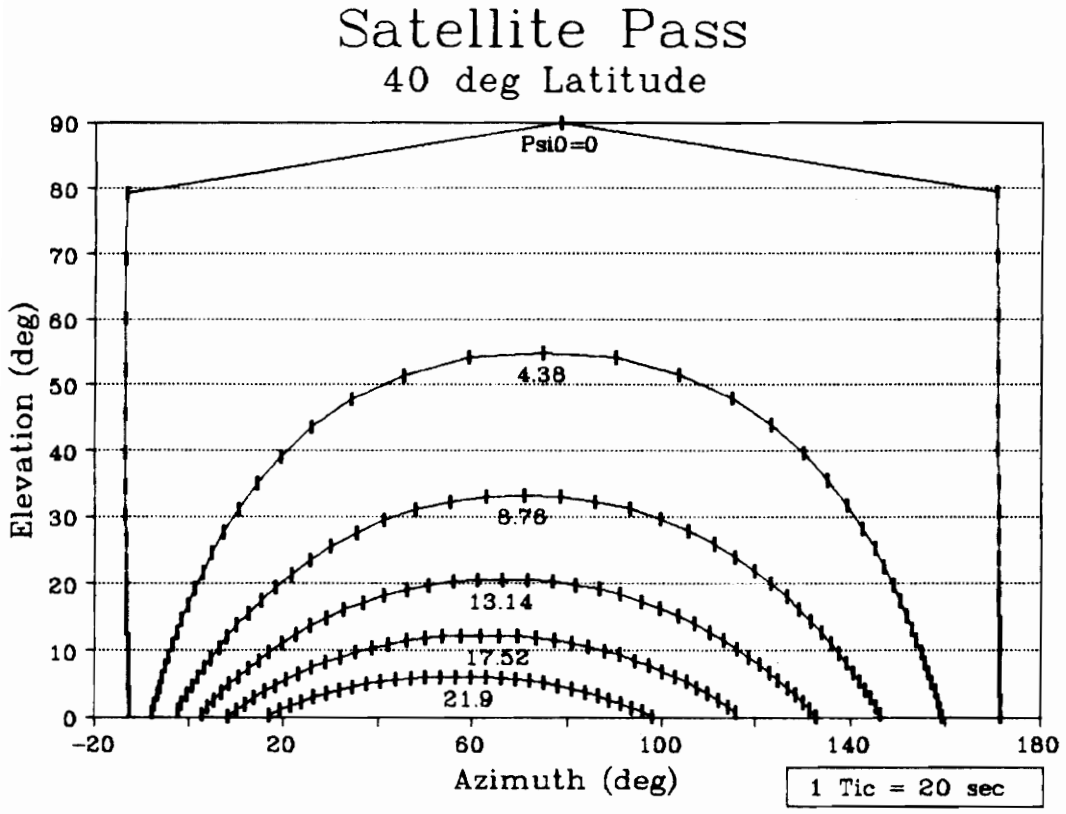

- Look Angles (in Degrees) from Ground Station to Satellite
- Ground Station at 4Ø° North Latitude
- Lower Passes Tend Slightly Toward North

Figure 1Ø: Azimuth-Elevation Trajectories for Ground Station at 4Ø° Latitude

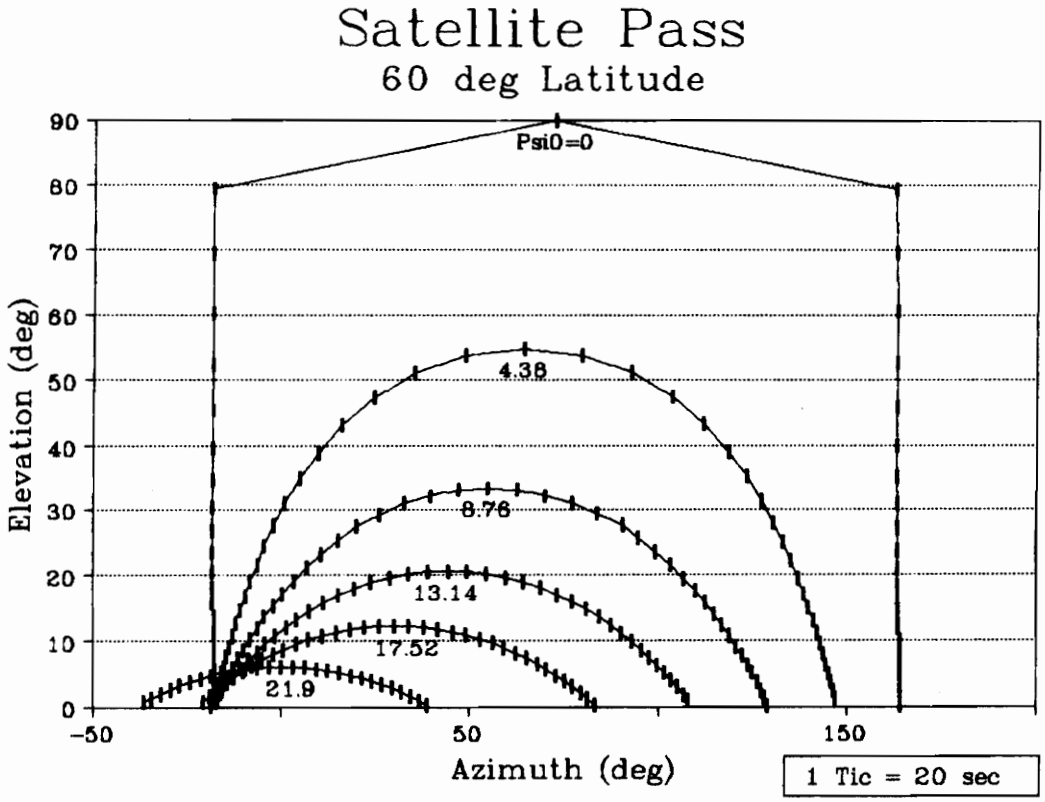

- Look Angles (in Degrees) from Ground Station to Satellite
- Ground Station at 60° North Latitude
- Lower Passes Tend More Toward North

Figure 11: Azimuth-Elevation Trajectories for Ground Station at 60° Latitude

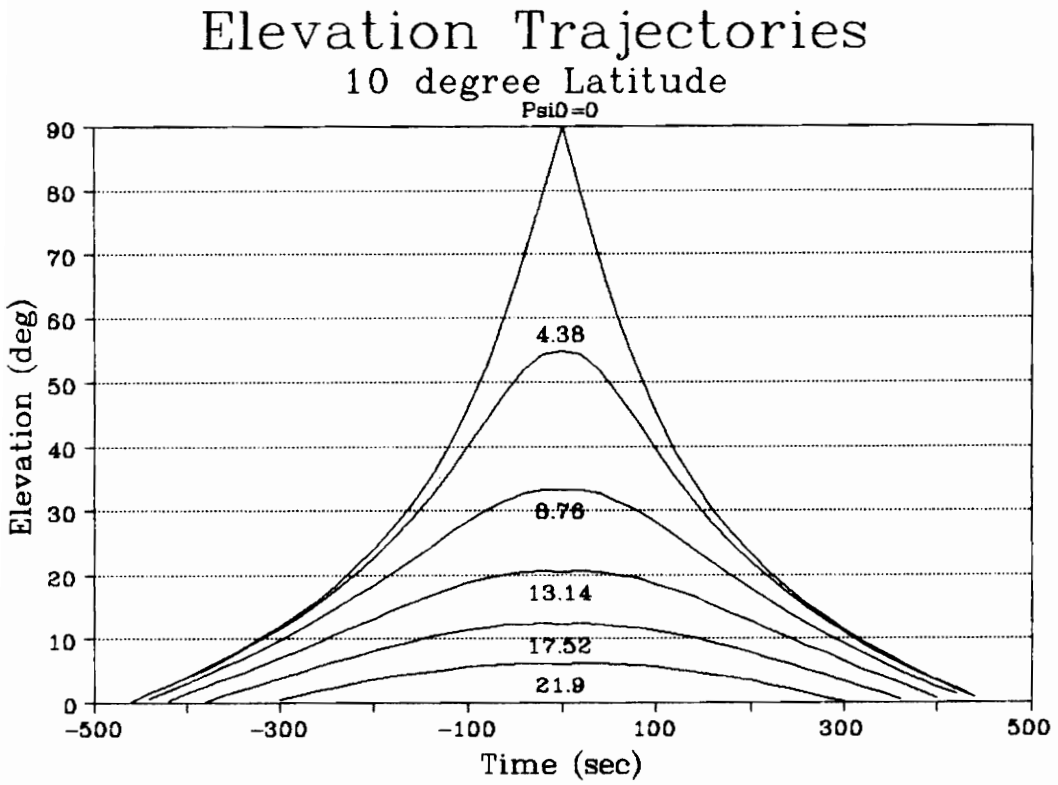

- Elevation Angle (in Degrees) from Ground Station to Satellite
- Ground Station at 1Ø° Latitude
- Satellite in Lower Elevations for Most of the Time it is Visible

Figure 12: Trajectories of Elevation Look Angles from 1Ø° Latitude Ground Station to Satellite for Various PsiØ

because the rotors were too slow for the highest elevation angles would not be that severe in terms of lost time.

3.2.1.2 Azimuth

As mentioned earlier, the azimuth trajectories are sensitive to the latitude of the ground station. Figure 13 shows a typical set of azimuth trajectories for a station near the equator. For passes with a small PsiØ, the rate of change of the azimuth angle is large near the time of closest approach but the rate approaches zero when the satellite is near the horizon. In contrast, when the satellite pass has a large PsiØ, the rate of change is nearly constant.

For the base station, communication to the passes with large PsiØ is more difficult because of the high rate of change of the azimuth look angle. Tracking is made difficult because the rotors move in discrete steps based on equal time intervals. When PsiØ is large, the satellite is likely to move out of the beam between rotor updates throughout the pass. Also, ephemeris errors will cause tracking problems for the low passes because the timing errors will produce large pointing errors. In contrast, tracking passes with small PsiØ during the time

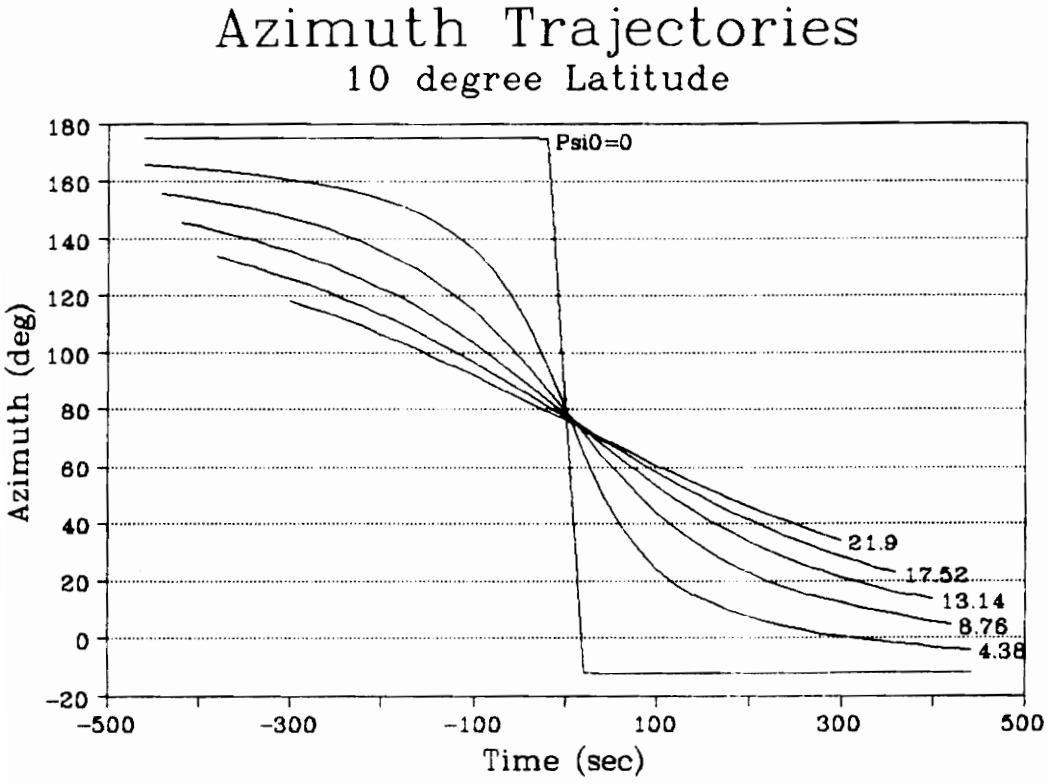

- Azimuth Angles (in Degrees) from Ground Station to Satellite
- Ground Station at 1Ø° North Latitude
- Tracking Rate (Slope) is Highest Near Center of Pass (t=Ø)
- Low Tracking Rates: PsiØ is Small & Satellite is Furthest from t=Ø.

Figure 13: Azimuth Look Angle Trajectories from Ground Station at 1Ø° Latitude for Various PsiØ

that the satellite is near the horizon is simplified because the azimuth look angle changes more slowly. Experience with operating the prototype base station with old ephemeris data showed that the easiest period to operate the satellite was during the low elevation portion of the passes with small PsiØ (i.e. passes that would pass nearly overhead).

For a portable station near the equator, some additional improvement in received signal to noise ratio may be obtained with an antenna with some directivity in the azimuth direction. The antenna beam can be pointed east or west depending on the pass. It may even be fixed, e.g. to always point west, but this means that communications is possible only with about half of the visible passes. For much more northern latitudes, the antenna may be pointed north to give a similar result. For example, if the ground station had azimuth directivity of 120° instead of 360°, then if everything else remains constant the antenna gain will increase by about 4.8 dB. This improvement would come at a cost of missed opportunities for communications. Section 3.3 presents a method for quantifying such costs.

3.2.1.3 Elevation Angles from the Satellite

The elevation angle from the satellite to the ground station is also important for the ground station. PACSAT will use a gravity-gradient boom that will help its antennas remain locally vertical. The elevation angle (measured from the satellite's nadir) can be translated to the gain available from the antenna, when the gain information is known.

A typical set of trajectories for satellite elevation angles are presented in Figure 14. Like the elevation angles from the ground station, this family of trajectories do not significantly change for different ground station locations. Also, the ground station position is typically near the satellite's horizon, which in this case is about 60°.

The elevation angle trajectories of Figures 14 and 12 indicate that the gain patterns typical of vertical dipoles or monopole antennas would be appropriate for both the satellite and the ground station because of the concentration near the horizon. In any event, communications near the horizon appears to be advantageous in terms of increasing the amount of time available for communications.

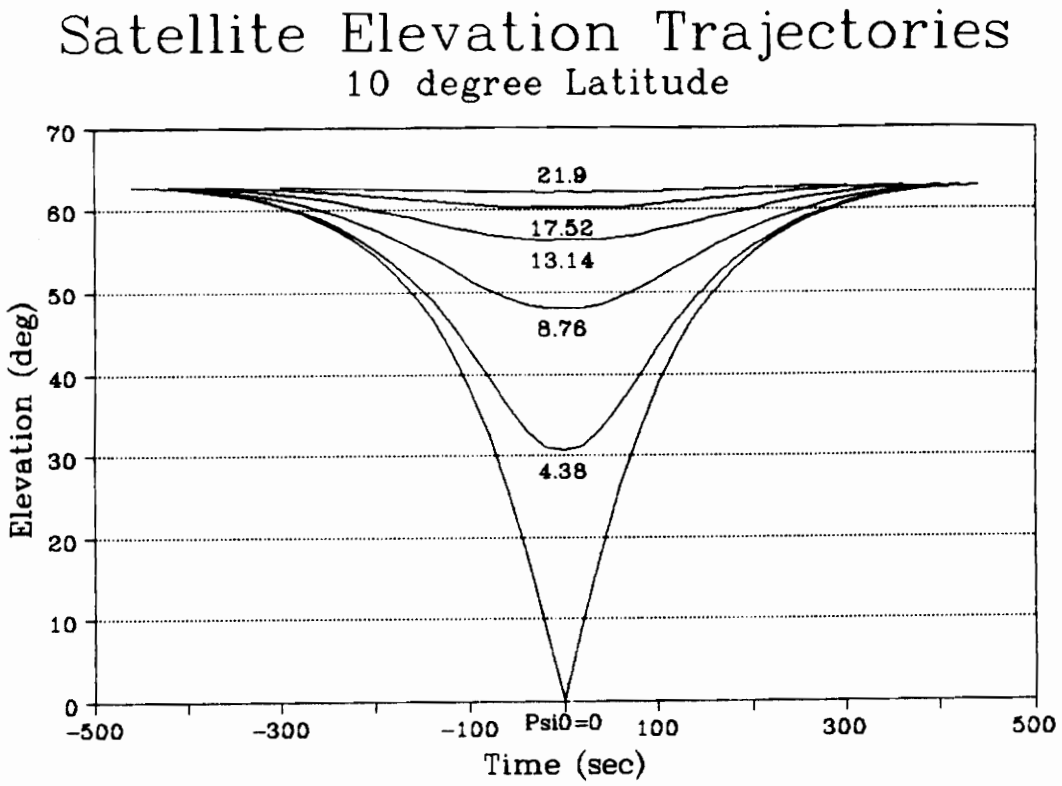

- Elevation Angles (in Degrees) from Satellite Nadir to Ground Station
- Ground Station at 1Ø° North Latitude
- Earth Horizon is at About 63°
- Ground Station Near Horizon Most of the Time

Figure 14: Trajectories for Elevation Angles from the Satellite's Nadir to a Ground Station at 1Ø° Latitude

3.2.2 Path Loss

Figure 15 shows typical path loss trajectories for downlink frequencies of 430 MHz (downlink) and 148 MHz (uplink). These trajectories do not depend much on the latitude of the ground station. There is about a 12 dB difference between worst case and best case path loss; however, the best case is with the satellite directly overhead.

An alternative approach for the portable station would be to use a zenith-directed antenna with a broad beamwidth (such as a turnstile over a groundplane) and concentrate on communications when the path loss is favorable. This approach can achieve about 5 dB of improved performance (assuming that the satellite had a compatible antenna pattern) before the favorable passes occur less frequent than once per day. Furthermore, if both the satellite and ground station used crossed dipoles over a ground plane, then there would be an additional improvement of up to 3 dB from the elimination of the polarization loss. However, because UoSAT3 uses a vertical monopole (which has a null at the satellite's nadir), the gain from reduced path loss would be reduced by the lower antenna gain from the satellite.

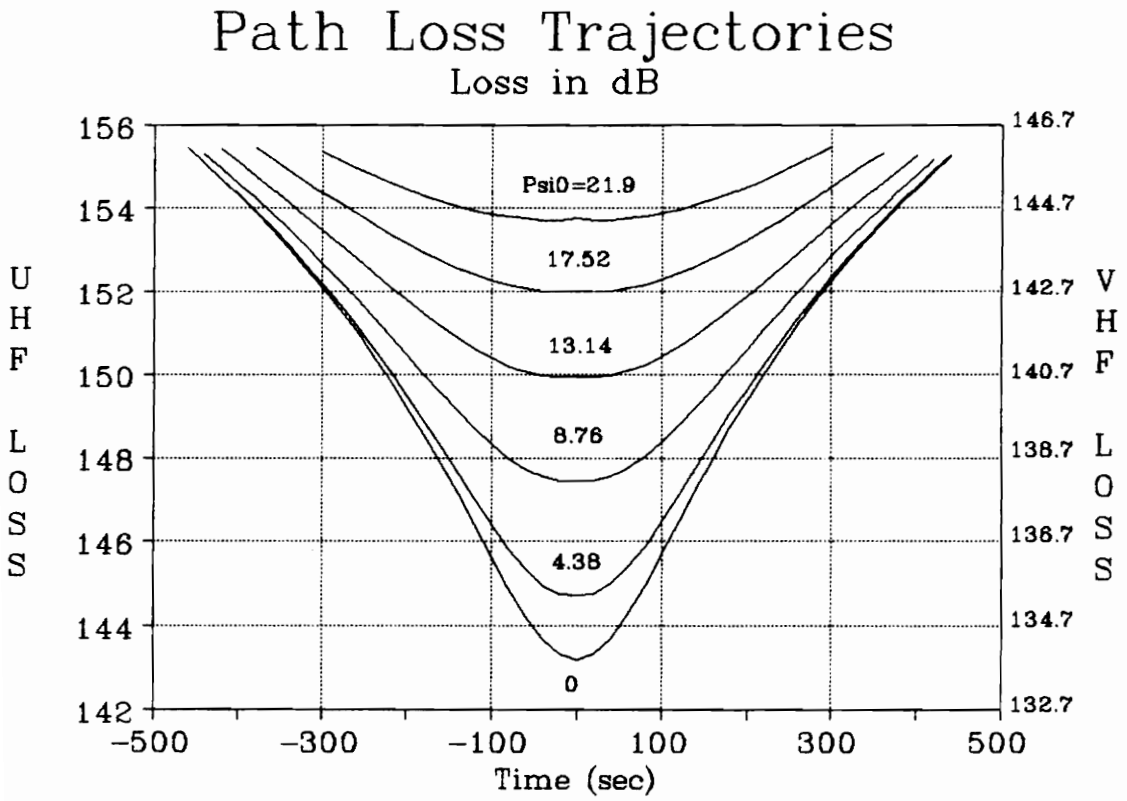

- Path Loss for UHF (430 MHz) and VHF (148 MHz)
- Ground Station at 10° N Latitude
- Reduced Path Loss for Overhead Passes
- For Max Utilization: Design for Max Path Loss (155 dB @UHF)

Figure 15: Typical Path Loss Trajectories for 430 and 148 MHz at Various Psi0

3.2.3 Doppler Shift

For VHF and higher frequencies, the doppler shift for LEO satellites becomes important. Plots of typical trajectories of doppler shifts are presented in Figure 16. These doppler shifts are for the UHF downlink frequency. The uplink doppler shift would follow the same curves except the magnitude would be scaled by about a third. The doppler shifts are affected by the latitude of the ground station because the effect of the earth's rotation (speed of about 460 m/s at the equator) decreases with increasing latitude. However, the effect of latitude is small because the relative speed of the satellite is about ten times the speed of the earth's rotation.

For near passes (small Psi0), the rate of change in doppler is very high (about 100 Hz/sec) near the time of closest approach but the rate of change is nearly zero as the satellite approaches the horizon. For far passes, the rate of change is more constant. Because the base station attempts to tune out the doppler shift by prediction based on time and satellite ephemeris, communications to the satellite is easiest for low Psi0 passes, but when the satellite is near the horizon. This result is also compatible with the experience of operating the prototype base station.

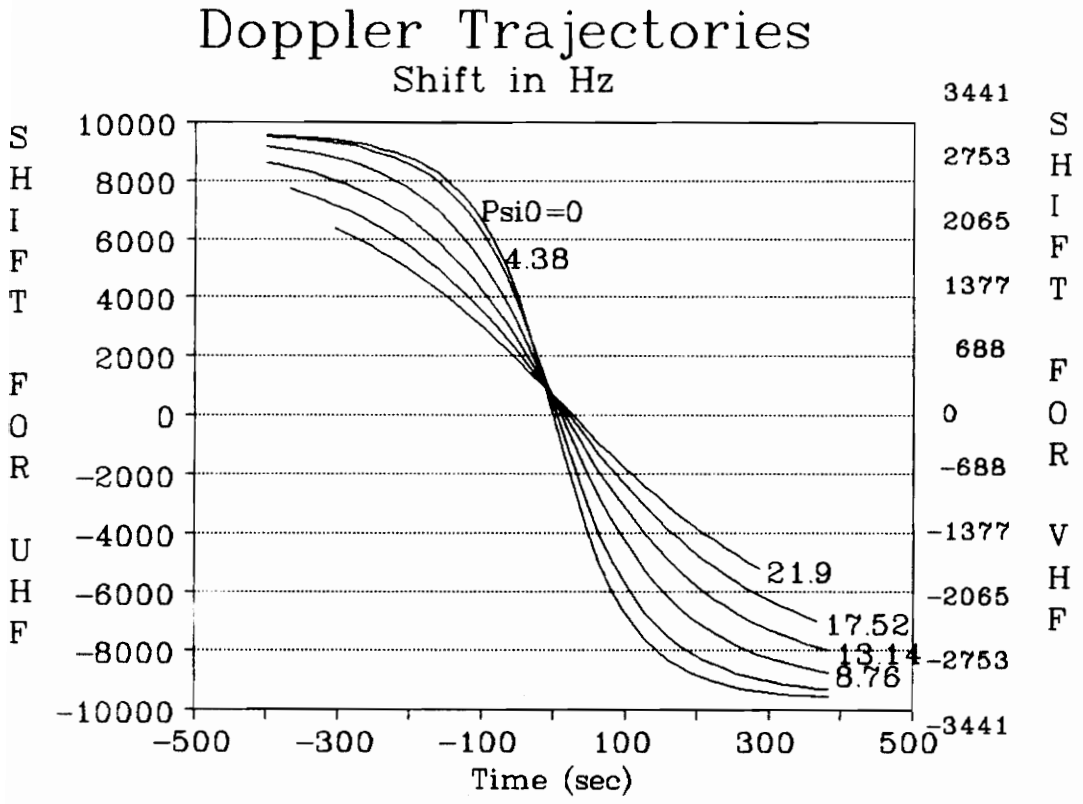

- Doppler: UHF(430) & VHF(148) MHz
- Ground Station at 10° N Latitude
- Max Doppler Rate (Slope) @t=0
- Lo Rates: Small Psi0 & Large t
- Doppler @t=0: Earth Rotation

Figure 16: Typical Doppler Shift Trajectories for 430 and 148 MHz at Various Psi0

By using a closed loop tuning approach which corrects the transceiver tuning by a measured tuning error instead of a predicted tuning error, the portable station is less affected by the rate of change in doppler.

3.2.4 Polarization Loss

The signal received from an antenna will depend on the polarization match between the signal and the antenna as well as the power gain pattern. Thus, a complete analysis of a link budget needs to include polarization loss. For the base station, this analysis is simplified by deliberately mismatching a linearly polarized signal with a circularly polarized antenna: the result is a constant 3 dB loss independent of the orientation of the signal polarization or the sense of the antenna polarization. Although considerable, the 3 dB loss is not easily regained without risking occasional deep fades due to polarization mismatch caused by satellite motion or by Faraday rotation. For example, circular polarization for both ends is a way to avoid Faraday rotation. However, circular polarization is difficult to achieve except in a limited beamwidth: outside that beamwidth the polarization will become more elliptical and may even switch its sense.

Thus, in order to get the full benefits of circular polarization, tracking antennas will be needed at both ends of the link. In contrast, small PACSAT satellites will most likely use antennas with broad fixed beamwidths.

Including polarization mismatch effects in the orbital analysis requires coordinate transformations to compare the relative orientations of the different antennas. Because the UoSAT3/PACSAT uses VHF and UHF links on which Faraday rotation is expected to dominate any geometric effects, a complete analysis was not done. Such an analysis would be more relevant for satellites with microwave links where Faraday rotation is less.

An estimate of the polarization loss from geometric considerations was made by computing a polarization loss caused by the difference in tilt of the local horizontal planes at the satellite and the ground station. This tilt angle is the angle Psi, the earth-centered angle between the ground station and the satellite. Figure 17 shows the polarization loss due to this tilt difference alone. Under this assumption the polarization loss due to differences in the tilt is less than a decibel.

The actual polarization loss will depend on the orientation of the antenna within the horizontal plane. The orbital analysis should be expanded to include orientation effects of the orbit so that the polarization

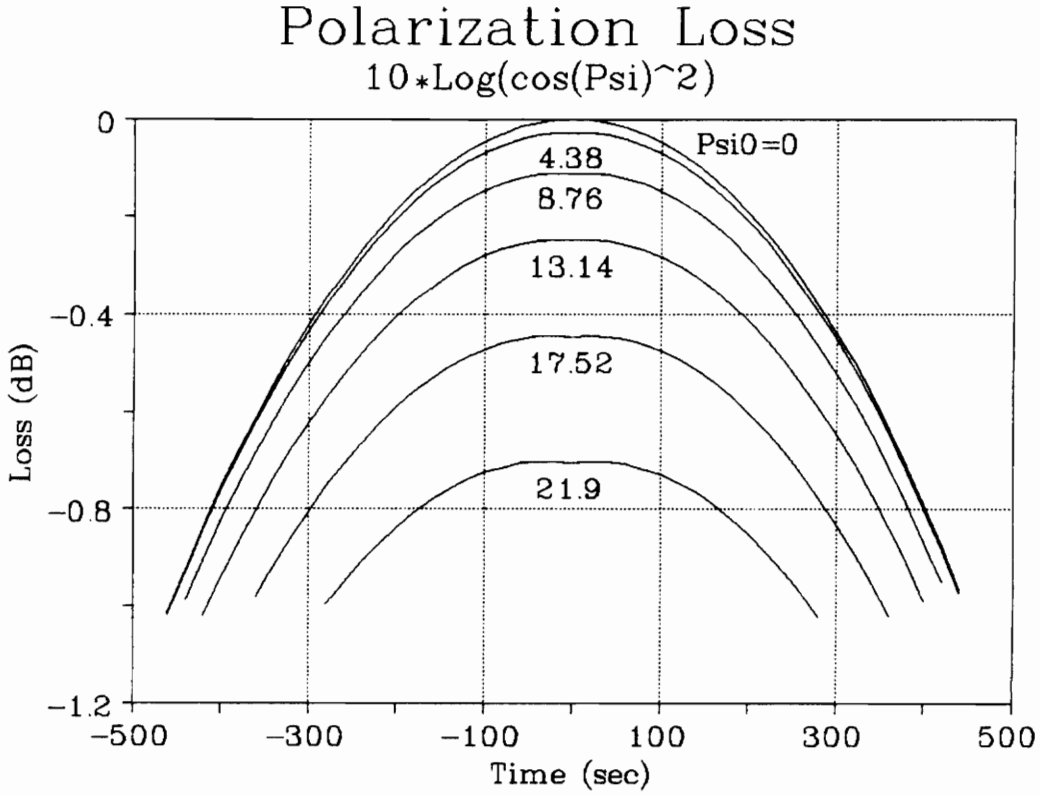

Figure 17: Polarization Loss Example

is fully accounted for, especially for microwave links. The analysis will be specific to particular antenna systems and pointing schemes.

Note that if the satellite and ground station both use vertical polarizations, then there is no mismatch because the antenna axes will always be coplanar.

3.2.5 A Trajectory Application: A Dynamic Link Budget

One potential application of the trajectory information presented in this section is to study a dynamic link budget for the PACSAT link. The dynamic parts of the link budgets presented in Chapter 2 are path loss and antenna gains. Secondary effects such as pointing errors due to high antenna slew rates or additional margins required for large tuning errors may also be included. Such a dynamic link budgets would also include polarization mismatch losses if the operating frequency is high enough (e.g., microwave) so that the random Faraday rotation can be ignored. For a particular satellite orbit, the path loss trajectories are independent of ground station design, but the other quantities in the link budget are very much dependent on

the choice of antennas, rotors, and transceivers used on both the ground station and the satellite.

As mentioned in Section 2.3, dynamic link budgets will be useful to predict performance in terms of how long and how often specific link margins for reliable communications will be exceeded. Since PACSAT ground stations with daily throughput requirements may not need to use the entire duration of the satellite passes, certain design simplifications may be possible while still meeting the throughput requirements. Because of the packet communications techniques used in PACSATs, the communication link can tolerate systematic fades (in the middle of a pass, for instance) and thus allow further simplifications of the link design.

For the specific case of the prototype PACSAT ground stations and the UoSAT3/PACSAT satellite, the primary dynamic effects are the path loss and antenna gains. The required antenna gain patterns of the satellite and ground stations are not available; however, the dynamic part of the link budget can be illustrated by assuming that the satellite and the portable station use vertical half-wave dipoles and the base station antenna gain is constant. These assumptions are for illustration only: while the portable station and the satellite use vertical monopoles, the patterns may be significantly different from the ideal

dipole pattern. For this approximation, the normalized pattern of a thin wire dipole was used:[19]

$$G(\theta) = \left[\frac{\cos(\pi l \cos(\theta)) - \cos(\pi l)}{\sin(\theta)} \right]^2,$$

where l is the length of the dipole in wavelengths and θ is the angle measured from the antenna axis. This pattern is normalized so that the peak gain is 1 and thus the actual peak gain (with respect to an isotropic radiator) of the antenna would have to be added as a fixed constant.

The dynamic part of the link budget for the base station with the above assumptions is presented in Figure 18. Note that only the dynamic part of the link budget is presented: the strictly static parts such as peak antenna gains, transmitter power, and receiver sensitivity are not included. The prominent effect of the vertical monopole is the deep fading that will occur when the satellite is nearly overhead (i.e., both time and PsiØ are small). The figure also shows that the minimum loss in signal power is only three decibels less than the signal power loss when the satellite is at the horizon, which is where the curves start. As shown in section 2.3, the base station has a margin of about nine decibels so that the deep fade on the

overhead pass will cause less than a minute of signal loss and thus it is not a major concern.

Figure 19 shows the effect on the dynamic budget when both antennas are vertical dipoles. This case corresponds to the portable station. Since the static link budgets for the portable station indicated low margins at 1Ø° in elevation, the curves in this Figure start when the satellite is 1Ø° above the horizon. For this arrangement, the loss at 1Ø° is only about a decibel more than the minimum loss. Furthermore, compared to the base station model, the fading will be longer and will occur for a wider range of PsiØ. The result is discouraging for the use of monopole whips for the portable station; however, this result is based on modeling the antennas as half wave dipoles. Vertical wire antennas can be designed to have gain patterns directed toward the higher elevations. Such designs are likely to result in less overall loss during parts of the passes as well as more static gain.

3.3 Distributions

The results of characteristics for the passes presented in section 3.2 can be generalized by information about the distribution of PsiØ over many passes. The

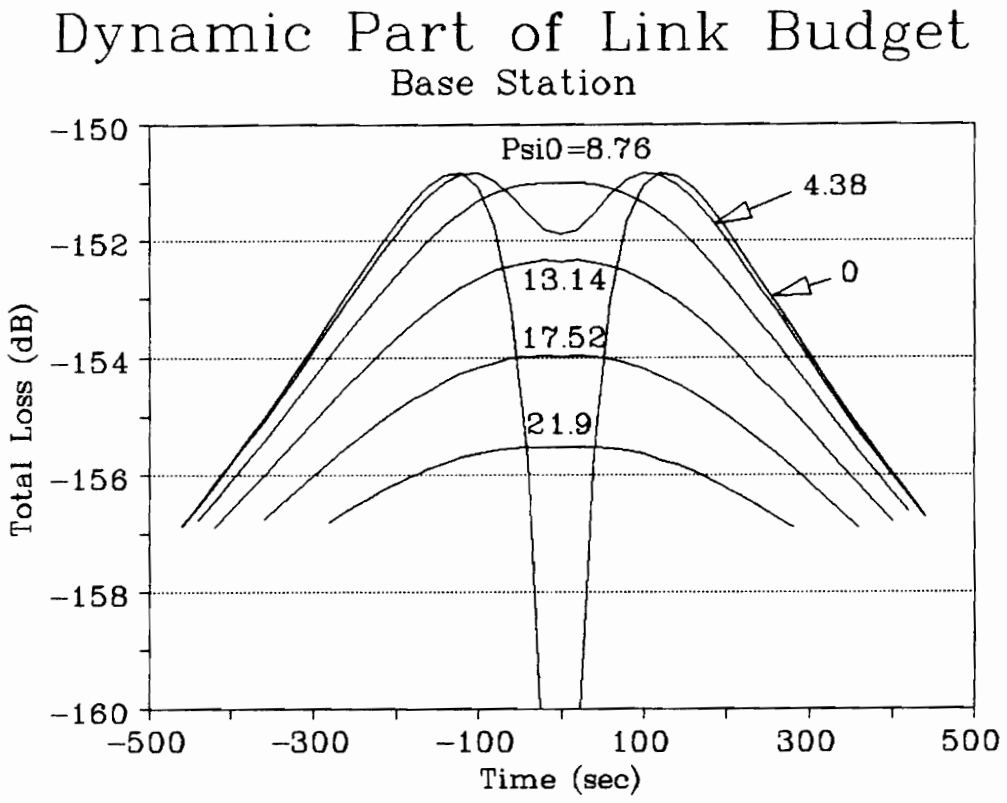

- Path Loss + Antenna Gain
- Constant Gain from Base Station Antenna, Ideal Half-Wave Dipole at Satellite
- Deep Fading Only For Satellite Directly Overhead

Figure 18: The Dynamic Part of the Link Budget for a Base Station and a Half Wave Dipole at the Satellite

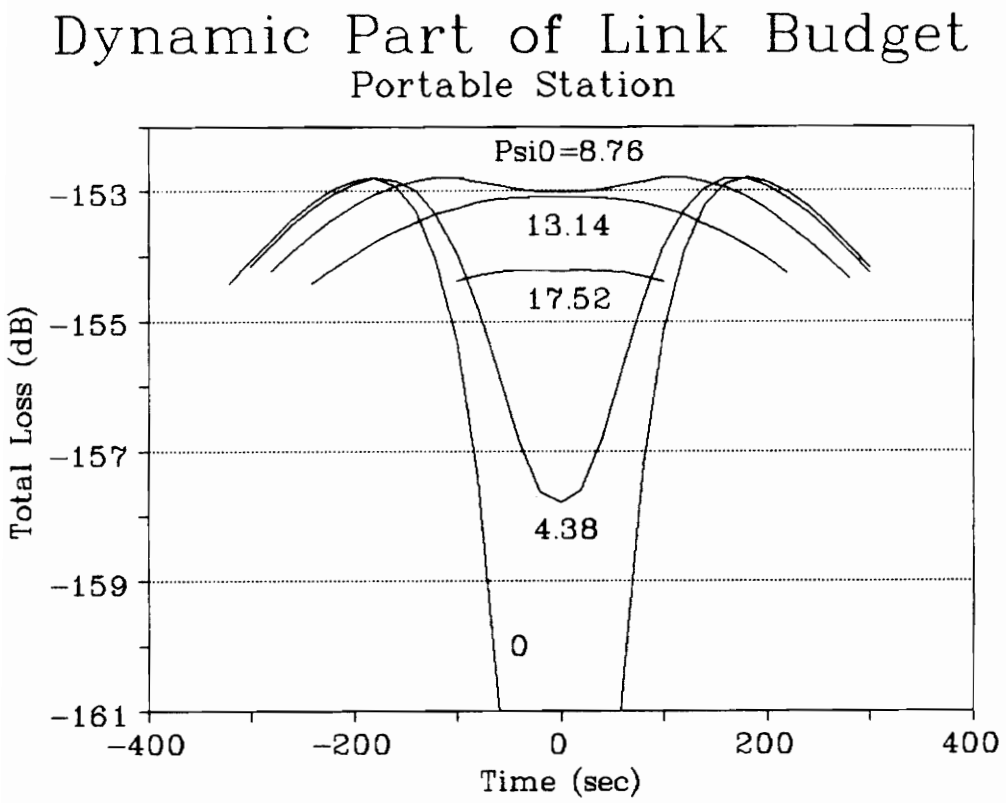

- Path Loss + Antenna Gain
- Ideal Half-Wave Dipole at Both the Satellite and Portable Station
- Trajectories Begin at 1Ø° Elevation
- Limited to Only About 1.5 dB Less Loss, and Fades are Deep and Long

Figure 19: The Dynamic Part of the Link Budget for Half Wave Dipoles at both the Satellite and the Portable Station

approach is to simulate the motion of the satellite over ten thousand orbits (approximately two years). The simulation of the satellite motion is carried out by moving the longitude of the ascending node (where the satellite passes the equator on its way north) of the orbital plane through increments determined by the earth's rotation and the nodal regression over the period of the satellite's orbit. The required results are computed once per orbit. This part of the analysis is presented in more detail in Appendix section A-5.

For a spherical earth, the orbital plane will stay fixed with respect to the fixed stars so that the earth rotates through the orbital plane. Because of the oblateness of the earth, the orbit is perturbed so that the orbital plane will precess, causing the position of the ascending node to move with respect to the celestial sphere. The effect of this nodal regression is illustrated in Figure 2Ø. When there is no precession, the orientation of the orbital plane with respect to the celestial sphere will not change as the Earth orbits the Sun as shown in Figure 2Øa. With nodal regression, the orbital plane rotates with respect to the celestial sphere as shown in Figure 2Øb. For certain choices of satellite altitudes and inclinations, the nodal regression can be made to make the orientation of the orbit with respect to

the Sun be constant. Such orbits are called solar synchronous because the satellite passes a ground station during the same period of the day throughout the year.[20] The UoSAT3/PACSAT is an example of a solar-synchronous satellite.

For each orbit, Psi∅ is computed and then recorded when it is less than the maximum Psi∅ visible from the ground station. A histogram of these Psi∅ angles is then compiled and the mean and standard deviation is computed. The number of nonvisible passes between the visible passes was also recorded. Furthermore, it was a simple task to extend the analysis to compute the time that the satellite was visible to a ground station when the ground station has a specified limitation on usable elevation angles.

3.3.1 Psi∅ Distributions

Figure 21 shows the distribution of Psi∅ for a ground station that is at 1∅° latitude. This latitude is typical for a portable station. For this ground station, the distribution is nearly uniform over all of the possible Psi∅ values. When the elevation limits are set from ∅° to 9∅°, about 31% of the orbits are visible. If a crossed dipole antenna over a ground plane were used, then the

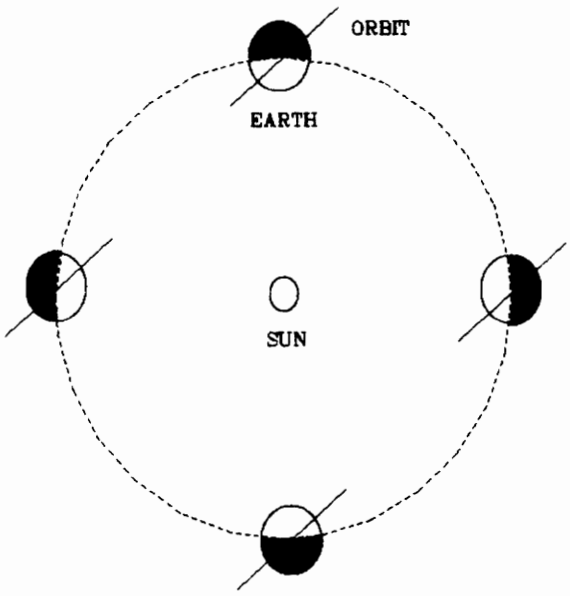

a) No Precession -- View From North

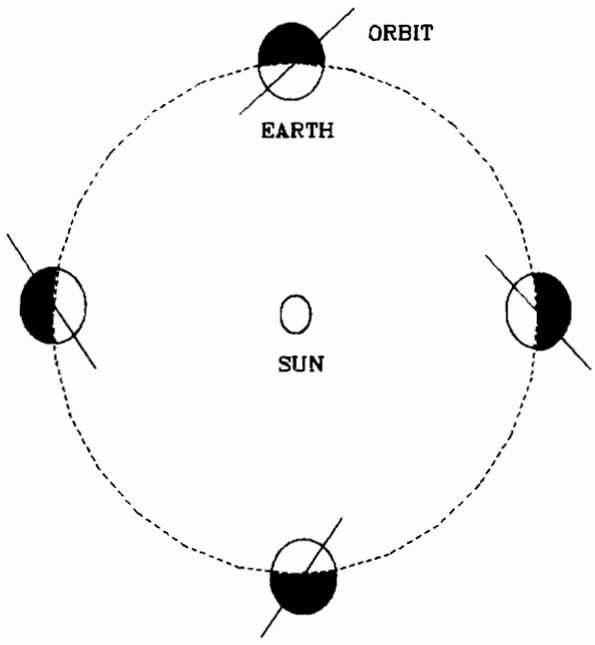

b) Precession From Oblate Earth

Figure 2Ø: Nodal Regression of the Orbital Plane as a Result of Perturbations from Earth's Oblateness

elevation limits may be from 2Ø° to 9Ø° in which case only 15% of the orbits would have visible passes. Half of the visible passes produce elevation angles of not more than 2Ø°.

Figure 22 is a distribution for a ground station at 4Ø° latitude, which is typical of a base station. Again, the distribution is approximately uniform. If a crossed dipole antenna over a ground plane were used, about 2Ø% of the orbits would have visible segments. As the latitude of the ground station increases, the distribution begins to favor the higher PsiØ and more orbits will have segments that will be visible by the ground station.

The uniform distribution of PsiØ for the more likely positions of the PACSAT ground stations makes interpretation of the above trajectories simpler. Since the trajectories were computed at equal steps of PsiØ, trajectories falling between any two adjacent plots would be equally likely. For example, in the look angle trajectories presented in Figure 9 there are six regions bound by the six plotted trajectories plus the horizon. Since four of this regions contain passes that do not exceed about 35° in elevation, the uniformity in PsiØ distributions implies that about 67% of the visible passes will not exceed 35° in elevation.

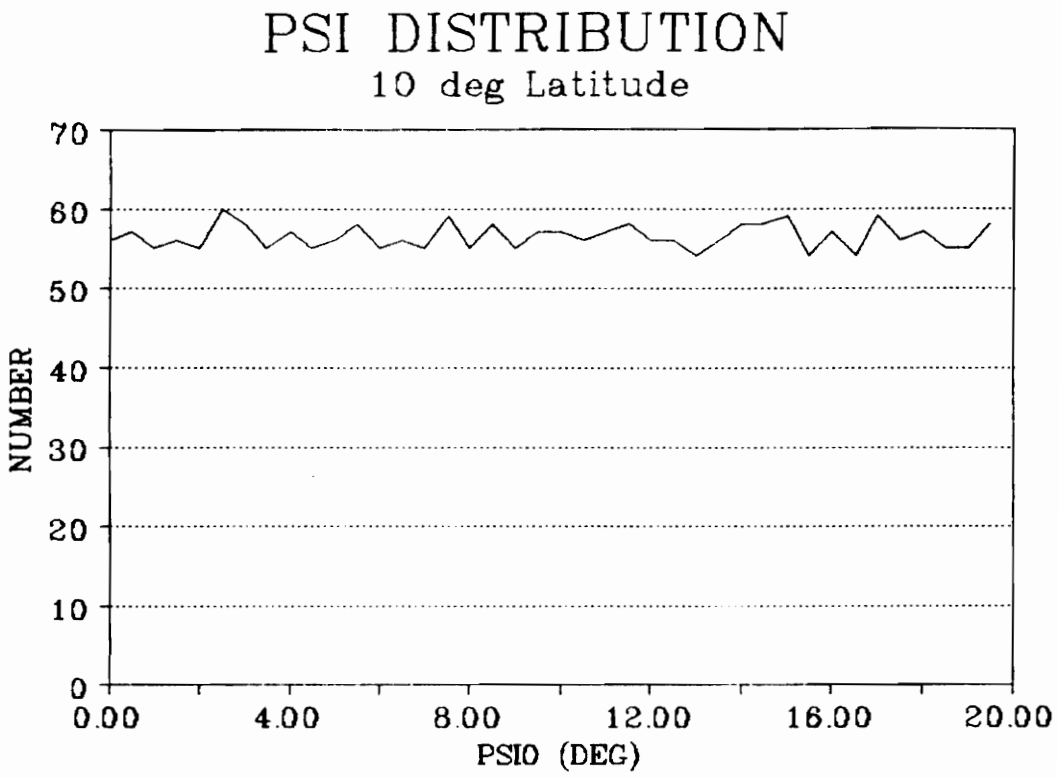

- Distribution of Psi∅ over 1∅,∅∅∅ consecutive orbits (about 2 years)
- Uniform Psi∅ Distribution for Ground Station near Equator
- For Solar-Synchronous 8∅∅ km orbit (UoSAT3)

Figure 21: Psi∅ Distribution for 1∅° Latitude

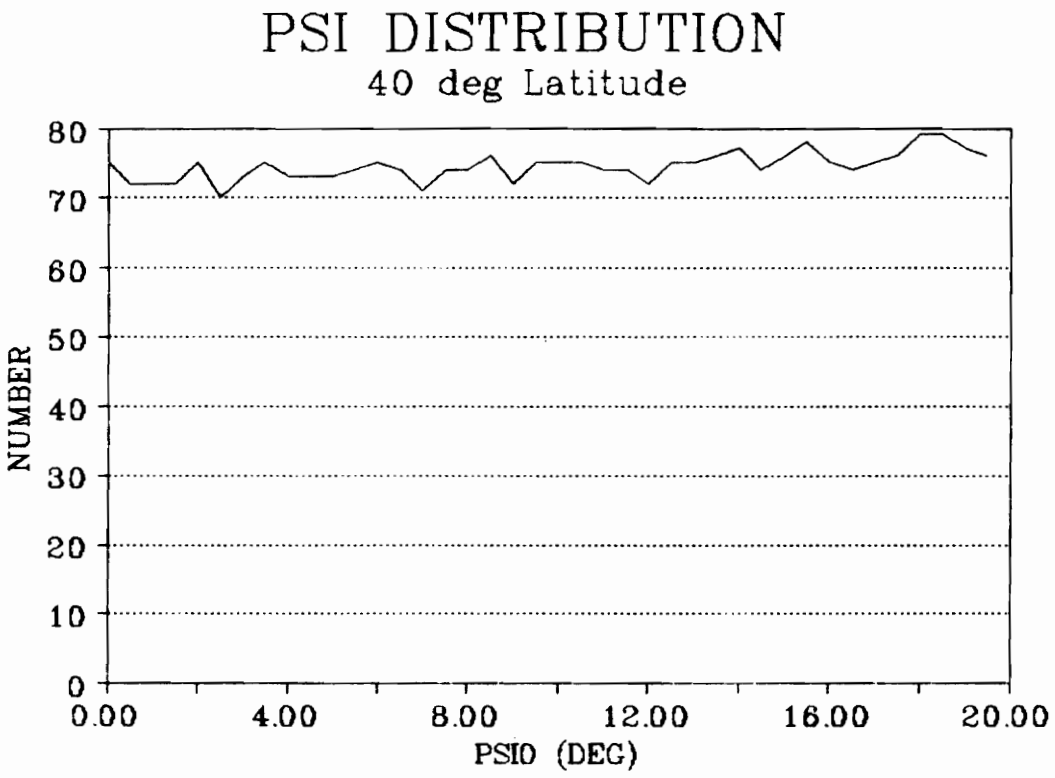

- Distribution of Psi0 Over 10,000 UoSat3-type Orbits
- For Ground Stations at Higher Latitudes:
  - Larger Psi0 are More Likely
  - Generally, More Orbits Are Visible
- For Ground Stations at 40° Latitude:
  - Psi0 Still Uniformly Distributed
  - About 24% More Orbits Are Visible

Figure 22: Psi0 Distribution for 40° Latitude

Uniform distribution arises in spite of the fact that the orbital plane passes over the ground station at about the same time every day because the orbital period is such that the satellite is in different parts of its orbit when the plane passes the ground station. It is possible to select an orbit where the satellite passes are synchronized with the nodal regression. The resulting distributions would not be uniform and would be dependent on longitude as well as latitude of the ground station.

3.3.2 Visibility Distributions

Distributions of visibility times and the number of orbits between visible passes were computed for the PACSAT ground stations in typical situations. The results are particularly important for the base station where visibility to the satellite must be maximized.

There are two aspects to the time distributions: visibility duration and visibility delay. The visibility duration distributions concern the relative frequencies of occurrence for specific durations given that the satellite is visible. The duration information is presented in pie chart form because it presents both density and cumulative information. The visibility delay concerns how many

orbits must occur before the satellite will be visible again. The delay distribution is presented as a histogram, but the delay is in terms of number of orbits. The number of orbits can be multiplied by the period to get a time delay, but an additional half period must be added if the two passes occurs at opposite times of the day.

3.3.2.1 Portable Station

The portable station typically would be near the equator and would use some sort of antenna that would have restrictions on elevation angles. Figure 23 shows the distribution of the durations of visibility for an ideal ground station that can communicate whenever the satellite is above the horizon. The distribution shows that the long duration passes are more likely than the short duration passes. As noted before, about 31% of the orbits have visible segments for such a ground station. The average visibility duration is about twelve minutes.

Figure 24 shows the distribution when the elevation angle is confined between 5° and 30°, which corresponds to the pattern of a vertical dipole. About 25% of the orbits have segments visible to the ground station, and the

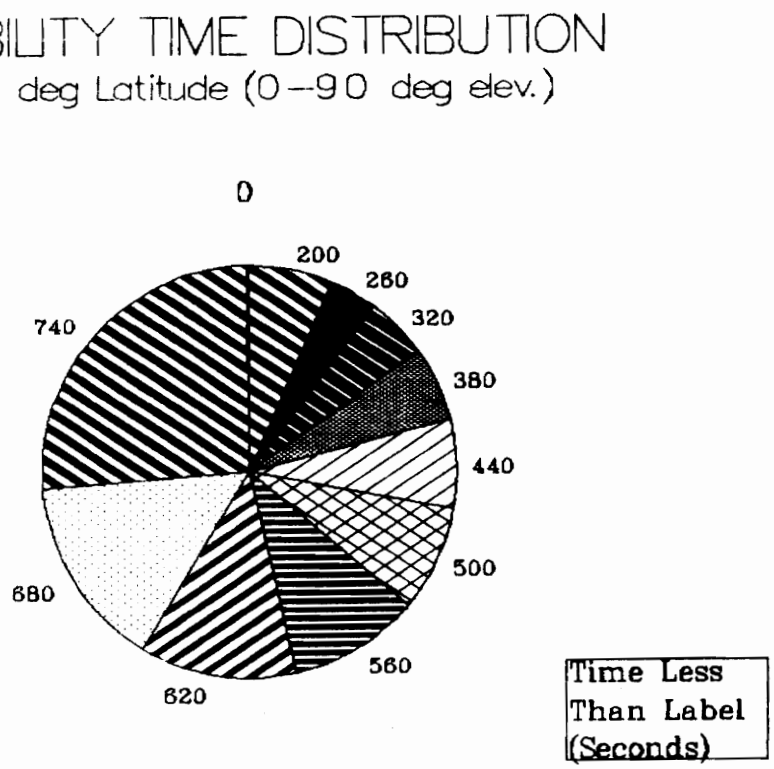

- Elevation Angles Limited only by Horizon
- More Than 25% of Visible Passes Have Durations of Greater than 680 Seconds
- Most Passes Exceed 3 Minutes in Duration

Figure 23: Duration Distribution for Ideal Ground Station (No Elevation Limit) at 10° Latitude

medium durations are favored. The average duration of visibility is reduced to about eight minutes from the twelve minutes of the ideal ground station.

Alternatively, a pattern such as that from a crossed dipole antenna over a ground plane would have a minimum elevation angle of about 20°. Figure 25 shows that for such an antenna, only 15% of the orbits would have visible segments and the average visibility time falls to about six minutes. The distribution of durations in Figure 25 show that the longer durations are slightly favored over the shorter ones.

From considerations of visibility, the portable station would benefit from an antenna pattern directed to the horizon. However, a more zenith-directed pattern will still result in considerable durations for communications. For a low throughput ground station, a limitation of as little as two minutes of visibility a day may be acceptable.

3.3.2.2 VITA Base Station

To maximize visibility to the UoSAT3 satellite, the ground station should be located as far north (or south) as possible and there should be line-of-sight visibility

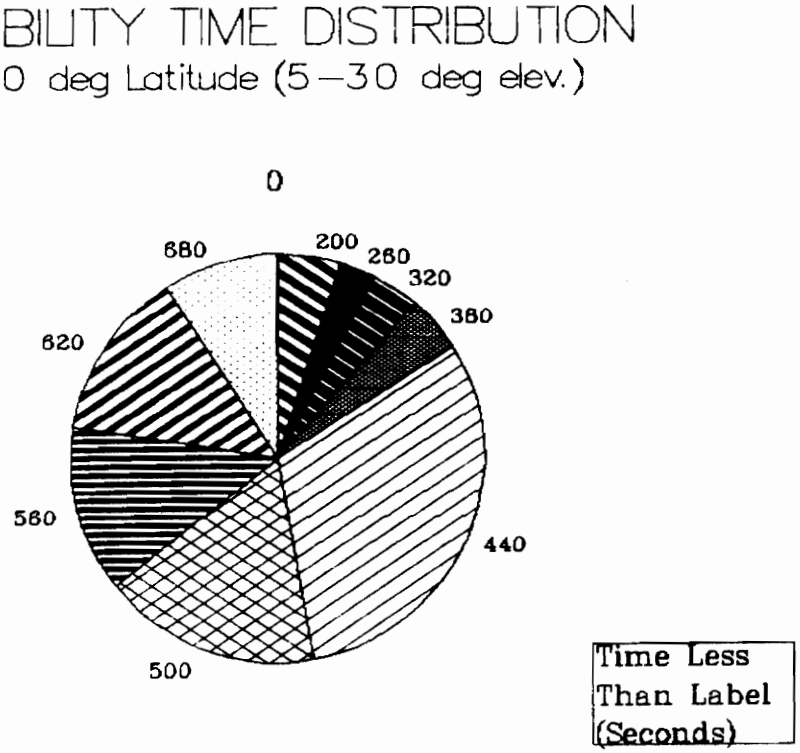

- Typical Elevation Limits for Vertical Whip
- Fewer Long Duration Passes
- Most Passes are Longer than 3 Minutes

⟹ Feasible Approach for Portable Stations

Figure 24: Duration Distribution for Vertical Dipole at 10° Elevation Angle (5°-30° Elevation Limit)

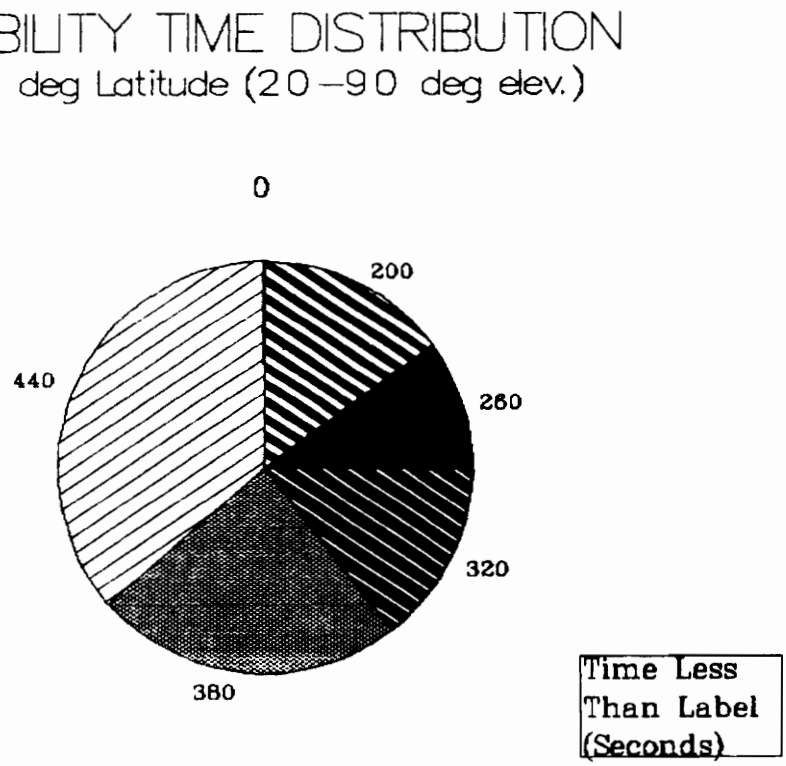

- Possible Elevation Limits for Horizontal Dipole over Ground Plane
- Long Duration Passes are Eliminated
- Most Passes are Longer than 3 Minutes, but Fewer than for Vertical Whip
- Feasible Approach for Portable Stations, but Compatible Satellite Required

Figure 25: Duration Distribution for 20°-90° Elevation Limit at 10° Latitude

to as near the horizon as possible. VITA headquarters in Washington D.C. is less than ideal because it is not very far north, and the surrounding buildings block off most of the low elevations.

For an extreme example, limiting the elevation angle to a minimum of 35° results in the distribution of visibility times shown in Figure 26. The average duration would be about 3.5 minutes and only 12% of the orbits would have visible segments.

Furthermore, the visibility delay distribution shown in Figure 27 indicates that there may be delays of up to a day and a half between visible passes. The length of time of the delay is approximately the number of orbits multiplied by the period, but if the satellite passes occur during the opposite general time of day (e.g., morning versus evening) an extra half period must be added since the satellite is seen during opposite halves of its orbit.

In contrast, if a portable station were used in the same area but where it had visibility to near the horizon, the resulting distributions of Figures 28 and 29 would result. The average duration is eight minutes and 34% of the orbits have visible segments.

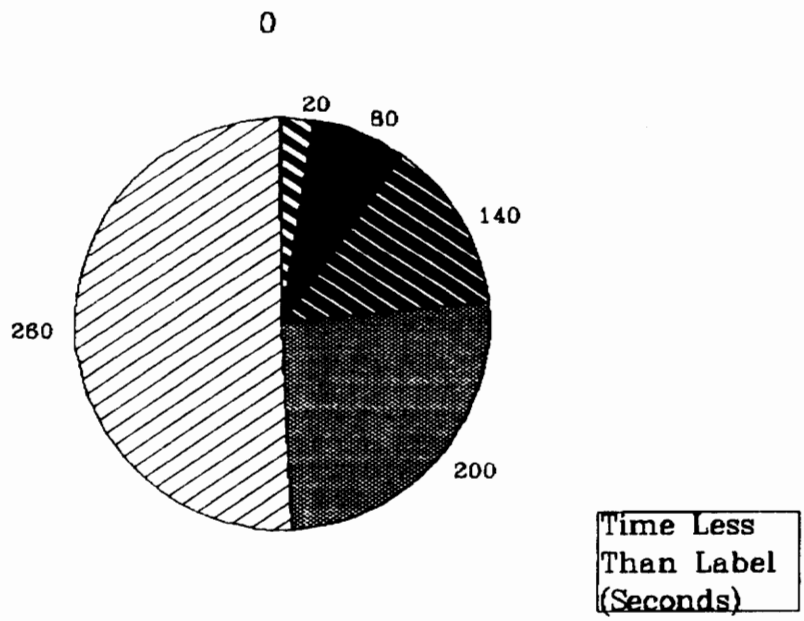

- Severe Elevation Limits from Geography and Noise
- Durations are Marginally Acceptable for Portable Station
- This Arrangement is Unacceptable for a Base Station

Figure 26: Visibility Duration Distribution for a Station at 40° Latitude and with a 35° Minimum Elevation Limit

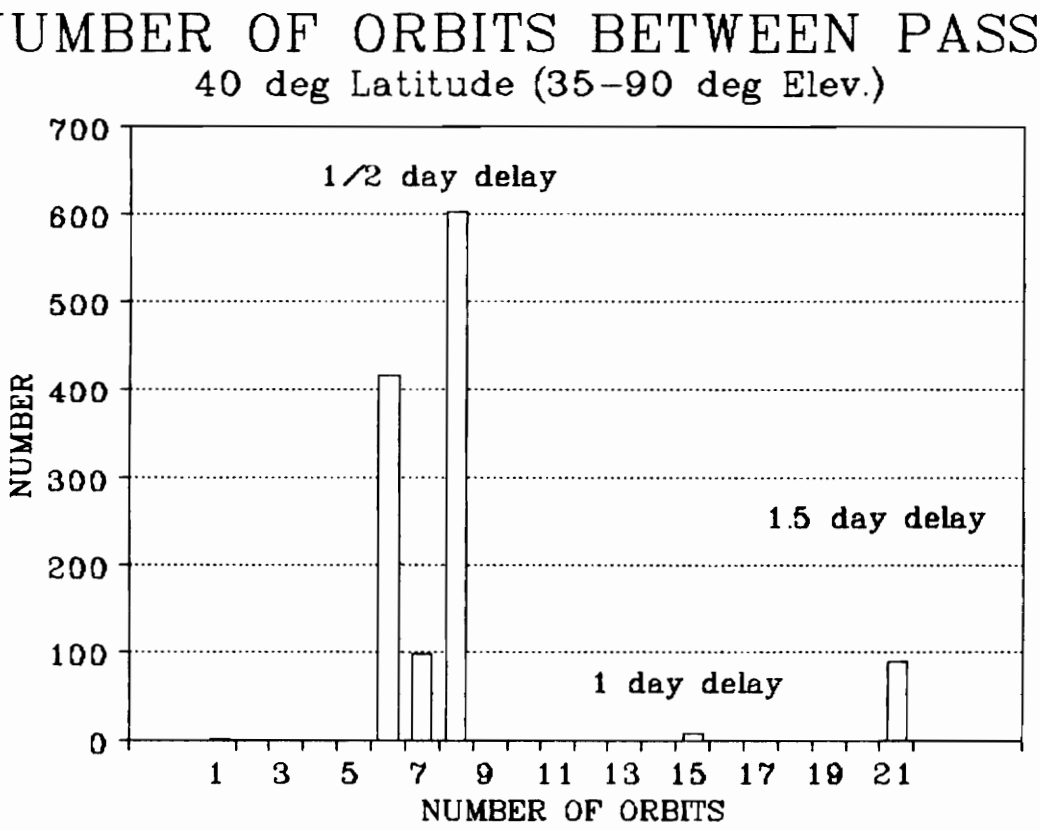

- Number of Orbits One Must Wait Before the Next Visible Pass -- About 14 Orbits per Day for UoSAT3
- One Day Delay too much for Base Station
- 1.5 Day Delay too much for Portable
- Access to Low Elevations is Essential!

Figure 27: Visibility Delay For a Station with a Minimum Elevation Limit of 35° at 40° Latitude

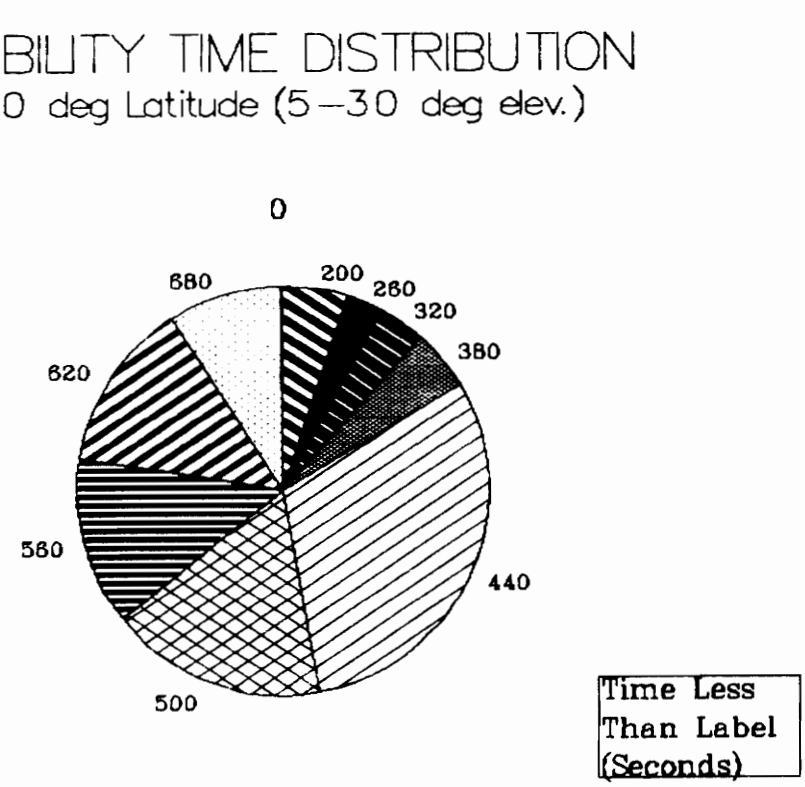

- Vertical Whip for 40° Latitude
- Similar to 10° Latitude Case
- Significantly Better than When Low Elevations are Blocked.

Figure 28: Visibility Duration for a Station at 40° Latitude and with a 5°-30° Elevation Window

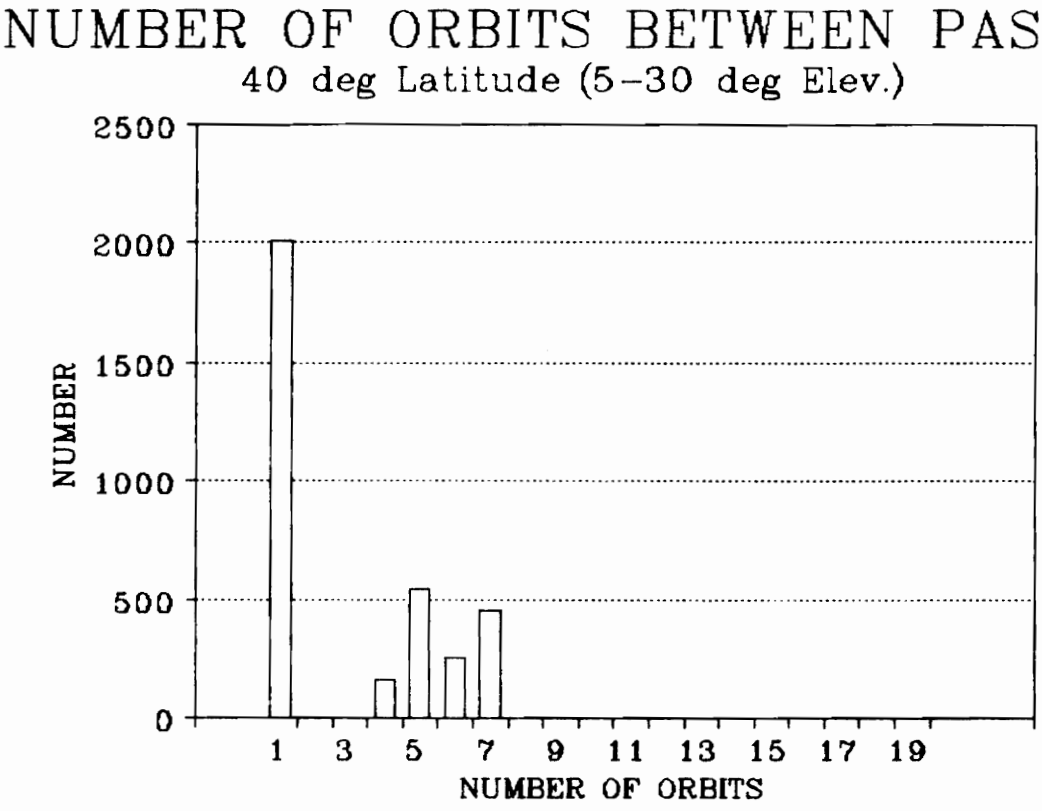

- Number of Orbits One Must Wait Before the Next Visible Pass -- About 14 Orbits per Day for UoSAT3
- Vertical Whip for 40° Latitude
- Never Longer Than a Half Day Delay
- Three Times as Many Visible Passes

Figure 29: Delay between Passes For Station at 40° Latitude and with a 5°-30° Elevation Window

Clearly, there is considerable advantage in locating the base station antenna so that it can communicate when the satellite is close to the horizon.

3.4 Orbit Prediction

As a result of the experience gained in the analysis of satellite orbits, writing a tracking program that predicts satellite position, given the satellite ephemeris, is relatively straightforward. Most of the equations are provided in The Satellite Experimenter's Handbook; however, an additional equation for computing the position of vernal equinox is required to find the longitude of the ascending node at the epoch time (i.e., the time at which the given satellite position occurred). An equation for the position of the vernal equinox is available in Satellite Communications by Pratt and Bostian.[21]

The resulting tracking program is not as sophisticated as programs such as Quicktrack, which may include the perturbational effects of the Sun and Moon. However, with two month old ephemeris, the simplified tracking program predicted satellite positions that were about two minutes off from Quicktrack's prediction. Note

that an operational PACSAT network will include automatic ephemeris updating so that the ephemeris data could be kept less than a week old, if necessary. In terms of accuracy, the simplified program appeared to give better results with the abnormally old ephemeris. In one case, the simplified program predicted a low pass that occurred but was not predicted by Quicktrack. The success of the tracking program helps to verify the above analysis since essentially the same equations were used.

A typical UoSAT3 ground track over a day was computed from the simplified program and is presented in Figure 3Ø.

3.5 Analysis Conclusions

The primary result from this analysis is the importance of communications at low elevation angles. The antenna pattern of the portable station is compatible with effective operation of the satellite. For the longest visibility windows, the base station antenna should be able to communicate as close to the horizon as possible.

Due to the rate of change of doppler shifts and look angles, the open loop tracking methods of the base station may have trouble tracking low elevation passes or high elevation parts of high elevation passes when the

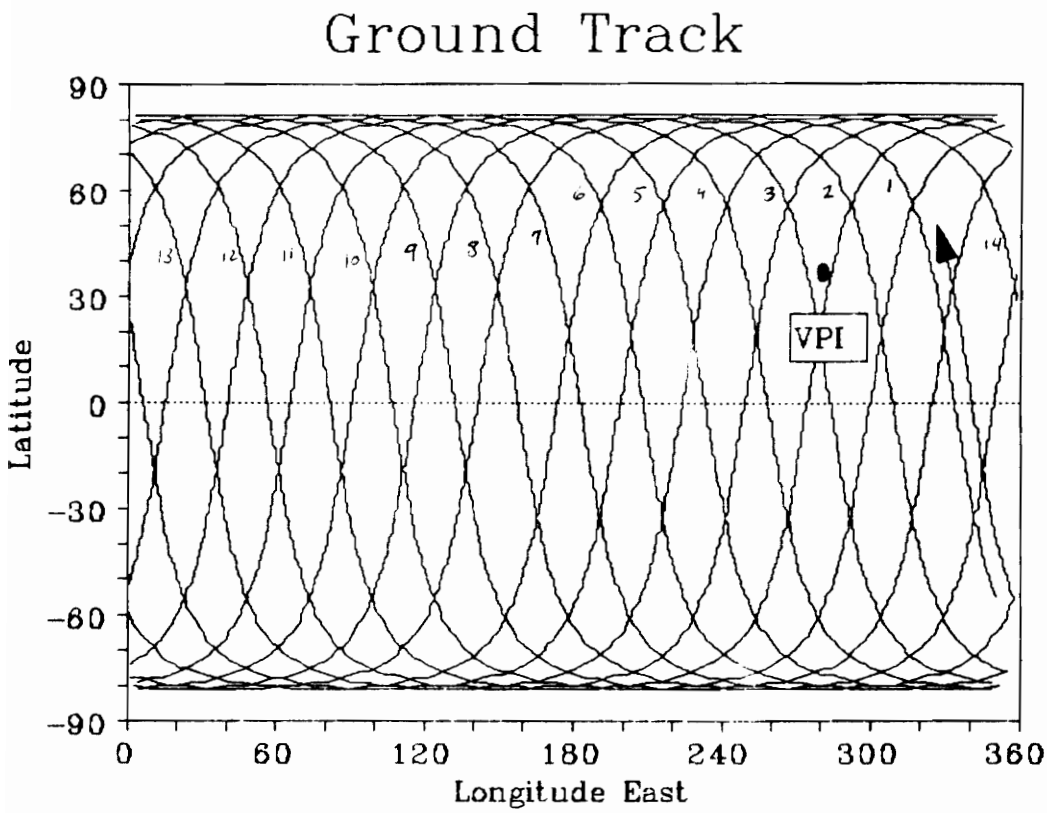

- Ground Trace of UoSAT3 over a 24 hour duration
- Mean Motion is about 14.3 orbits per day
- Simpler tracking software

Figure 30: Typical UoSAT3 Ground Track over 24 Hours

ephemeris data is old. The least difficult parts to track are the low elevation parts of the high elevation orbits.

An alternative approach of using crossed dipoles on both the portable station and the satellite has considerable advantages from reduction of both path loss and polarization loss. The visibility durations for such antenna patterns should be more than sufficient for portable ground stations with low throughput requirements.

Chapter 4

An Analysis of the CPFSK for PACSAT

PACSAT uses a 9600 baud modulation technique that is becoming popular for amateur radio operation. The advantage of this technique is that it obtains direct FSK performance by using existing FM voice transceivers for both modulation and demodulation. The transmitted signal will fit within a 20 kHz FM voice channel, and thus this modulation is also attractive for many commercial uses.

The actual modulation, often referred to as a form of CPFSK (continuous phase frequency shift keying), is a generalization of the conventional FSK which changes between two frequencies instantaneously. With this form of CPFSK, the frequency shift occurs gradually and smoothly across the bit interval to reduce the bandwidth of the transmitted signal. The frequency shift due to a bit can be extended over more than a single bit interval to reduce the bandwidth even more. The performance of this type of modulation is competitive with standard modulations such as MSK and even PSK.

Descriptions of this type of modulation can be found in the literature.[22,23] However, these descriptions are generally in terms of optimal filter theory. Optimal filters are becoming simpler to implement with the availability of VLSI technologies and signal processing ICs. Also, systems consisting of optimal filters and precision modulators can spread a bit transition over several bit periods (partial response signaling) to improve performance. Although optimal receiver theory is practical for applications that use coherent receivers, it does not provide an adequate explanation of the performance of the modulation scheme used for UoSAT3/PACSAT.

The 9600 baud modulation used on UoSAT3/PACSAT was designed within the amateur radio community to use existing FM voice transceivers. The modulation has been used in many terrestrial packet networks, particularly for backbones connecting local digipeaters and packet-radio bulletin board systems. This modulation is easy to implement and performs very well.

Figure 31 shows a block diagram of the communications system for the UoSAT3/PACSAT. The transmit and receive paths are separated to show the processing sequence. The transmitted signal is actually CPFSK but the communications system may be modeled as a polar binary

channel which begins at the input to the FM transmitter and ends at the output of the FM receiver.

Analysis of this modulation is made different because the modulation uses neither a precise modulator nor an optimal receiver. Although analytic results for performance of an optimal receiver may be used for the purposes of comparison or estimation of a performance bound, an analysis of the actual transmitter and receiver used would be more appropriate. Such an analysis treats the digital signal as a smoothed polar binary signal that is transmitted through a channel consisting of a FM transmitter and receiver. The FM channel is treated as a noisy channel with SNR improvement obtained from the FM demodulation, but the FM channel also has nonlinearities resulting from phase distortions from the IF filter. Although the frequency modulated polar signal is identical to a CPFSK signal, analysis of the polar binary signal is appropriate since the actual demodulator detects the polar binary signal instead of the CPFSK signal.

This modulation method is also subject to performance degradation due to real filters and tuning errors (from doppler shifts). These degradations are analyzed separately.

In this chapter, the PACSAT communications system and its modulation are described in more detail. The PACSAT

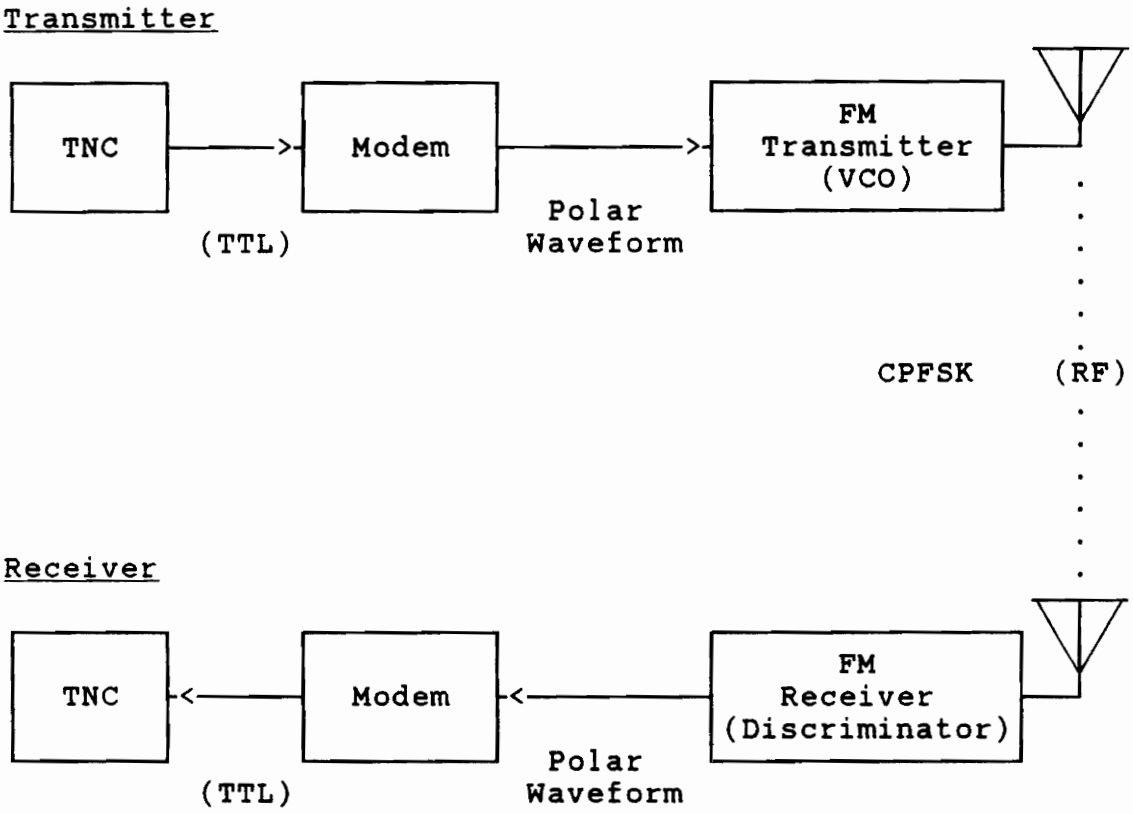

Figure 31: Block Diagram of the Essential Features of the PACSAT Communications Channel

receiver is analyzed in terms of optimal FSK receivers and then in terms of polar binary signal detection. The degradation in performance due to the filter and mistuning is analyzed last. These analyses apply to the discriminator approach and are specifically relevant to the base station. Some of the results may also apply to the portable station, but the portable station approach is not explicitly analyzed here. A separate analysis of the performance of the portable station is presented in a paper from UVa.[24]

4.1 PACSAT Communication System

The following sections describe relevant features of each block identified in Figure 31.

4.1.1 TNC (Transmit)

The operation of the AX.25 protocol was addressed in Section 1.2.1 of this thesis. The TNC is a product that implements this protocol and communicates with the computer. For this discussion of the communication channel, the relevant aspects of the transmit side of the

TNC concerns the bit stuffing feature and the baseband coding.

The TNC does the link-level processing of the AX.25 frames. On the transmit end, the TNC assembles the packets and controls the link. When the TNC is not sending any data, it sends a string of AX.25 flags which are unique words ("Ø1111110" in binary). The TNC formats the incoming data into information fields, appends the necessary control and address fields, and then marks the beginning and ending of the frame with the unique word flags. The transmitted data within the AX.25 packets are prevented from containing randomly generated flags by the TNC stuffing a "Ø" bit after each string of five "1" bits which are not part of flags.

The TNC also does baseband coding for NRZ-S which causes a level change whenever a "Ø" bit is transmitted. A string of "1" bits would cause a constant level and thus a DC component; however, the bit stuffing feature helps to limit this undesirable effect.[25]

4.1.2 Modem (Transmit)

The 96ØØ baud modem is a separate unit from the TNC although it is mounted within the same enclosure. It

generates the signal that modulates the voltage-controlled oscillator (VCO) within the transmitter. The modem scrambles the NRZ-S signal from the TNC by using a 16 stage random sequencer. The scrambled signal is then shaped via a PROM table.

The specific shaping of the analog waveform, which modulates the transmitter, is chosen to minimize the intersymbol interference (ISI) of the signal at the receiver output. The shaping is approximately raised-cosine in either the time or frequency domain and the pulse shape is spread over two bit periods. These pulse shapes meet the Nyquist condition for zero ISI.[26] The modem also sets the modulation index, h, by the adjustment of a potentiometer. In contrast to optimal systems for CPFSK, the receiver for this application does not require precise control of h from the transmitter.

In the UoSAT3/PACSAT link, the transmitted signal is predistorted to cancel out the distortion expected from the receiver's IF filter. This method of link equalization is easy to accomplish by programming the PROM table with a predistorted wave shape. Because the equalized signal is designed to reduce phase distortion, the power spectrum of the transmitted signal should be approximately the same as the unequalized signal. However, the equalized signal will perform better with

narrow IF filters to which the signal was designed, and worse with wider filters, compared to unequalized signals.

4.1.3 FM Transmitter

In most modern transceivers, FM is generated directly from a VCO where the controlled element is a varactor diode. The base station transceivers like the Kenwood TS-790A generally produce the FM at some IF frequency and then mix the signal to the desired transmit frequency. Fixed frequency transmitters such as the Kantronics DVR2-2 used for the portable station may modulate an IF with a reduced modulation index and then multiply both the frequency and the deviation to get the desired output. Both techniques are compatible with this signal; however, the baseband circuitry (especially the microphone limiter and filter) may have to be bypassed.

Many of the smaller tunable transceivers such as handheld units and mobile units attempt to modulate the output frequency by directly modulating the VCO inside the frequency synthesizer loop used for tuning. In such an approach, the synthesizer will tend to correct the frequency deviations from the modem and result in a high

low-frequency cutoff. Such transceivers are not easily modified to handle these 9600 baud signals.

4.1.4 FM Receiver

FM voice receivers demodulate the signal at an intermediate frequency, typically 455 kHz. Instead of using IF filters that are optimized for data, the PACSAT receivers will use the filters already installed in the transceivers. In the Kenwood transceiver, there are three IFs and each has a narrow band (15 kHz wide) crystal filter. In the modified Kantronics transceiver, there are also three IFs; however, the IF filters become progressively narrower for each stage and the narrowest filter is 30 kHz wide. Multiple narrow band filters improve the selectivity (interference rejection) of the receiver, but narrow band filters are expensive at the higher IF frequencies. Using fewer filter stages gives a smoother transition and a more linear phase response, which is important for digital data.

Demodulation is typically done by an FM discriminator. The discriminator converts the FSK signal to a polar binary signal. In most modern transceivers, the discriminator is an IC-based quadrature detector which

detects the phase difference between the signal and the signal filtered by a low Q tank circuit. The low Q tank circuit delays the signal and when the delay is short compared to the modulation, the phase difference is proportional to the frequency deviation. From a different perspective, the tank circuit has a linear phase response in the frequency domain so that it will convert frequency deviation into phase deviation. Thus, the quadrature detector converts frequency modulation into phase modulation which is demodulated by the phase detector.

The portable station uses a PLL (phase-locked loop) demodulator to lock onto the signal received with doppler shift. The PLL circuit was designed by UVa.[27] The PLL outputs a voltage proportional to the frequency deviation like other discriminators. The PLL circuit uses a wide bandwidth input filter to capture the signal despite tuning errors but the loop bandwidth of the PLL is small so that the FM threshold of the PLL will be comparable to that of a discriminator with ideal tuning and a narrow IF filter. This property of the PLL is analogous to the use of PLLs for threshold extension detectors which typically are used for wide band FM signals.[28]

There are several approaches to compensate for doppler errors. A common approach used for Oscar Phase-3 satellite work is to use a transceiver with fine tuning

steps to tune out the doppler either in a closed-loop fashion by manually tuning the radio, or by tuning according to a schedule from a tracking program. The latter approach may be automated but it is open-loop: it does not correct or even monitor actual errors in tuning. The base station uses the latter approach.

As mentioned earlier, the portable station uses a PLL circuit to automatically tune out the doppler shift. This approach is promising since it requires neither an accurate tracking program nor an expensive interface to a computer.

Other approaches are to include some closed loop control either by analog automatic frequency control or by returning tuning error information to the computer that is otherwise doing open-loop control. Another proposed approach is to use a discriminator circuit with a wide input bandwidth like that of the PLL circuit: this approach is analyzed in a later section.

4.1.5 Modem (Receive)

The receive side of the modem samples the signal, recovers the clock, and descrambles the data. The baseband filter is on the modem board and it has a

bandwidth of about 7200 hertz. The descrambling is noteworthy since it will convert an input bit error to three bit errors spread over a 16 bit interval.

4.1.6 TNC (Receive)

The receive side of the TNC does the NRZ-S decoding, flag detection, bit destuffing, and packet disassembly. The differential nature of the NRZ-S decoding will convert a bit error into two successive bit errors. There will also be some more errors introduced by the bit destuffing but these errors are probably not significant due to the rarity of bit stuffing in the first place.

4.1.7 Receiver Side Conclusion

The receiver side of the 9600 baud link demodulates the CPFSK signal with an FM discriminator (either a quadrature detector or a PLL demodulator) to generate a polar binary signal that is then detected to produce digital data. The FM demodulation may give some FM improvement if the signal is above threshold and the modulation index is high enough. The digital side of the

receiver will generally multiply by six the bit errors from the detector. Because these bit errors will occur close together, the CRC of the AX.25 frame will be less effective in detecting errors, and thus bit errors inside accepted frames will be more likely. But the bit error multiplication should not effect the block error rate much because these bit errors will usually all occur in the same frame.

Although the above is considered the extent of the communications system, the RS-232 link between the TNC and computer is also important. RS-232 is an asynchronous link that does not have a provision for error recovery or even for detection of missing data. Missing data is likely for this system because the computer will be busy doing many things as well as handling the RS-232 port. Because the RS-232 is asynchronous, it may be the weakest link in the entire system.

4.2 PACSAT Modulation

The modulating waveform used in the PACSAT system is one of the waveforms provided on the PROM in the PacComm NB-96 modem. This waveform is two bit intervals wide to meet the Nyquist condition and adjusted to do some

equalization on the channel. The actual waveform is probably close to a two-interval spectrally raised-cosine pulse, which is abbreviated 2SRC. For the analyses in this document, a two-interval raised-cosine (time) pulse (2RC) is used to approximate the actual waveform. There is little difference between these two pulse shapes in the time domain, but because the derivative of 2SRC pulses has a discontinuity at the transitions, the spectrum of 2SRC will be a little wider than the spectrum of 2RC pulses.

The PACSAT modulation uses a modulation index, h, of Ø.75 which corresponds to a peak deviation of 36ØØ Hz for 2RC, 2SRC, and 1REC (one-interval rectangular) pulses. For these pulse shapes, the peak deviation is $h*R_b/2$.[29] The modulation index is defined so that after a single bit is sent, the total phase shift caused by that bit will be $h\pi$ radians. Smaller h values give FSK which would be affected less by tuning errors but they are also less resistant to noise than larger values of h. Unlike optimal receivers, a single PACSAT receiver can decode a wide range of h values. For example, in the Satellite Communications Laboratory at Virginia Tech, data was sent across the room with a modulation index of about Ø.3, judged by the spectrum of the signal.

4.2.1 FSK Spectra

The spectrum of the modulation gives an indication of how much tolerance to tuning errors the receiver will have. For an initial approximation, the receiver should be able to handle tuning errors until those errors cause a significant amount of the signal to be cut off by the IF filter. For example, an approximation of the tolerance can be measured as that tuning error that causes the frequency where the signal spectrum is three decibels down from the peak to coincide with the frequency where the filter response is three decibels down from the peak response.

Another important use of spectral information is in determining whether a modulation fits within an allocated channel. For example, a voice FM channel may be allocated 20 kHz of bandwidth, which means that the signal should be down by 40 to 60 dB at the channel edge in order to prevent adjacent channel interference.

The spectrum of the CPFSK modulations was computed by using an FFT (fast Fourier transform) routine in a simulation of a CPFSK signal modulated by a random data sequence. The spectrum was computed from the complex envelope representation of the CPFSK signal. Complex envelope analysis is useful for narrow band signal

analysis because the complex envelope is a baseband signal, which easier to analyze.[30] A Hanning window was used on the CPFSK signal to help smooth the estimated spectrum. The estimated spectrum was further smoothed by selecting the maximum magnitude values of five FFTs for different data. Finally, the resulting log magnitude of the spectrum was further smoothed by averaging each sample in the frequency domain with the two nearest samples on either side, i.e., a moving average over five samples. More details about the process of generating the spectra are presented in Appendix B.

Figure 32 shows a comparison of the computed spectrum for a MSK signal (1REC with h=Ø.5) with the theoretical spectrum.[31] An equation for the theoretical spectra of 1REC CPFSK signals is available in Proakis' Digital Communications.[32] Although the FFT estimate is not as smooth as the analytic result, the relative magnitudes and positions of the side lobes closely match those of the analytic spectrum.

The PACSAT modulation was simulated by using 2RC waveforms for modulation instead of 1REC. A comparison of the CPFSK spectrum (for 2RC pulses) in Figure 33 and the MSK spectrum in Figure 32 have the same modulation index (Ø.5) illustrates that premodulation pulse shaping has the effect of a bandpass filter after the modulator when no

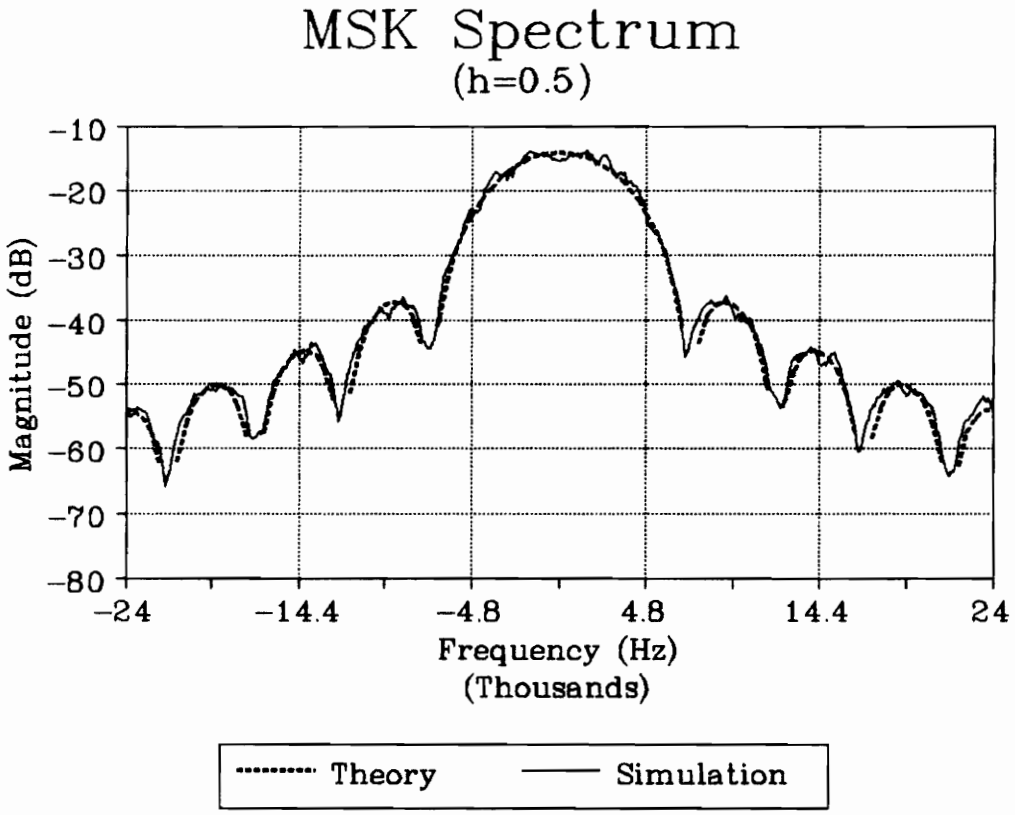

- The Estimation Approach Accurately Measures the Main Lobe
- Sidelobe Peaks are Accurate
- Nulls are Less Accurate
- Notes:
  - Frequency Relative to Center Frequency
  - Magnitude Relative to Arbitrary Value

Figure 32: Classical MSK Spectrum: A Comparison of the Analytic Spectrum with the Simulated Spectrum Using FFTs

pulse shaping is used. The practical importance of this effect is that baseband pulse shaping is easier and less expensive than narrow band filtering.

The spectrum for the modulation index used on PACSAT (h=.75) is plotted in Figure 34. Compared to MSK, this spectrum is flatter and occupies more of the 20 kHz channel. Outside of the channel, the PACSAT modulation has a lower spectral density than the MSK modulation despite the higher modulation.

4.2.2 Receiver Performance

The analysis of the receiver performance consists of two steps. In the first step, the performance of an idealized model of the receiver is analyzed. Two models are considered: an optimal filter model and a model for polar binary signals through an FM channel. The second step analyzes degradations due to the imperfections of the real receiver. The degradations are expressed as a loss in SNR such that additional signal power would be required to restore performance to that of the ideal model. The degradations considered are signal distortions and additional noise. Both of these degradations result from using real filters and from tuning errors due to the

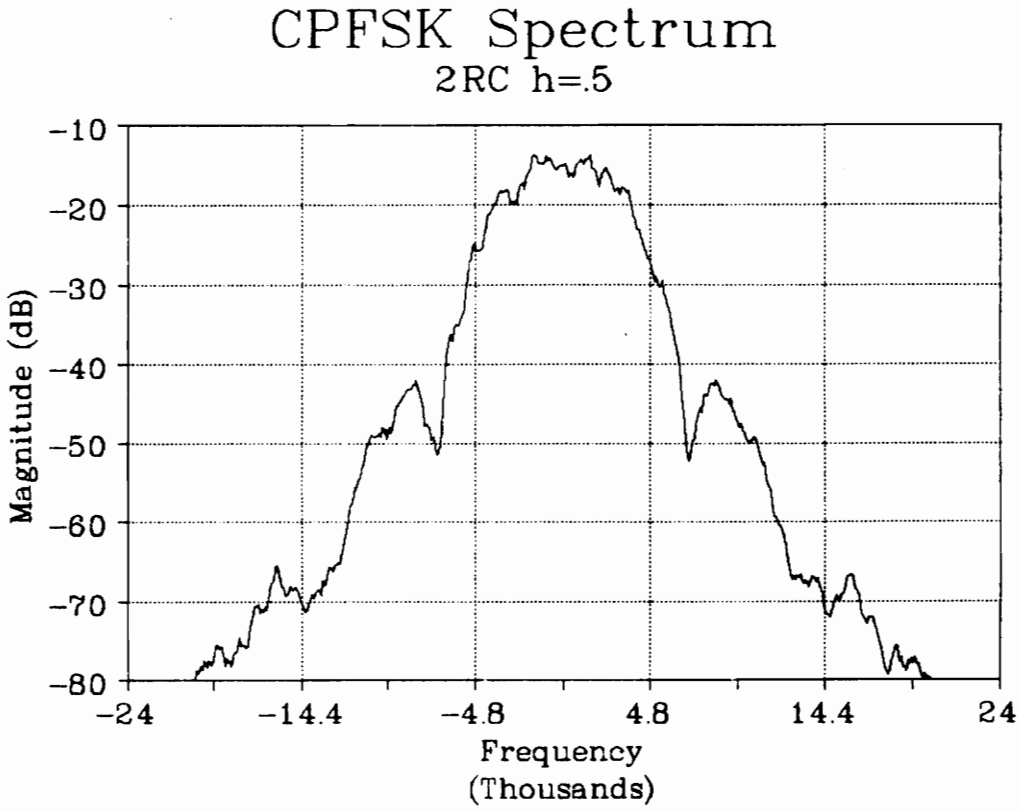

- 2RC MSK Spectrum
- Premodulation Shaping Similar to Postmodulation Filtering
- Relative to 1REC MSK:
  - Same Main Lobe Magnitude
  - Less Side Lobe Magnitude

Figure 33: Spectrum of CPFSK for 2RC Pulses with h=Ø.5: A 2RC-MSK

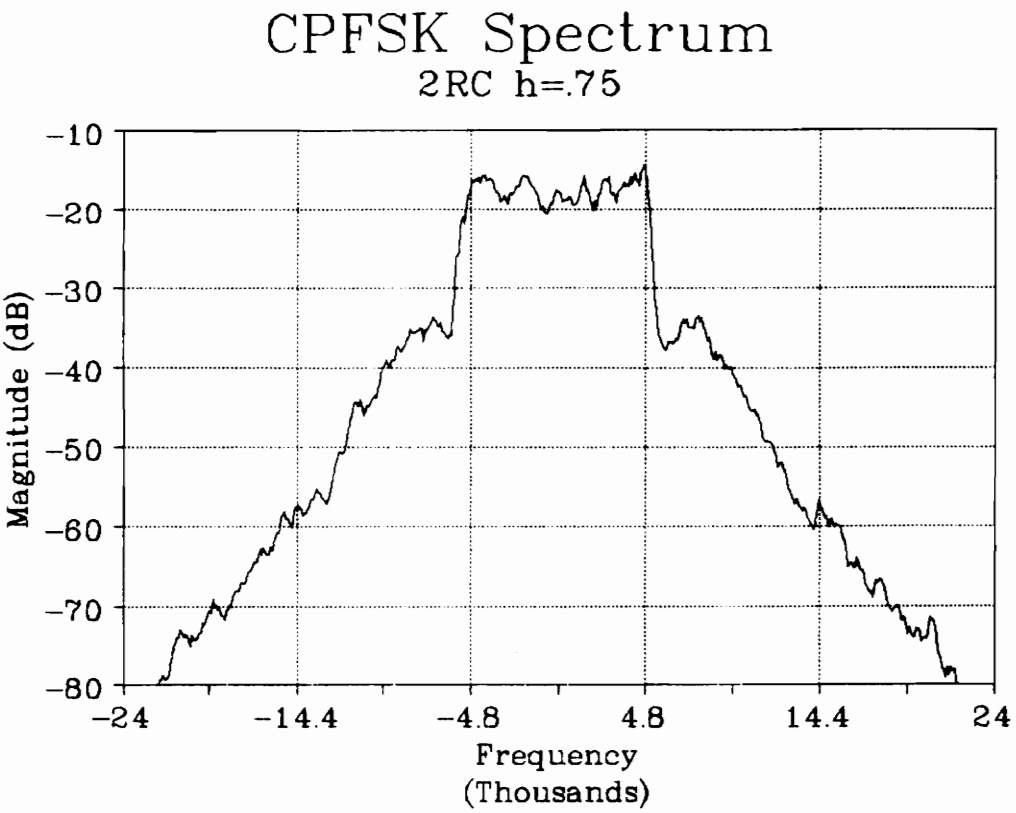

- Similar to UoSAT3 Modulation
- Fills More of a 20 kHz Channel
- Relative to 1REC MSK:
  - Wider Main Lobe, but
  - Less Side Lobe Magnitude

Figure 34: PACSAT Modulation Spectrum: 2RC Pulses with h=0.75

doppler shift of the signal. Except for the optimal filter model, the analyses in the two steps involves treating the polar binary signal as an analog signal.

4.2.3 Ideal Receivers

The two idealized receivers are actually quite different. Optimal filter receivers are optimal among the class of linear filters in the presence of white Gaussian noise.[33] The performance is optimized with a filter that passes all of the signal energy but only the part of the noise that is correlated with the signal.[34] As a result, the optimal receiver treats the modulated signal like an AM signal and resembles a DSBSC (double sideband suppressed carrier) receiver.[35]

The alternative approach is to use an FM demodulator to convert the signal into a measure of its instantaneous frequency. This conversion is inherently a nonlinear process that has two important effects. Firstly, the output noise level decreases with increasing input signal level. And secondly, the reduction in bandwidth resulting from converting a signal into its instantaneous frequency leads to an improvement in SNR at the output. Because of the nonlinearity, the improvement will disappear when the

signal level is too small, i.e., there is a threshold effect.

4.2.3.1 Optimal Receiver

The optimal receiver for CPFSK modulated by 2RC pulses consists of four filters matched to the four possible signals resulting from the overlapping pulses. The bit decision is based on the filter with the largest output. Because the pulses overlap, there is also information in the sequence of selected filters as would happen with convolutional coding. Thus, this information can be exploited for some additional improvement by Viterbi decoding techniques.[36] For pulses spread over only two bit intervals, the effect of Viterbi decoding is expected to be minimal and it is ignored in this analysis.

For optimal receivers, the input signal will generate responses in each filter according to how closely the input signal is correlated with the signal to which the filter is matched. When two filters are used, the ideal pair of signals produce full negative correlations in their opposite's filter and this condition is termed antipodal and applies to BPSK.[37] When more filters are involved, the various signals may be selected to be

mutually orthogonal in order to make the design easier.[38] For two signals, the bit-error probability can be expressed in terms of the correlation as follows:[39]

$$P_e = Q\left[\sqrt{(1-p)\frac{E_b}{N_\emptyset}}\right],$$

where p is the cross-correlation of the two signals (p=-1 for PSK). When the individual pulses are confined within single bit intervals, there will be only two possible signals.

The cross-correlation is straight forward to compute for the two-signal case.[39] Figure 35 shows the cross correlations (rho) for two types of pulse shapes extending over a single bit period, 1RC and 1REC. The cross-correlation is plotted versus the modulation index, h. The 1REC (rectangular) pulse shapes apply to classical CPFSK which includes MSK (h=Ø.5). Note that the optimum modulation index for 1REC is h=Ø.715. Although both shapes perform equally well at h=Ø.5, the 1RC case performs significantly worse than 1REC at h=1.Ø. Thus the performance of the 1REC pulse shapes, which is well documented, does not serve as a good prediction of performance for other pulse shapes.

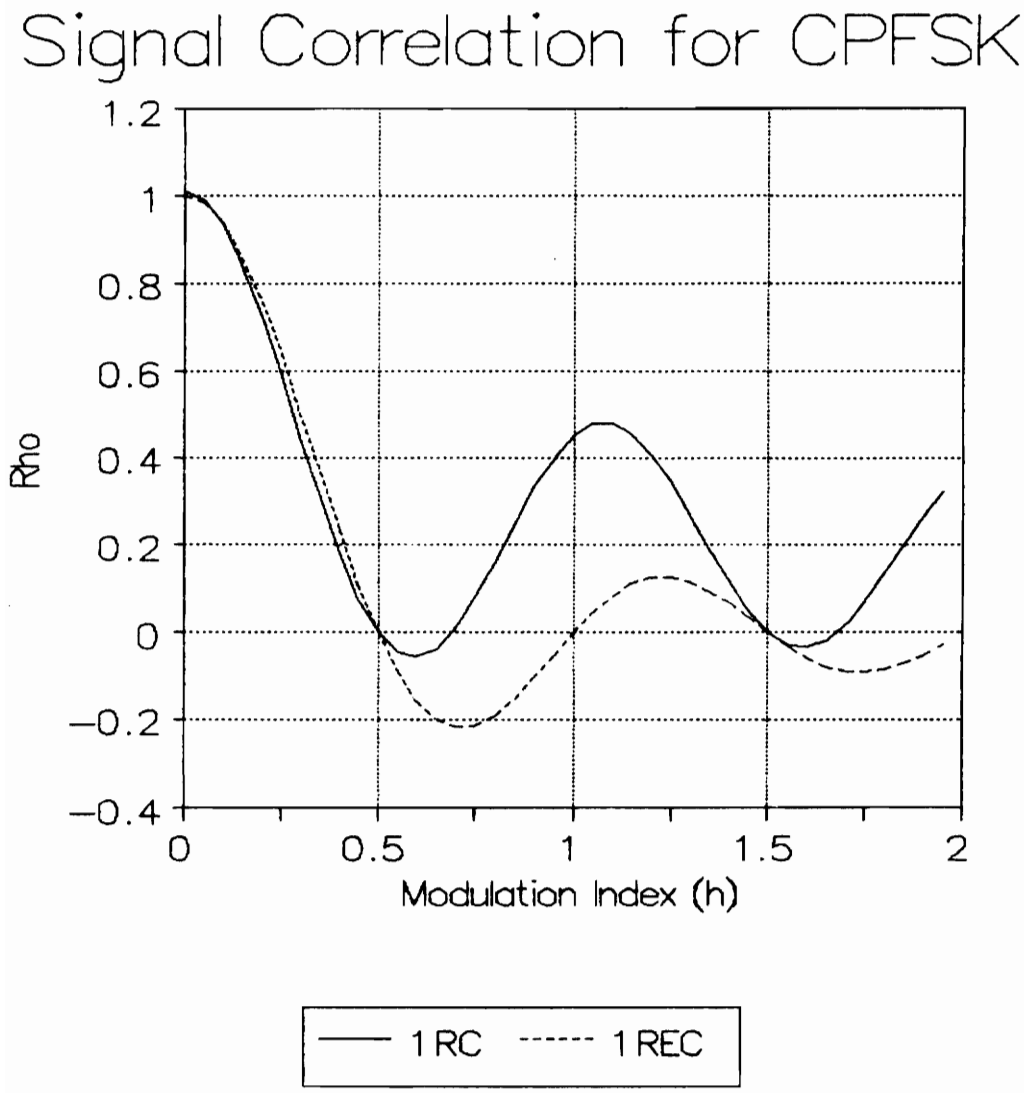

Figure 35: Dependence of Cross Correlations for 1REC and 1RC pulses on Modulation Index

When the individual pulses are spread over two bit periods there will be four possible signals depending on the combination of two adjacent bits. For a four-signal modulation, the cross-correlation must be computed for every pair of signals. For 2RC signals, there are four distinct cross correlations for the six possible combinations. The individual cross correlations are plotted against modulation index in the top plot of Figure 36. Assuming that the transmitted data are independent and equally probable, then an average of the six possible cross-correlations would serve as a good measure of the overall performance of the receiver. This average is shown on the bottom plot in Figure 36. According to the averaged cross-correlation, the optimal modulation index is about Ø.6, which is less than for 1REC: however, the optimal correlation value is about the same for both pulse shapes.

4.2.3.2 Polar Binary with FM

The alternative approach to analysis is to consider what actually is done in the PACSAT ground station receiver. The shaped waveform is frequency modulated to generate the CPFSK signal. At the receiver, the CPFSK is

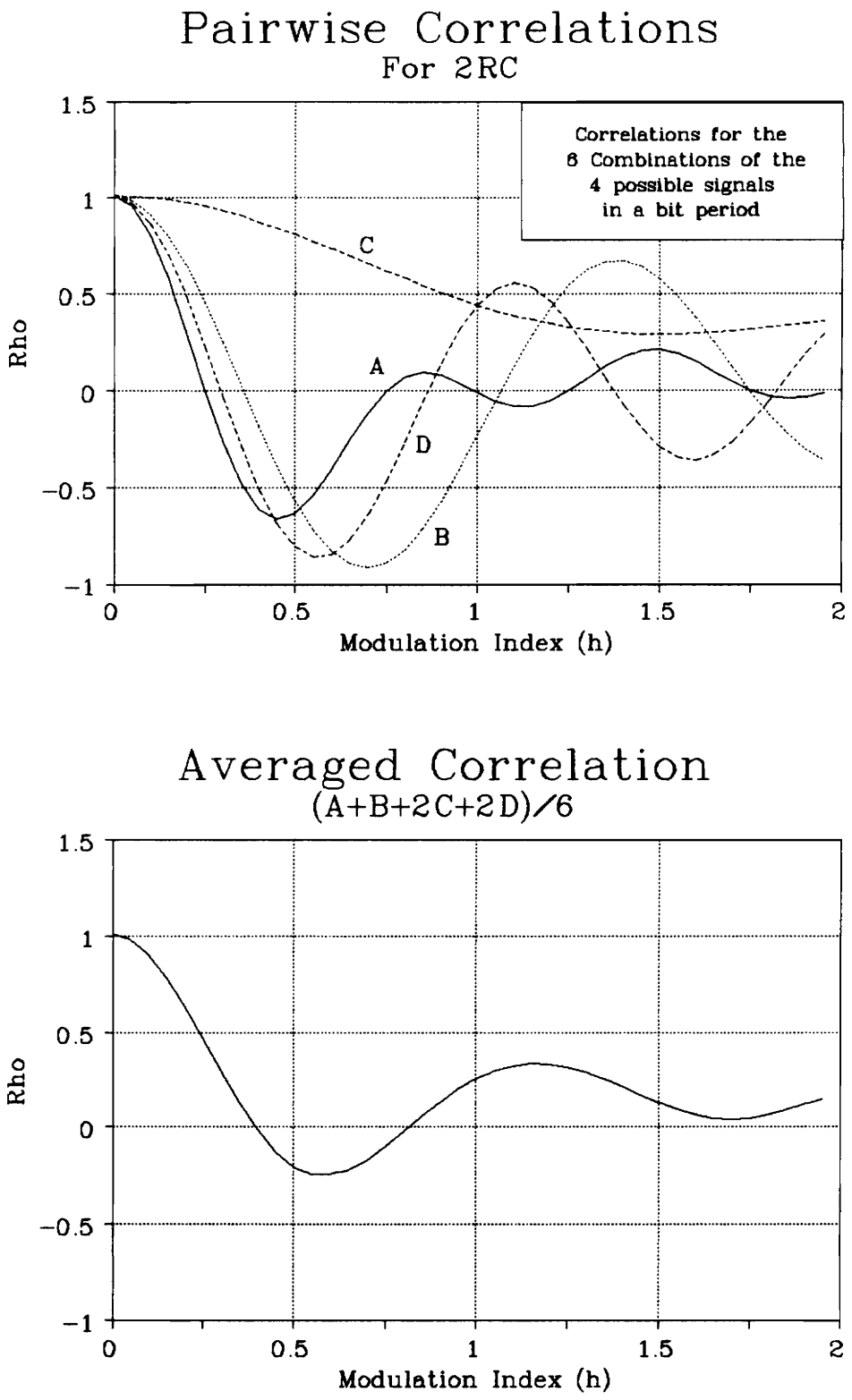

Figure 36: Cross Correlations for 2RC Pulses vs. Modulation Index

frequency-demodulated to restore the polar binary signal. Although the waveform extends over two bit intervals, the intersymbol interference at the sampling instant is assumed to be zero. Thus, at the sample time, the signal consists of the transmitted peak deviation and noise from the discriminator. The output noise power from a discriminator when the output signal is the desired frequency deviation (i.e., there is no scaling) is:[40]

$$N = \frac{N_{\emptyset} B^3}{(3 S_c)},$$

where B is the baseband bandwidth, S_c is the carrier (input signal) power, and $N_{\emptyset}$ is the noise power spectral density. For approximation purposes, the baseband bandwidth can be expressed as a fraction of the bit rate; thus, $B=\beta R_b$, where B is the baseband bandwidth and β is between Ø.5 and 1 (the NB96 modem uses a value of Ø.75). The frequency deviation is $hR_b/2$. Furthermore, when the input noise level is small, the statistics of the output noise density is approximately Gaussian because the output noise becomes proportional to the derivative of the quadrature component of the input noise (assumed to be Gaussian).[41] Therefore, the bit-error probability can be expressed as

$$Pe = Q\left[\frac{f_d}{\sqrt{2N}}\right],$$

which can be rewritten as

$$P_e = Q\left[\sqrt{\frac{3h^2}{8\beta^3}\,\frac{E_b}{N_\emptyset}}\right],$$

where E_b is simply S_c divided by the bit rate.

The last equation is of the same form as the expression for the optimal filter:

$$P_e = Q\left[\sqrt{\alpha\,\frac{E_b}{N_\emptyset}}\right],$$

where α is a scaling factor. Since the bit error rate equation for MSK is the above equation with an α of one, the α factor can be considered as the $E_b/N_\emptyset$ improvement compared to MSK.

The predictions of the two approaches can be compared by plotting α versus h. Figure 37 shows that for small deviations, the optimal receiver will perform better than the discriminator. However, as h exceeds about Ø.7 for β of Ø.5 or about 1 for β of Ø.75, the discriminator would

be expected to perform better than the optimal filter. The optimal receiver performance for 1REC pulses is also plotted for reference. Figure 38 is the same plot of as Figure 37 where α is scaled in dB.

The PACSAT modulation uses a modulation index of Ø.75 and the ground stations use a ß of Ø.75. Figure 38 shows that the ground stations will require 3.5 dB more $E_b/N_Ø$ than a coherent receiver to achieve the same bit error rate. When compared to the ß=Ø.5 discriminator, the ground stations require about 5 dB more $E_b/N_Ø$ for the same bit error rate. If ß is constant but the modulation index is increased to 1.5, the discriminator should perform about 3 dB better than a coherent receiver for the same signal.

The analysis of the polar binary signal through an FM demodulator indicates that the demodulator approach may perform better than an optimal receiver. The reason that this is possible is that the optimal receiver theory optimizes linear receivers whereas the FM demodulator is a nonlinear receiver. Several points about the above analysis should be noted. First, the analysis assumed that the noise level was low enough that the output noise can be considered Gaussian and that the SNR is above threshold. However, SNR decreases and the threshold increases as the modulation increases; thus, the

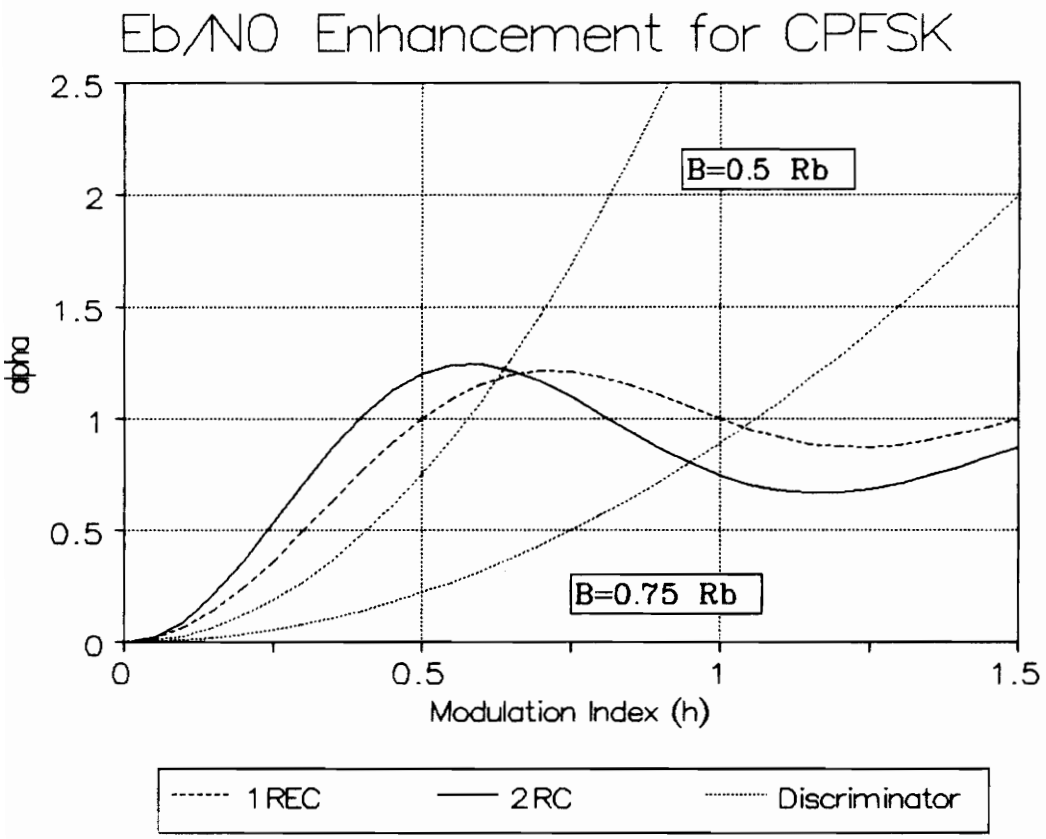

- Comparison Between Coherent Receivers (2RC and 1REC pulses) and Discriminators
- Coherent Receivers Perform Better than Discriminator for Small h
- UoSAT3/PACSAT System Uses B=Ø.75 Rb and h=Ø.75

Figure 37: Eb/NØ Enhancement vs. h: Coherent Receivers (1REC & 2RC pulses) and Discriminators (β= Ø.5 & Ø.75)

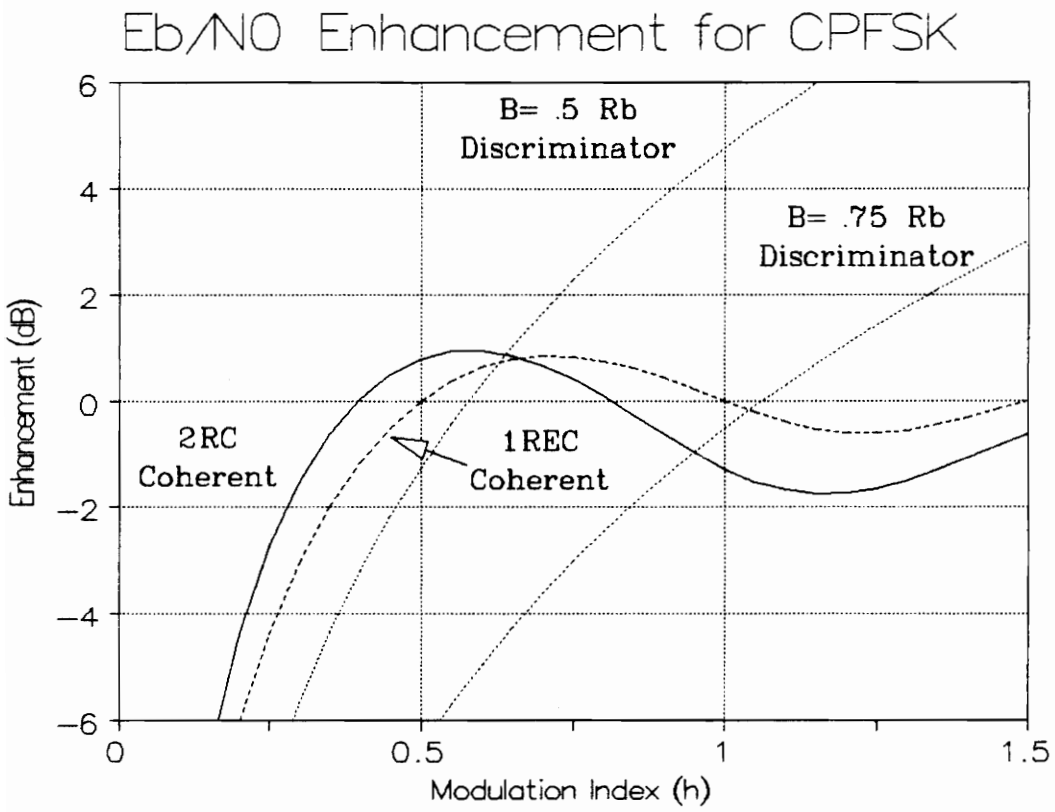

- UoSAT3/PACSAT System Uses B=Ø.75 Rb and h=Ø.75:
- Performance is 3 dB less than that of Coherent Receivers
- Possible Improvements: Better Receiver or More Modulation

Figure 38: Eb/NØ Enhancement (in dB) vs. h: Coherent Receivers (1REC & 2RC pulses) and Discriminators (β= Ø.5 & Ø.75)

enhancement from FM plotted in Figure 37 will level off and decrease to zero at some point depending on the available signal power: the enhancement curve for FM depends on the value of $E_b/N_\emptyset$. In high noise conditions, the threshold effect will cause the performance of the optimal receiver to exceed the FM demodulator performance even for large modulation indexes. In moderately high noise conditions, the output noise from the discriminator will become less Gaussian and more dependent on the discriminator implementation. Finally, the above analysis also does not include the effects of click noise which will occur even with high $E_b/N_\emptyset$. Like FM threshold, Click noise will increase as the modulation index increases and thus will limit the improvement.

4.2.4 Degradations

Degradations come from excess noise from tuning errors and distortion from the real filter with tuning errors. The IF bandwidth will also determine the FM threshold effect but as long as the signal is above threshold and thus effect the bit error rate. However, an analysis of the threshold effect will not be presented in this thesis.

4.2.4.1 Excess Noise from Tuning Errors

When a FM demodulator receives a signal with a tuning error, the output is the desired signal with a DC offset corresponding to the tuning error, assuming that the signal is not distorted by the IF filter. As a result, a candidate approach to dealing with the doppler errors is to use a discriminator preceded by a filter that is wide enough to handle the worst case doppler. This approach will introduce a performance degradation because the wider filter will let in more noise power to the discriminator. Also, the mistuning will cause even more noise to appear at the output of the discriminator.

With no tuning error and low input noise levels, the FM demodulator has an output noise spectrum that varies as the square of the frequency because the demodulator is approximately a differentiator of the IF noise (for high SNRs). The noise is in effect filtered by a frequency response of

$$H(f) = C\ j2\pi\ f,$$

where C is a scale factor. With a tuning error of f_d, the filter response changes to

$$H(f) = C\ j2\pi\ (f-f_d).$$

As a result, the output noise power density varies as $(f^2+f_d^2)$ instead of just f^2. After integration over the baseband bandwidth, the additional noise due to the tuning error results in a degradation of

$$D = \frac{1}{1 + 3(f_d/B)^2} .$$

For an illustration, the output noise level will double, leading to a 3 dB degradation when the tuning error is just 1/3 of the baseband bandwidth (2400 Hz for the PACSAT ground stations).

4.2.4.2 Distortion Degradation

Distortion results from using real IF filters which have nonlinear phase responses and variable amplitude responses in the frequency domain. The distortion of the filter is exacerbated by a tuning error which will cause the signal to move from the center of the filter's response.

Base station transceivers such as the Kenwood TS-790A use several monolithic crystal filters in cascade. The crystal filter is essentially a coupled resonator and thus the response will have some amplitude ripple and some

corresponding phase distortion. The crystal filters are usually installed in the circuit with an impedance match to give a response with minimum ripple. As a result, the crystal filter may be modeled as a Butterworth (maximally flat) filter. Due to the number of filters in cascade, the overall response will have a sharp cutoff and correspondingly sharp phase distortions at the band edges. Increased distortion can be expected when the signal approaches the band edge of the filter.

To quantify this distortion, a simulation of the basic components of the communication system was performed to produce eye patterns which then can be evaluated for degradation. This simulation is noiseless and thus the results will indirectly indicate system performance in the presence noise. Figure 39 shows a block diagram of the elements simulated. A random data sequence was converted into a signal consisting of 2RC pulses. Frequency modulation by the waveform was represented in its complex envelope form. The response of the IF filter for a mistuned FM signal was computed in the frequency domain. Finally, the quadrature detector multiplied a sample of the signal with an adjacent sample. (The delay path includes a 90° phase shift so that the correct components of the complex envelope have to be multiplied to get the desired result.) The modulation index of the signal was

Ø.5 and the filter was a 15 kHz wide eighth order Butterworth filter. Appendix C provides more details about the implementation of this simulation.

The accuracy of the simulation can be improved with a better model of the receiver. For examples: a limiter can be inserted between the filter and the discriminator; a more accurate crystal filter model may be used; and the delay of the quadrature detector can be replaced with a model of an LC tank circuit. These components were left out to simplify the simulation program.

A typical eye pattern is shown in Figure 4Ø. There is no doppler shift for this eye pattern; thus, the distortion is from the filter. An ideal eye pattern for a zero ISI waveform would have the various traces converge to two points at the sample instant. Distortion spreads the traces apart at the sampling instant and in effect closes the eye. The degradation due to the eye closing is the amount of increased signal power required to restore the performance to that of a zero ISI eye pattern. This degradation can be computed from the ratio of the width of the eye opening to the width of the overall signal.[42]

Figure 41 shows a high degree of distortion resulting from a doppler shift of only 3 kHz in a 15 kHz bandwidth filter. The eye is substantially closed by this point. Figure 42 shows an eye pattern for no doppler shift but

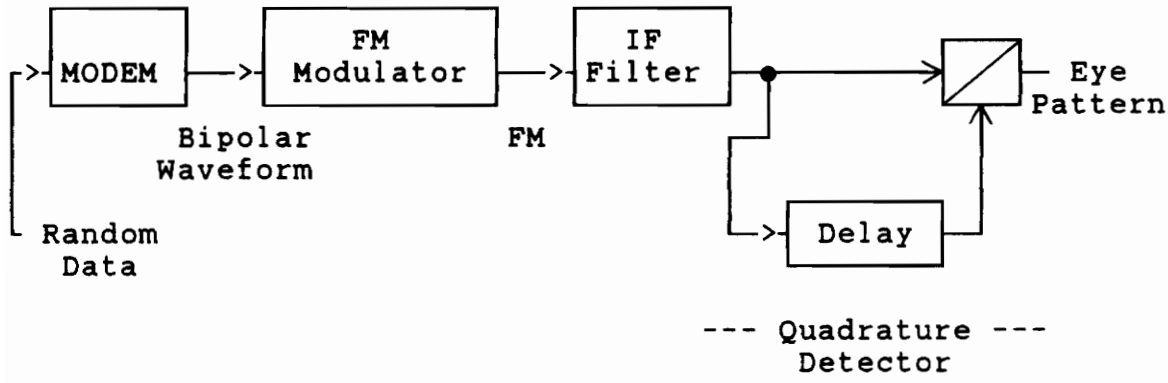

Figure 39: Block Diagram for Simulation to Generate Eye Diagrams

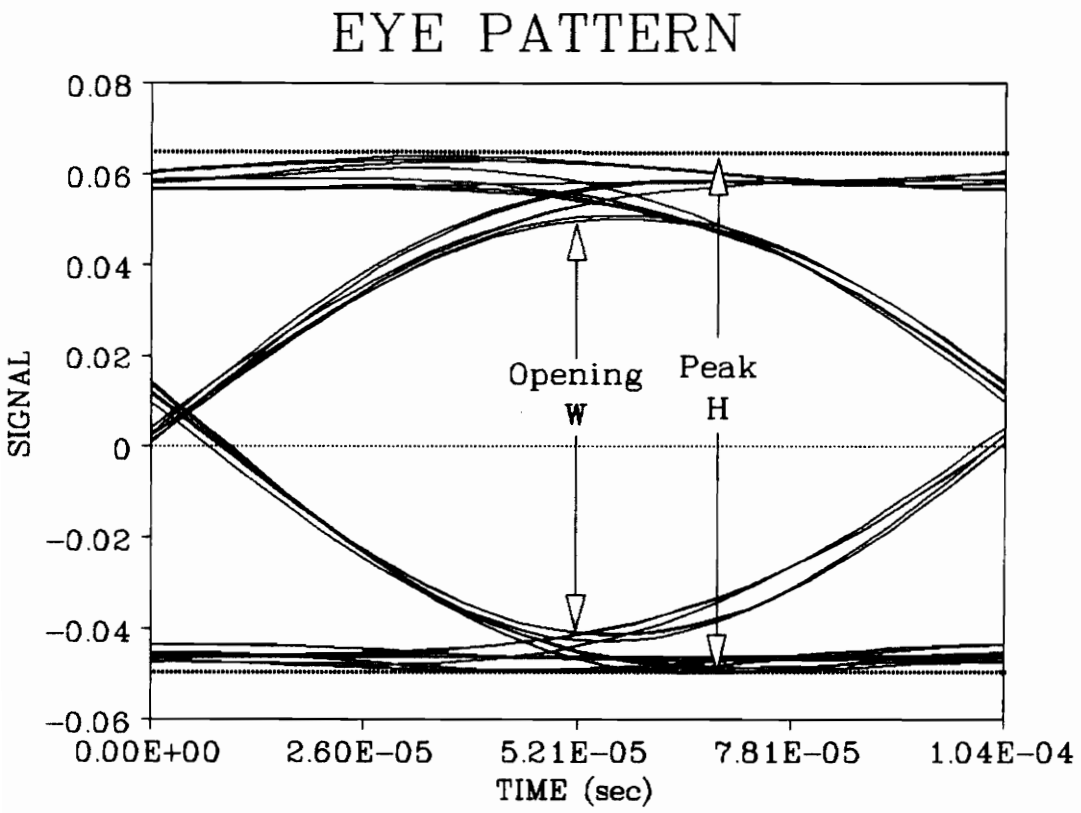

- Eye Pattern for 9600 Baud CPFSK with 2RC Pulse Shaping
- 15 kHz IF Bandwidth Typical for 20 kHz Channel
- No Tuning Error: Eye Closing Due to Filter
- Degradation is 20Log(W/H)≈ -2 dB

Figure 40: Eye Pattern for 15 kHz Filter, No Doppler, 2RC pulses at 9600 baud

with a 30 kHz wide filter that would be used to accept worst case doppler shifted signals. This pattern is almost ideal.

4.2.4.3 Total Degradation

Figure 43 shows the total degradation for the real receiver with tuning errors. The eye-pattern degradation was computed for several doppler shifts for filters of 12, 15, and 30 kHz bandwidths. The resulting degradations were added to the degradation due to increased noise from mistuning. The modulation index is 0.5 for these results.

Figure 43 indicates that the wider bandwidth filter performance is superior because it degrades more gracefully than the narrower bandwidth and it performs better with small tuning errors. There is still over 10 dB of degradation at the maximum doppler shifts of 9 kHz for UHF. However, compared to the 12 kHz bandwidth approach, the 30 kHz bandwidth will require about 4 dB more signal power to stay above threshold. For small tuning errors of less than about 300 Hz, the performance of the narrower filters can be improved with the addition of equalization on the link, as is done on the UoSAT3/PACSAT link. When the link is equalized for the

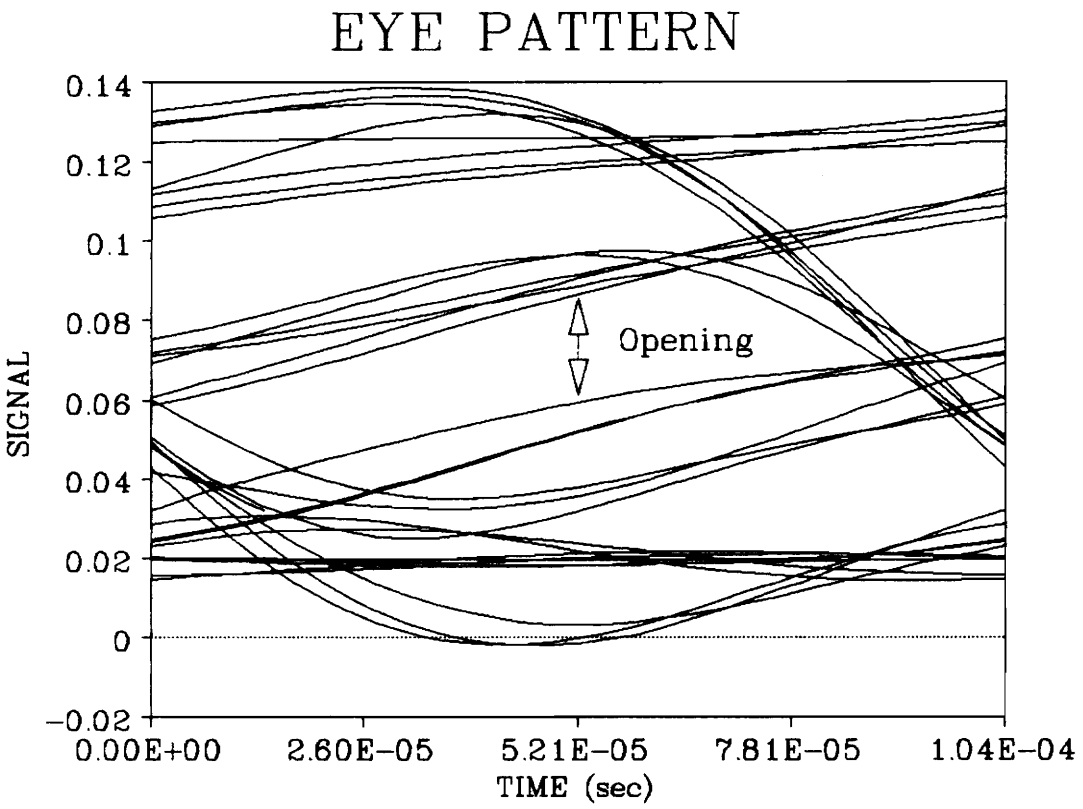

- 3 kHz Tuning Error
- 9600 Baud 2RC CPFSK, 15 kHz IF
- Degradation is ≈ -10 dB

Figure 41: Eye Pattern for 3 kHz Doppler (15 kHz Filter, 2RC Pulses, 9600 baud)

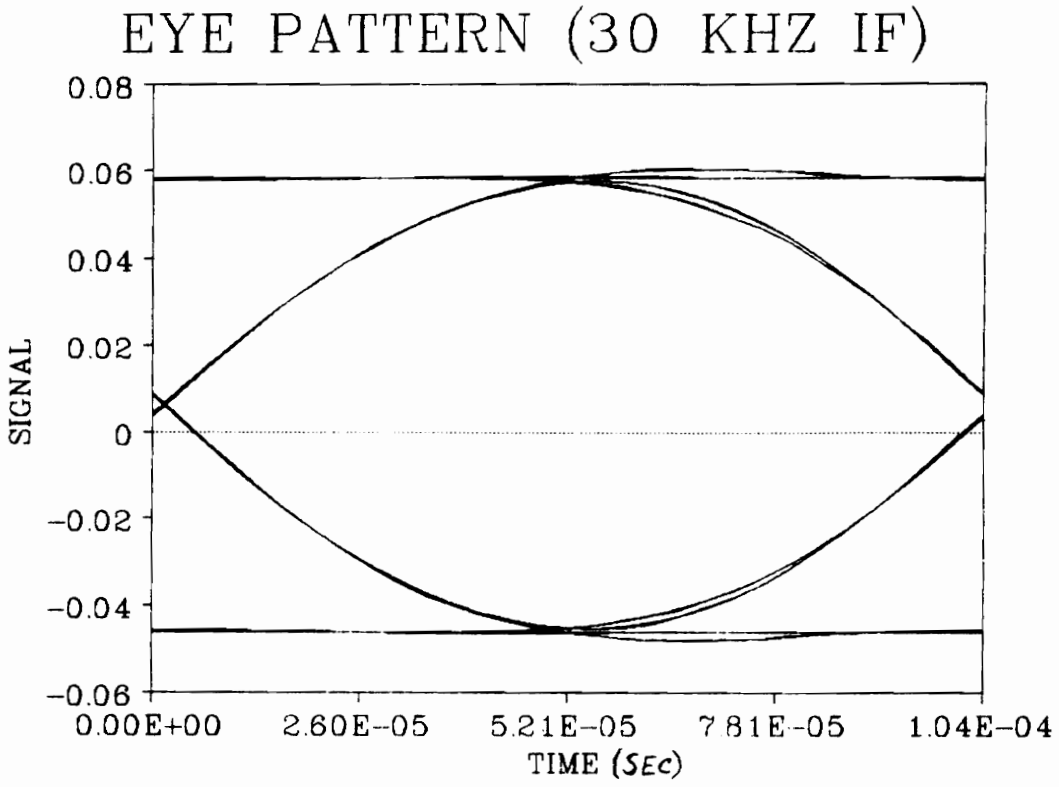

- 3Ø kHz IF, No Tuning Error
- Nearly Ideal Eye Pattern
- Trade-off Between Filter Distortion and FM Threshold

Figure 42: Eye Pattern for 3Ø kHz Filter, No Doppler, (2RC Pulses, 96ØØ baud)

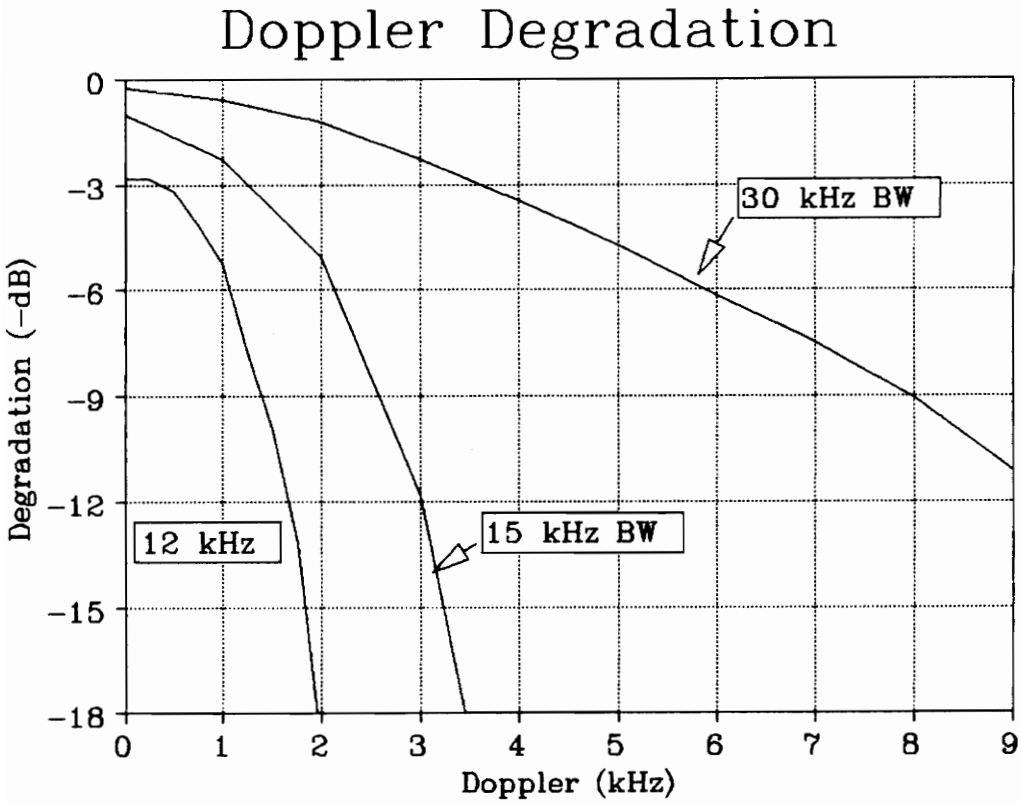

- Degradation Measurements For Several Bandwidths and Tuning Errors
- Equalization may Improve the Performance for Small Errors
- The 3Ø kHz Filter has 9 dB of Degradation with 8 kHz Tuning Error
- Tuning Accuracy is Preferred over a Wide Band Discriminator

Figure 43: Total Degradation vs. Tuning Error and IF Filter Bandwidth (Unequalized 2RC pulses at 96ØØ baud)

narrower bandwidth, then the narrower bandwidth filter will perform better than the wider filter for small tuning errors.

4.2.5 Base Station Performance

The above model of a base station using h=.5, an IF bandwidth of 15 kHz, a ß of Ø.5 (B=48ØØ Hz), a discriminator receiver, and open-loop doppler tracking indicates that the receiver should operate with a total degradation of about 3.5 dB compared to ideal MSK: -1.25 dB FM enhancement with 2.25 dB distortion degradation.

The actual base station would be better modeled by the following parameters: h=Ø.75, ß=Ø.75, and an IF filter bandwidth of between 12 kHz and 15 kHz. The FM enhancement for the above parameters would be -3 dB. The degradations would be about 3 dB from distortions by tuning errors which are assumed to be less than 5ØØ Hz. Therefore, the performance of the base station based on the Kenwood transceiver is expected to be about 6 dB worse than MSK. The actual degradation is less because the modem waveform is predistorted to compensate for the distortion of the narrow filters.

Given a modulation index of Ø.75, some improvement may be achieved through better receiver design. By using less sharp IF filters, the degradation due to filter distortion can be reduced. A better, narrower baseband filter may also be used for some additional improvement. Baseband equalization would be difficult because the distortion results from time-varying (doppler dependent) nonlinearities. For the selected modulation index, a careful design of a discriminator-based receiver may be able to reduce the overall degradation to less than 1 dB.

Although the 6 dB degradation with respect to MSK is significant for even an LEO satellite link, this degradation is acceptable on terrestrial links which usually have large signals. Because the modulation allows 96ØØ baud transmission in a voice channel by using inexpensive FM transceivers, the degradation is acceptable for many commercial and amateur radio applications. These advantages are also important for cheap ground stations for PACSATs.

4.2.6 Some Alternative Systems

The performance of the receiver can be improved by increasing h, but this will increase the bandwidth of the

transmitted signal. The increased bandwidth lets in more noise and increases the threshold level. Assuming that the signal remains above the threshold, the modulation index would have to be increased to about 2 before the receiver performance matches that of an optimal receiver for MSK, i.e., when the FM enhancement equals the degradation. Carson's Rule for FM bandwidth estimates that this much increased modulation will require a channel that is about 71% larger than for h=Ø.75. In contrast, an optimal filter would not provide additional enhancement when h is increased.

4.2.7 Other Bit Rates

Given that a channel of 2Ø kHz is available, it may be better utilized with a smaller bit rate. When the bit rate is decreased, the modulation index can be increased and still stay within the channel. To estimate performance at lower bit rates, Carson's rule is used for a total available bandwidth of 16.8 kHz which was chosen to match the result for the 96ØØ baud case. The minimum SNR at the receiver is determined by the threshold which is assumed to be relatively constant at about 13 dB.[43] Because $E_b/N_Ø$ is related to SNR by B/R_b and B is kept

relatively constant, the minimum $E_b/N_\emptyset$ will increase as the inverse of the bit rate. More signal will be required to begin communication, but once the signal is above threshold, the performance will be very good.

When the bit rate is 4800 baud, the modulation index can be increased to 2.5. Assuming that an unmodified modem is used, β=.75, the FM enhancement will be 7.4 dB. This enhancement is over 10 dB more than the enhancement for 9600 baud. Even when a distortion degradation is included, the receiver should perform about 4 dB better than MSK when the signal is above threshold. In other words, at threshold the bit error rate is approximately the same as MSK with an $E_b/N_\emptyset$ of 23 dB. By comparison, the same link for MSK would have an $E_b/N_\emptyset$ of about 19 dB although it will occupy much less of the allocated channel.

Reducing the bit rate to 1200 baud, which has been used on the UoSAT3, the modulation index can be increased to 13 which will give an enhancement of 21.7 dB. With degradation, the link will perform 18.7 dB better than MSK, although the minimum $E_b/N_\emptyset$, for a 13 dB threshold, will be 25.2 dB. This link would be essentially error free.

4.2.8 Link Design with Polar Binary FM

The above improvements are based on the same link budgets: the minimum SNR is 13 dB, determined by the threshold. To be able to reduce overall signal power requirements, the IF bandwidth will have to be reduced. When the maximum bandwidth to achieve threshold is determined during the link design, the bit rate and modulation index can be chosen to fit both the noise bandwidth and channel bandwidth requirements.

Chapter 5

Summary and Conclusions

Prototype ground stations were designed and assembled based on established practice in the amateur radio community. These ground stations are relatively inexpensive and will function to some degree. They have been built more for evaluation and testing of both the hardware and the overall concept than being finished products. Several improvements of the ground stations have been identified: some of these improvements will be required for an operational system while other improvements will enhance the performance.

An analysis approach for time-varying characteristics of the PACSAT orbit was developed. This approach divided the analysis into small routines that can be run on a relatively low-end personal computer. Most routines run in less than a minute on a AT-type computer consisting of an 8 MHz 80286 processor and an 80287 coprocessor. This analysis illustrated the importance of having accurate information for open-loop tracking, which was confirmed by

experience. Also, this analysis identified pass characteristics that either can benefit the design of a portable station or can severely limit the throughput of a base station.

The physical level communications systems for PACSAT was analyzed in terms of both optimal receiver theory and FM theory applied to polar binary signals. The difference between optimal receivers and FM demodulators is essentially the distinction between analog AM (coherent) and FM receivers. With a change in the PACSAT communications system, the simple FM receiver may perform much better than an optimal receiver. The analysis also indicated receiver changes that can improve the existing communications link. These characteristics will require substantial changes to the base station receiver but many of the characteristics are already in the portable station receiver.

The development of ground stations for PACSAT applications has been successful. Prototype ground stations have been developed to maximize use of existing products. The evaluation of these products and the overall PACSAT concept has identified specific requirements for production ground stations. The ground stations will need special purpose designs where the requirements can not be met by existing products. The

design and manufacture of these special purpose products are best done by manufacturers or software companies.

5.1 Prototype Ground Stations

Both the base station and the portable station have been prototyped. The prototype base station is functional but there are features that can be improved. The prototype ground station design is considerably different from the base station. The need for portable and inexpensive stations constrains the PACSAT concept.

5.1.1 Prototype Base Station

The prototype base station combined amateur radio products for both OSCAR (satellite) applications and packet radio applications. Its design is straightforward application of state-of-the-art products. Although the prototype is functional, the component parts are not necessarily inter-compatible nor compatible with PACSAT operation. New products, especially software products, are needed to make reliable ground stations.

The base station computer is a reasonably capable computer that is almost identical in performance to the selected portable station computer. The major exceptions are the addition of the math coprocessor, standard XT-type expansion ports, and EGA graphics; however, only the expansion port is absolutely required. The primary deficiency of this computer is that it is too low-end compared to what the protocol developers are assuming. The new 9600 baud protocols being developed for PACSAT will probably require the use of more expensive computers such as 20 MHz 80286 machines if the protocols have to be run on general purpose computers. The protocol development should be constrained to be able to be run on low-end computers so that the complete PACSAT network can be quickly and inexpensively set up; therefore, the PACSAT link should use a slower bit rate so that less expensive computers can be used.

The base station TNC is typical of the available TNCs in that they are built around slow 8 bit processors (typically a 4 MHz Z80). The trend has been to develop smaller and more portable TNCs with more user-interface software functions instead of faster TNCs with machine interfaces. This trend is explained by the popularity of the 1200 baud operation which is adequately handled by these TNCs. For 9600 baud, high efficiency, automated

packet communications with full-duplex file transfers, much faster TNCs are required. Furthermore, the desired TNC will have an interface that is appropriate for software control instead of user control. The electrical interface between the TNC and the computer should be changed from RS-232 to a synchronous interface. Although the recently introduced Kantronics Data Engine does not provide the desired interface, its internal architecture is more appropriate for high speed communications yet it is much less expensive than a full personal computer with the same capabilities. Also, the AX.25 link layer protocol is inappropriate for PACSAT applications primarily because of the excessively sized address fields and of the lack of the more sophisticated services for a commercial application. The special protocol requirements of PACSATs deserves further research.

Kansas City Tracker is not at all compatible with the needs of a PACSAT ground stations. The controller software runs asynchronously with the other software processes and is a major cause of the need for a faster computer. For the control of rotor positions, KCT uses software to close the control loop. For tuner control, KCT derives doppler scaling factors from doppler entries stored in a table and then computes in real time interpolated values for tuning. KCT does not allow any

other use of the RS-232 link to the tuner. In contrast, a PACSAT ground station will require a controller that uses a hardware control loop for rotor control, that allows full use of the radio control link, and that uses precomputed values of position and doppler shifted frequencies. Synchronization with the communications software in the computer is a desirable feature; for example, the rotor should be delayed from sweeping 360° from southeast to southwest while a file transfer is in progress. The ground station control software needs more development and customization for PACSAT applications.

The transceiver works fairly well with the 9600 baud signal. However, the small modifications required to make the transceiver operate with 9600 baud signals should not have been necessary. Some form of automatic frequency control (internal to the radio) is desirable. For example, the microcontrollers inside most modern transceivers could automatically tune the transceiver based on a schedule table downloaded in advance from a computer: this will free the computer from real-time control of the transceiver. Also, the completely automated approach used by the portable transceiver may be more than sufficient for the base station as long as uplink tuning is not required.

The available tracking software does not meet the PACSAT requirements. The tracking programs have too many features that are not required and yet do not offer the desired features. The ideal tracking program for the PACSAT concept is a command-line driven program that generates a table consisting of time, look angles, and absolute doppler-shifted frequencies for the next several passes. A summary table of pass times and visibility durations (or throughput capacity) is also desirable. Instant Track has a nice interface but it can only control the rotors with its own routines using the KCT hardware, and it offers no form of output to a file. Quicktrack can load the KCT tables for control of both the rotor and the radio, and it can output to a file. Unfortunately, Quicktrack has a difficult interface and it does not reliably generate a doppler table. Also, Quicktrack's doppler entries in the table is the amount of tuning error for just one of two frequencies. It was demonstrated that a simple customized tracking program is not difficult to write.

5.1.2 Prototype Portable Station

The portable station uses more recently introduced products for amateur radio use. Its design departs significantly from the standard practice and the design of the base station.

The portable computer used is almost identical to the prototype base station computer. As long as the PACSAT protocols do not require a more capable computer, it should work well. However, due to the amount of software envisioned and the need for security, the portable computer requires a hard-drive which greatly impacts its weight, power consumption, and cost. A re-evaluation of the PACSAT concept is desirable in order to identify ways to eliminate the need to carry a hard drive. Carrying a box of many diskettes (and backups) is an option, but it is not desirable. Outside of possibly turning the other ground station elements on and off, the computer will not have to control the rest of the hardware.

The prototype transceiver uses parts from several sources. The various parts include the VHF transceiver, a UHF-VHF downconverter, a power amplifier, and a PLL demodulator circuit. These parts should be integrated into a single transceiver that is further capable of full-duplex radio operation. Also, the receiver antenna

port should have DC power for the preamp inserted on the coax cable. Because the operator has no indication that the transceiver is not working, the integrated unit should include a self-test feature for receiver (and preamp) sensitivity and transmitter power. The satellite should use a receiver with at least the same tracking ability as the portable transceiver's PLL circuit in order to avoid expensive uplink tuning by the ground station. Uplink tuning will also reduce the bandwidth available in the channel since, for commercial applications, the spectrum must stay within the channel even after compensation for doppler shift.

The TNC and modem are miniature, low power versions of the base station units. Again, the PACSAT protocol may require a faster TNC but TNCs like the Data Engine are less acceptable for portable operation due to their increased power consumption and cost. The PACSAT protocols should be designed so that the lower efficiency of the portable station does not severely impact the link efficiency at the satellite. In other words, where multiple portable stations are involved, the satellite should be able to handle multiple simultaneous connections in order to reduce the burden on any ground station.

The power supply for the portable station is best provided by house current with an uninterruptible power

supply, if needed. The station can operate with 10 Watt solar panels with storage batteries but such a supply will not support extended computer operation. However, the use of packet store-and-forward technology implicitly assumes extensive computer use to generate and use the files that are being transferred. Long operation from batteries will require batteries that are too large for portability, but these batteries may be acceptable for more permanent applications where house current is not available or unreliable.

The antennas for the prototype station use vertical polarization instead of the circular polarization (CP) recommended by Surrey. In the absence of Faraday rotation, these antennas will work better than CP antennas. The antennas will have a pattern that is directed toward the horizon which is compatible with the satellite's antenna pattern and compatible with long visibility windows. A different approach would be a horizontal polarization with a pattern directed at the zenith and thus see the satellite with less path loss but for a shorter time. In either case, the antennas will have to be mounted outdoors, clear from any obstacles, and on a high mast (probably at least six feet high).

The required RF cabling will have a significant impact on the portability of the station. For

flexibility, weight, and cost reasons, lossy cables such as RG-58 are preferred. Less lossy cabling is heavier, less flexible, and/or much more expensive. While the loss on the downlink can be mitigated somewhat by a preamp at the antenna, the loss on the uplink will waste amplifier power and thus increase the drain on the battery (if used).

5.2 Orbit Analysis Results

The PACSAT orbit analysis allowed the dynamics of satellite passes to be studied by simulation on a computer. Instead of running a tracking program like Quick-Track for a large number of passes which would take a long time, the presented approach separated the analysis of the pass dynamics from the analysis of the statistics of occurrences. As a result, the statistics of over two years worth of orbits can be done on a personal computer in less than five minutes.

This analysis indicated the importance of communications to low elevation angles. This fact has greatest importance to the base station located in an urban area such as VITA's headquarters location in Arlington, Virginia. Because the VITA headquarters is

located in an area surrounded by taller buildings, their antenna will be denied access to the benefits of communications during low elevations of the passes. The simulations also show that the low elevation portions of high peak elevation passes are the least sensitive to inaccurate or old ephemeris data.

The simulations show that the portable station can operate with a zenith-directed pattern which would take advantage of the lower path loss to the satellite. However, to make such a system work, the satellite would need a compatible antenna.

5.3 FSK Analysis

The analysis of the FSK modulation illustrated the fundamental difference between optimal receivers and FM demodulators. For the modulation used for PACSAT, an optimal receiver could operate about 7 dB better than the discriminator approach. However, by changing the modulation to 4800 baud with a modulation index of 2.5 to occupy the same bandwidth, the advantage between the two receivers may be reversed.

The analysis also identified areas where the receiver design can be improved. The base station receiver can

benefit from a wider IF bandwidth and the NB-96 modem would benefit from a better baseband filter. Some of these benefits may not be realized because the transmitted signal is pre-equalized for a specific type of transceiver. Receiver equalization is difficult because the channel has nonlinear, time varying distortions.

The difference between optimal receivers and FM-polar receivers indicates that the respective link design procedures should be different. Unlike the case with optimal receivers, the improvement from FM demodulation can not be used directly to reduce SNR requirements. FM links have to be designed so that the received signal to noise ratio is above the receiver threshold. Once threshold is achieved then the improvement may be realized.

FM demodulators are better for applications where the occupancy of an allocated channel would require a modulation index of greater than one and where such occupancy could still operate over threshold. The FM demodulator approach is especially appropriate for links with low bit rates, high signal levels, or low bit error rate requirements.

Optimal receivers are best for links with low signal levels or high bit rates. The optimal receiver is preferred when the modulation index is less than about

Ø.7. The transition that determines which approach is preferred is about the same as the transition that separates analog AM and FM modulations.

The optimal receiver is preferred for satellite links carrying voice, FAX, or Bell-type AFSK modem traffic. On the other hand, it appears that PACSAT applications can benefit from the FM approach especially if the baud rate is reduced to 48ØØ baud or less.

5.4 Conclusions

This research and the associated project has been very interesting and educational. There are many more challenges related to the PACSAT concept than what has been discussed. These challenges are worth pursuing because there is very likely a strong commercial demand for PACSAT services even outside of VITA and its associates.

The work described in this thesis should be expanded. The ground stations need more development to reduce cost and improve effectiveness. The orbital analysis approach can be refined to be applied to different problems. Other aspects of PACSAT orbits can be studied such as studying alternative orbits that would be more appropriate for a

certain distributions of ground stations. The use of FM discriminators for CPFSK modulations should be studied further to see if it may be useful for other applications and if the performance can at least approach the performance of coherent receivers. The entire theory of partial response CPFSK appears to need more development to include FM theory. Even if discriminators are inherently inferior to coherent receivers, the increasing popularity of the use of discriminators for special purpose low-cost links demands a theory that can predict their performance and give guidance for the design of the link.

References

1. R. J. Diersing and J. W. Ward, "Packet Radio in the Amateur Service," IEEE Journal on Selected Areas in Communications, Vol. 7 No. 2, pp 226-234, Feb. 1989.

2. M.R. Davidoff, The Satellite Experimenter's Handbook, Newington, CT: American Radio Relay League, 1985, chapters 1-3

3. S. Horzepa, Your Gateway to Packet Radio, Newington, CT: The American Radio Relay League, 1989.

4. M. Schwartz, Telecommunications Networks: Protocols, Modeling, and Analysis, Reading, Mass: Addison-Wesley, 1987.

5. ARRL, AX.25 Amateur Packet-Radio Link-Layer Protocol, Version 2.Ø, Newington, CT: American Radio Relay League, October 1984.

6. M. Schwartz, Information, Transmission, Modulation, and Noise, New York: McGraw-Hill Book Company, 198Ø, p. 549.

7. S. Horzepa, Your Gateway to Packet Radio, Newington, CT: The American Radio Relay League, 1989, page 3-12.

8. B.S. Hale, ed., The ARRL Handbook for the Radio Amateur, 66th edition, Newington, CT: American Radio Relay League, 1989, pp. 19-37,19-38.

9. James H. Polaha, An Analysis of Low-Earth-Orbit Satellite Communication Systems, M.S. Thesis, Blacksburg, VA: VPI&SU, Department of Electrical Engineering, May 1989.

1Ø. S.G. Wilson and B. Humphreys, Design and Test of a TNC/FSK Demodulator for PACSAT, Unpublished Report to Virginia Tech, June 4, 199Ø.

11. Mischa Schwartz, Information, Transmission, Modulation, and Noise, New York: McGraw-Hill, 1980, p. 386.

12. Steven G. Wilson and Bruce M. Humphreys, Analysis and Measurement of PACSAT Data Link Bit Error Rate, report to Virginia Tech, May 17, 1990.

13. G. Hall, The ARRL Antenna Book, Newington CT.: The American Radio Relay League, 1988, pp. 24-18.

14. G.R. Jessop, VHF UHF Manual, Avon, UK: Radio Society of Great Britain, The Bath Press, 1989, p. 8.33

15. T. Pratt and C.W. Bostian, Satellite Communications, New York: John Wiley and Sons, 1986, chapter 2.

16. M.R. Davidoff, The Satellite Experimenter's Handbook, Newington, CT: The American Radio Relay League, 1985, chapters 8-10.

17. W.H. Beyer, ed., CRC Standard Mathematical Tables, Boca Raton, Florida: CRC Press, Inc., 27th edition, 1984. pp. 145-148.

18. R.R. Bate, et al, Fundamentals of Astrodynamics, New York: Dover Publications, Inc, 1971, p. 154.

19. C.A. Balanis, Antenna Theory: Analysis and Design, New York: Harper & Row, 1982, p. 120.

20. R.R. Bate, et al, Fundamentals of Astrodynamics, New York: Dover Publications, Inc, 1971, p. 156.

21. T. Pratt and C.W. Bostian, Satellite Communications, New York: John Wiley and Sons, 1986, p. 21-22.

22. A.P. Clark, "Modulations and Modems", Satellite Communication Systems, ed. B.G. Evans and T. Tozer, UK: IEE, 1987, Chapter 9.

23. C.-E. Sundberg, "Continuous Phase Modulation", IEEE Communications Magazine, Vol. 24, No. 4, pp 25-38, Apr. 1986.

24. S.G. Wilson and B.M. Humphreys, Analysis and Measurement of PACSAT Data Link Bit Error Rate, Report to Virginia Tech, May 17, 1990.

25. B.S. Hale, ed., The ARRL Handbook for the Radio Amateur, 66th edition, Newington, CT: American Radio Relay League, 1989, p. 19-39.

26. F.G. Stremler, Introduction to Communication Systems, second edition, Reading, Mass: Addison-Wesley Publishing Company, 1982, pp. 367-370.

27. S.G. Wilson and B. Humphreys, Design and Test of a TNC/FSK Demodulator for PACSAT, Report to Virginia Tech, June 4, 1990.

28. U.L. Rohde and T.T.N. Bucher, Communications Receivers: Principles and Design, New York: McGraw-Hill, 1988, pp. 418-420

29. C.-E. Sundberg, "Continuous Phase Modulation", IEEE Communications Magazine, Vol. 24, No. 4, p. 26, Apr. 1986.

30. S. Haykin, Communication Systems, New York: John Wiley and Sons, 1978, pp. 357-361.

31. F.G. Stremler, Introduction to Communication Systems, second edition, Reading, Mass: Addison-Wesley Publishing Company, 1982, p. 601.

32. J.G. Proakis, Digital Communications, New York: McGraw Hill, 1983, eq. 5-23.

33. S. Haykin, Communication Systems, New York: John Wiley and Sons, 1978, chapter 7.

34. T.T. Ha, Digital Satellite Communications, New York: McMillan Publishing Company, 1986, pp. 385-393.

35. F.G. Stremler, Introduction to Communications Systems,second edition, Reading, Mass: Addison-Wesley, 1982, p.574,580.

36. C.-E. Sundberg, "Continuous Phase Modulation", IEEE Communications Magazine, Vol. 24, No. 4, p. 31, Apr. 1986.

37. S. Haykin, Communication Systems, New York: John Wiley and Sons, 1978, p.555.

38. U.L. Rohde and T.T.N. Bucher, Communications Receivers: Principles and Design, New York: McGraw-Hill, 1988, p. 425.

39. S. Haykin, Communication Systems, New York: John Wiley and Sons, 1978, p. 555.

40. M. Schwartz, Information, Transmission, Modulation, and Noise, third edition, New York: McGraw-Hill, 1980, p.405.

41. M. Schwartz, Information, Transmission, Modulation, and Noise, third edition, New York: McGraw-Hill, 1980, p. 403.

42. F.G. Stremler, Introduction to Communications Systems,second edition, Reading, Mass: Addison-Wesley, 1982, p. 526.

43. R. Mudry,"Calculation of Strikes/Sec", EE 4974 report, Blacksburg: VPI&SU, April 10, 1990.

Appendix A

Orbit Equations

The equations for the orbit analysis are derived from basic spherical trigonometry. The relevant derivations are outlined in the following sections and in the order in which they are computed.

The analysis in the first section sets up the geometry for the point of closest approach. For convenience, that point occurs at time zero. The analysis of the dynamics is split into two parts: the effects of the orbit are described in the third section, and the effects of the rotation of the Earth are described in the fourth section. Finally, the basic relations for look angles and range are described.

These equations were all derived from basic spherical analysis.[1] However, by solving for the latitude and subsatellite point of the satellite at $\Phi_{\emptyset}$ instead of the azimuth look angle, equations found in standard orbit tracking programs may be used instead. For notational

convenience, this appendix uses phi, Φ, to represent the Psi discussed in the main body of this thesis.

A.1 Phi$\emptyset$

The orbit analysis depends on finding an orbit with a specified minimum separation angle, $\Phi_\emptyset$, from a ground station at a particular latitude. Figure A-1a shows the desired geometry. The known quantities are: orbit inclination, i; ground station latitude, l_o; and $\Phi_\emptyset$. The desired quantity, the azimuth angle at closest approach, $\alpha_\emptyset$, can be derived from the relationships between the two spherical triangles shown in Figures A-1b and A-1c.

From Figure A-1b, the following equation is derived by using the law of cosines for spherical triangles:[1]

$$\sin(l_s)=\sin(l_o)\cos(\Phi_\emptyset)+\cos(l_\emptyset)\sin(\Phi_\emptyset)\cos(\alpha_\emptyset).$$

And from the law of sines, the following can be derived:

$$\cos(\beta)=\cos(l_o)\sin(\alpha_\emptyset)/\cos(l_s).$$

The quantities in Figure A-1c are defined by a right spherical triangle and are related as thus:

$$\sin(\beta)=-\cos(i)/\cos(l_s).$$

The above equations can be combined by using the trigonometric identity:

$$\sin^2(\beta)+\cos^2(\beta)=1.$$

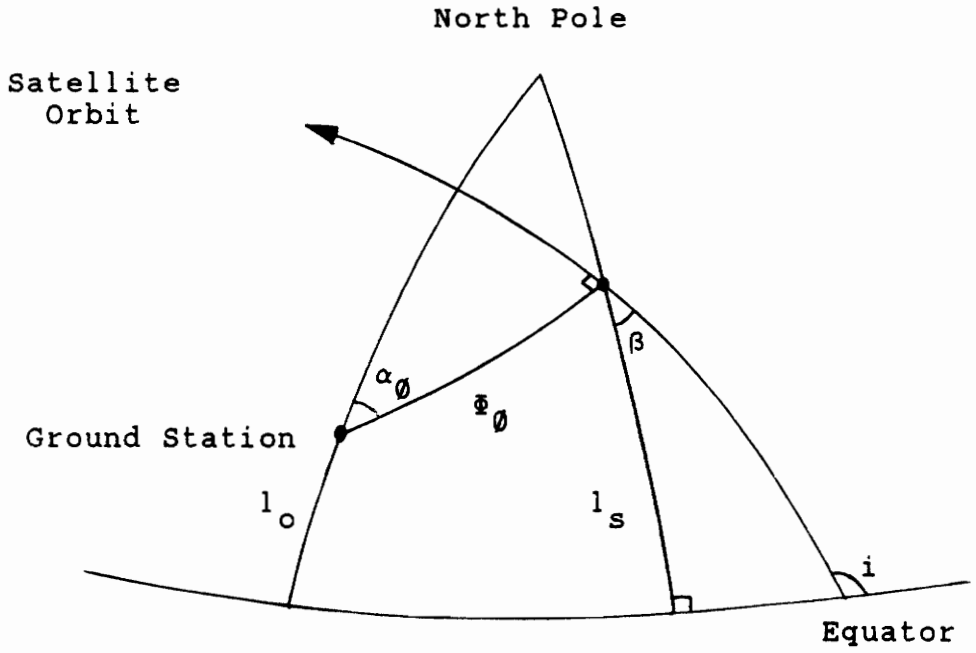

a) Overall Picture

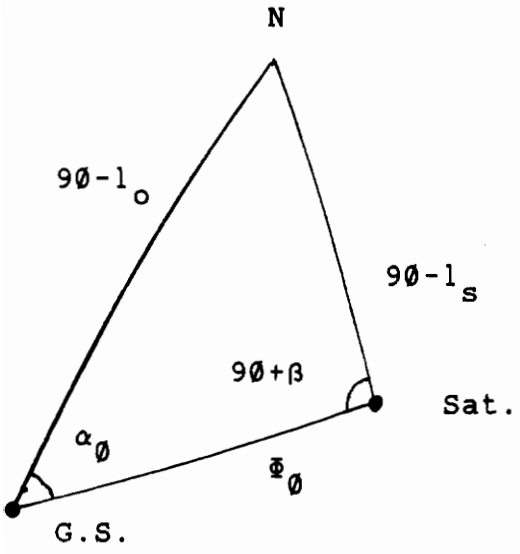

b) Top Triangle

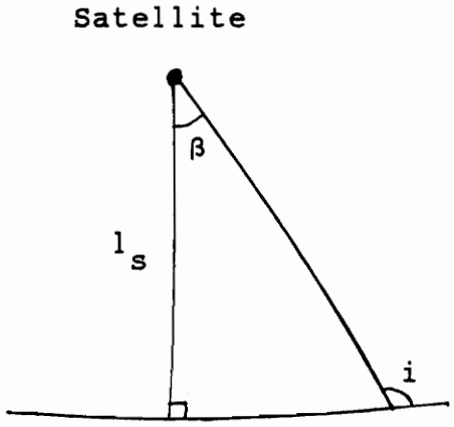

c) Bottom Triangle

Figure A-1: Geometry For Placing An Orbit Given Phi∅

After some manipulation, the following quadratic equation for $\cos(\alpha_\emptyset)$ can be derived:

$$A*\cos^2(\alpha_\emptyset)+B*\cos(\alpha_\emptyset)+C=\emptyset;\ \text{therefore,}$$

$$\alpha_\emptyset = S_2\cos^{-1}(-B+S_1*(B^2-4AC)^{\frac{1}{2}})/2A,$$

where

$$A=\cos^2(l_o)\cos^2(\Phi_\emptyset),$$

$$B=-\sin(2l_o)\sin(2\Phi_\emptyset)/2,$$

$$C=\sin^2(i)-\cos^2(l_o)-\cos^2(\Phi_\emptyset)\sin^2(l_o),\ \text{and}$$

$$S_1=\pm 1, \quad S_2=\pm 1.$$

There are four solutions for $\alpha_\emptyset$: two solutions result from the quadratic equation and two solutions result from the arccosine function. Figure 43 shows the geometric relationships of the four solutions when the ground station is in the northern latitude. In the northern hemisphere, the principal value of the arccosine function gives a solution for the ground station to the west of the point of closest approach. The selected sign, S_1, in the solution of the quadratic equation is determined by whether the ground station is between the orbital plane and the equator ($S_1=+1$) or above the plane ($S_1=-1$). These solutions have different characteristics but, except for determining the look angle azimuth, these differences are minor.

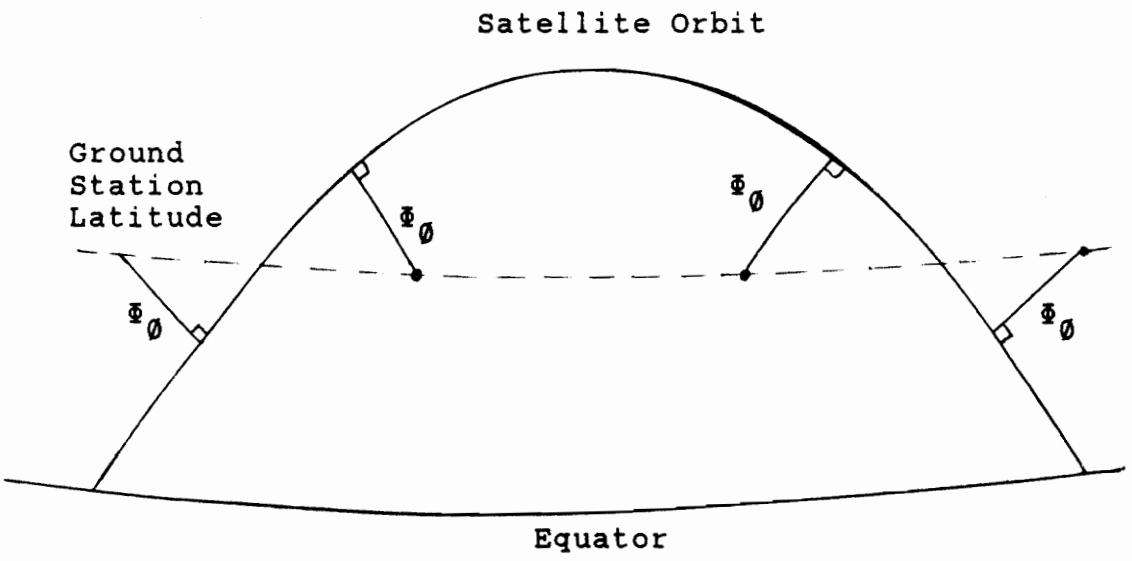

Sign Variables in Solution:

S_1=-1	1	1	-1
S_2= 1	-1	1	-1

Figure A-2: Geometry of the Four Solutions for Azimuth

A.2 Effect of Satellite Orbit

Figure 43 shows the geometry of the satellite displaced from the point of closest approach by a true anomaly, θ. For LEO satellites, the true anomaly can be approximated by the mean anomaly (which has a constant angular rate) since the orbits are nearly circular. For a more precise analysis that includes the effects of orbital eccentricity and argument of perigee, Kepler's equations[2] can be used to solve for the true anomaly which would then have to be adjusted to measure from the point of closest approach.

Ignoring the motion of the Earth, a new angular separation, Φ, and azimuth angle, α, can be computed from the known variables, θ, $\alpha_\emptyset$, and $\Phi_\emptyset$ as follows:

$$\cos(\Phi)=\cos(\theta)\cos(\Phi_\emptyset), \text{ and}$$

$$\alpha =\alpha_\emptyset-\sin^{-1}(\sin(\theta)/\sin(\Phi)).$$

The longitudinal difference, b, between the ground station and the satellite is

$$b=\sin^{-1}(\sin(\Phi)\sin(\alpha)/\cos(l_s))$$

$$b=90^\circ-b, \quad \text{if } \cos(\Phi)<\sin(l_\emptyset)\sin(l_s)$$

where l_s is the latitude of the subsatellite point:

$$\sin(l_s)=\sin(l_o)\cos(\Phi)+\cos(l_o)\sin(\Phi)\cos(\alpha).$$

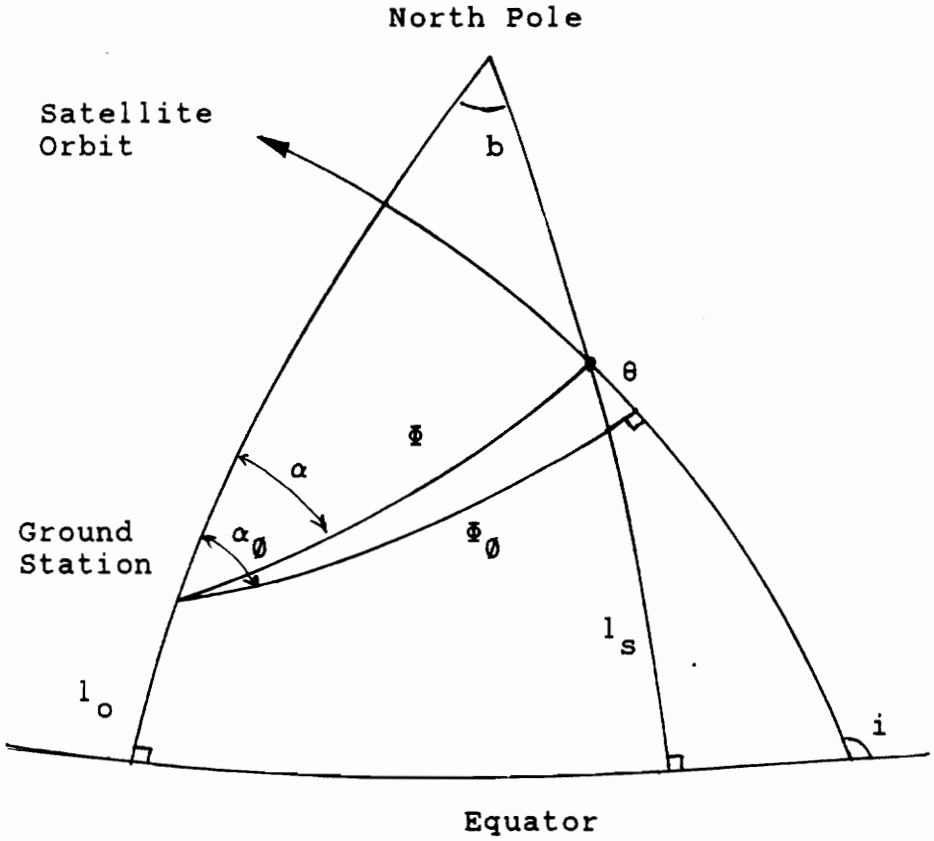

Figure A-3: Effect of Satellite Orbital Motion

A.3 Effect of Earth's Rotation

The final step is to move the Earth under the satellite. The earth rotates at a constant rate of one revolution per sidereal day. In addition, the orbital plane will precess according to the perturbation caused by the Earth's equatorial bulge. This precession is called nodal regression and it only amounts to a few degrees (less than 10°) per day[3] and thus may be ignored. The total rotation rate including the nodal regression is[2]

$$\dot{\Omega}=7.2921154e\text{-}5+2.00996e\text{-}6*(R_e/R_o)^{3.5}\cos(i) \quad \text{rad/sec.}$$

The geometry of this motion is shown in Figure 43. The rotation of the earth reduces the angle b so that new α and Φ angles can be computed as follows:

$$\cos(\Phi')=\sin(l_s)\sin(l_o)+\cos(l_s)\cos(l_o)\cos(b-\dot{\Omega}t)$$

$$\alpha'=\sin^{-1}(\sin(b-\dot{\Omega}t)\cos(l_s)/\sin(\Phi'))$$

$$\alpha'=180-\alpha', \quad \text{if } 0<b<\dot{\Omega}t.$$

A.4 Other Characteristics

Once the relative positions of the satellite and ground station are fixed, the other characteristics can be computed. The relevant geometry is shown in FIGURE 43. The relevant equations are simply:

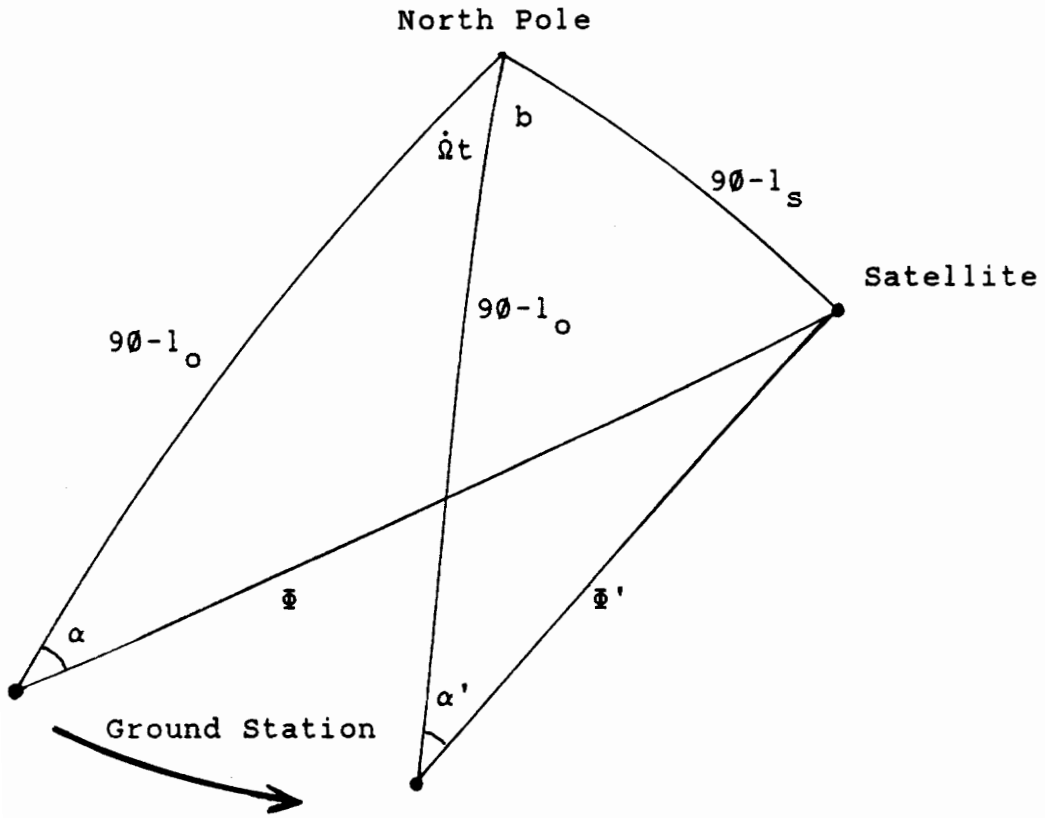

Figure A-4: Effect of Earth's Rotation

$$\text{Range}=R'=(R_e^2+R_s^2-2R_eR_s\cos(\Phi'))^{\frac{1}{2}}$$

$$\text{Elevation}=\cos^{-1}(R_s\sin(\Phi')/R')$$

$$El_{Sat}=\sin^{-1}(R_e\sin(\Phi')/R')$$

where the elevation will be negative when the satellite is below the horizon. Path loss can now be computed directly as

$$L_p=20\text{Log}(4\pi*R'*F_c/c)$$

where F_c is the frequency and c is the speed of light.

Doppler is computed directly from the range rate, $\dot{R}$, as

$$F_d=F_c\dot{R}/c$$

where $\dot{R}$ is the vector sum of the derivative of the range computed for the geometry for a fixed earth and the relative velocity due to the rotation of the Earth:

$$\dot{R}=\dot{\Omega}R_eR_o(\sin(\dot{\Omega}t)\cos(\Phi_\emptyset)/R-$$
$$\cos(l_o)\sin(\alpha')\sin(\Phi')/R')$$

where R is the range computed like R' except under the assumption that the Earth does not rotate.

Finally, the polarization loss is approximated as

$$L=10\text{Log}(\cos^2(\Phi')).$$

The polarization loss results from the misalignment of the local horizontal planes; however, the actual loss also depends on the orientations of the individual antennas. The point is that the angle Φ is an important contributor to the misalignment of local coordinates. One area for

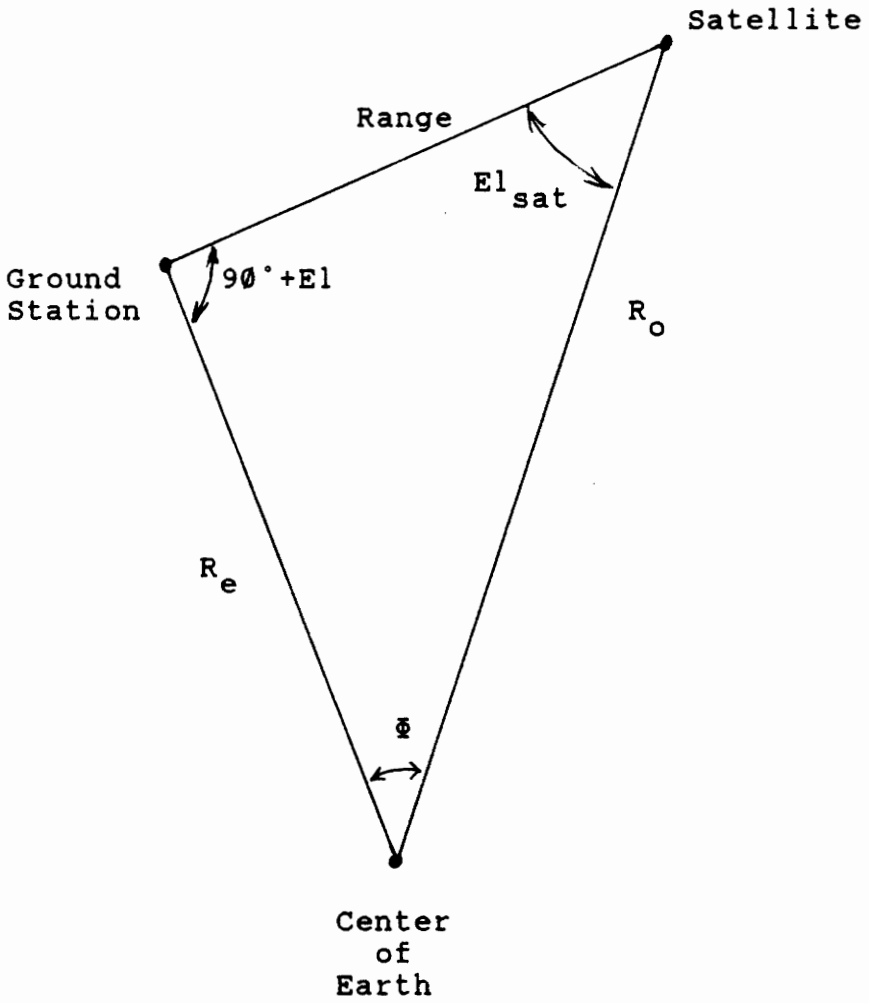

Figure A-5: Basic Geometry for Elevation and Range

further development of these equations is to incorporate antenna patterns (including polarizations) so that a complete and dynamic end-to-end link budget can be computed throughout the pass.

A.5 Distributions

The equations for the distributions are basically the same as above except that the angle $\Phi_{\emptyset}$ is computed for each consecutive pass. Starting the simulation with the satellite over the equator, each pass can be defined as beginning at the relative longitude, Ω, where the satellite passes over the equator at integral multiples of the satellite period. This model assumes a circular orbit. For an eccentric orbit, the period would be from perigee to perigee, but the perigee itself would move (apsidal precession) due to perturbation of the Earth's bulge.

From the equator, $\Phi_{\emptyset}$ is computed along with the true anomaly from the equator. Since the earth rotates as the satellite orbits, the orbit has to be rotated in proportion to the computed true anomaly and thus the $\Phi_{\emptyset}$ angle is solved iteratively. Only one iteration was used

for this study. The following equations were used to compute this iteration:

$$a=\cos^{-1}(\cos(l_o)\cos(\Omega))$$

$$A=\sin^{-1}(\sin(\Omega)\cos(l_o)/\sin(a))$$

$$\Phi_{\emptyset}=\sin^{-1}(\sin(a)*\sin(i-A-\pi/2))$$

$$B=\cos^{-1}(\cos(a)/\cos(\Phi_{\emptyset}))$$

iterate above with $\Omega'=\Omega+\dot{\Omega}T_P*B/2\pi$

The geometry for these equations is shown in Figure 43.

Once $\Phi_{\emptyset}$ is determined and found to be small enough to be visible for the minimum elevation angle for the ground station, then the same equations described in the previous sections are used to compute azimuth at closest approach. The elevation limits are related to $\Phi_{\emptyset}$ limits as follows:

$$\Phi_{\emptyset m}=\cos^{-1}(R_e\cos^2(e_m)\cdot (1+\tan(e_m)((R_s/(R_e\cos^2(e_m)))-1)^{\frac{1}{2}}/R_s),$$

where m represents either the minimum value of elevation for the maximum value for $\Phi_{\emptyset}$ or the reverse and e is the elevation angle.

In addition, the visibility time for the pass is computed for the given elevation limits by computing the range of true anomaly, θ, that is visible. The visibility time computation assumes that the true anomaly is the mean anomaly (i.e., a circular orbit) and thus visibility time is proportional to interval of visible true anomalies:

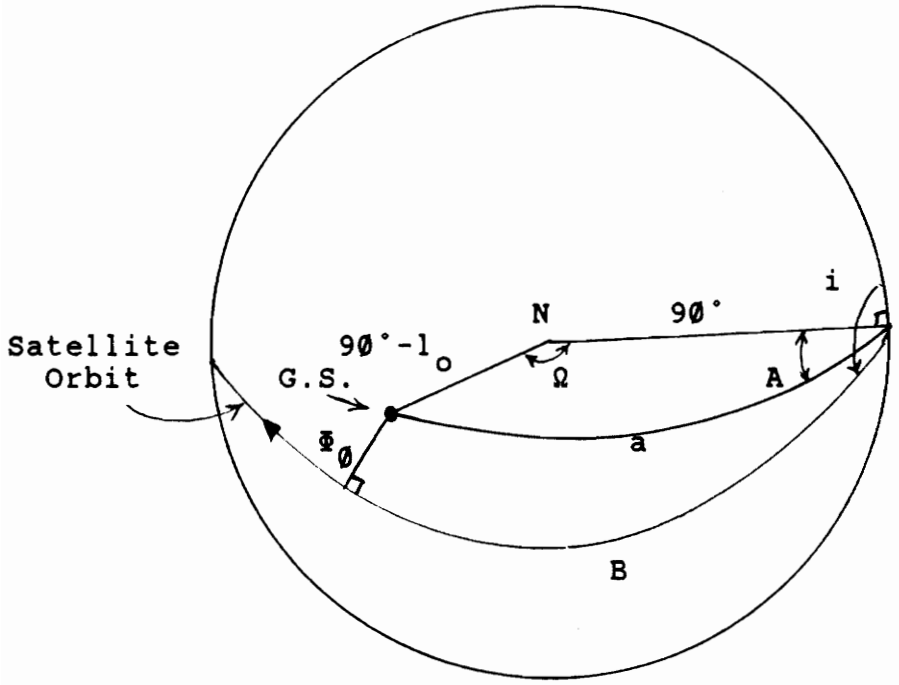

Polar View

Figure A-6: Geometry for Finding PsiØ

$$\theta_{min}=\cos^{-1}(\cos(\Phi_{min})/\cos(\Phi_{\emptyset}))$$

$$\theta_{max}=\cos^{-1}(\cos(\Phi_{max})/\cos(\Phi_{\emptyset}))$$

$$T=T_P(\theta_{max}-\theta_{min})/\pi,$$

where T_P is the period.

References

1. W.H. Beyer, ed., CRC Standard Mathematical Tables, 27th Edition, Boca Raton, FL: CRC Press, Inc, 1985, pp. 145-148.

2. M. Davidoff, The Satellite Experimenter's Handbook, Newington, CT: The American Radio Relay League, 1985, chapter 8.

3. R.R. Bate, et al, Fundamentals of Astrodynamics, New York: Dover Publications, Inc., 1971, pp. 156-157.

Appendix B

CPFSK Spectral Estimation

The spectra of the digital modulation described in chapter 4 were estimated from computation of a Fast-Fourier Transform (FFT) on the complex envelope of samples of a simulated signal. A block diagram of the process is shown in Figure B-1. The individual blocks of this process are described in the following sections.

B.1 Data Generator

The data generator is simply a random number generator. Most computer languages have pseudorandom number functions that generate independent random numbers that are uniformly distributed between Ø and 1. These random numbers can be converted into digital data by selecting either a digital 1 when the random number exceeds a set value or a digital Ø otherwise. By using a set threshold value of Ø.5, the resulting bit values will

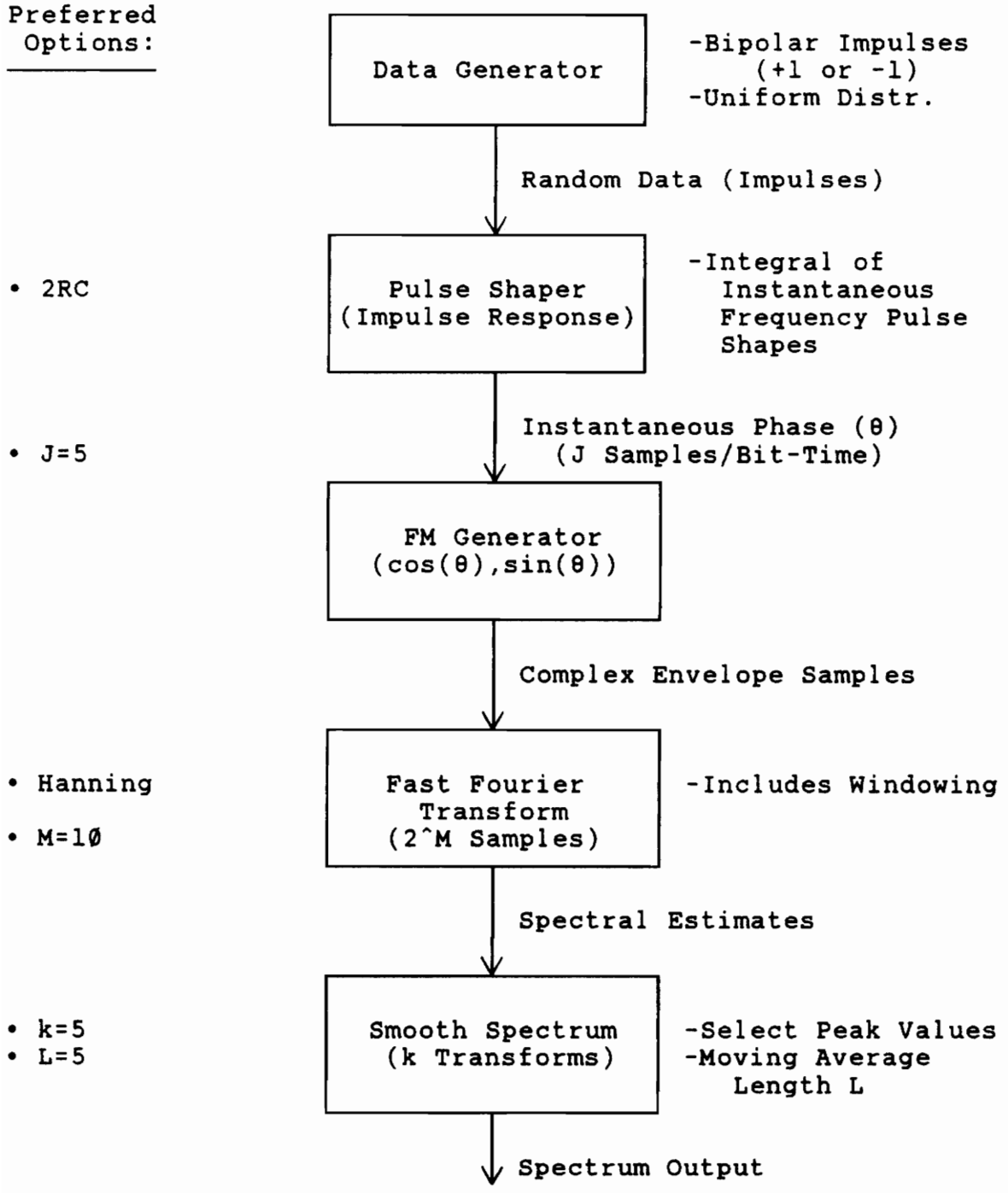

Figure B-1: Process to Compute CPFSK Spectrum

be equally probable. Since the analyzed system used a data randomizer prior to modulation, the bit probabilities should be nearly equal.

Other threshold values may be used when the bit values are not equally probable and the resulting spectrum will change accordingly. Also, if a specific data stream is known to be transmitted (e.g. a string of AX.25 flags), that stream may be used as data to study its effects on the spectrum.

B.2 Pulse Shaper

The random data stream is converted into samples of the continuous phase by simulating a filter with an impulse response that is the integral of the desired instantaneous frequency pulse shape.

The random data is represented as a sequence of digital impulses (of +1 or -1) separated by J-1 samples with a value of zero. The value of J is determined by the desired maximum frequency, F_{max} of the spectral estimate:

$$J=2F_{max}/R_b,$$

where R_b is the bit rate.

The pulse shaping is simulated as a filter response in the frequency domain because it is simple to program.

The output frequency response, Y(f), of the digital data is:

$$Y(f)=X(f)\cdot S(f)/j2\pi f,$$

where X(f) is the Fourier transform of the desired pulse shape for the instantaneous frequency and S(f) is the Fourier transform of the impulse data stream. The inverse Fourier transform is used to get the desired phase samples, θ, in the time domain. The FFT is used to compute the Fourier transforms; however, since the FFT and inverse-FFT form an exact transform pair (i.e., the original time sequence can be recovered from the frequency domain representation), no windowing should be used for the computation of the phase sequence.

B.3 FM Generator

The complex envelope of the FM signal, $\hat{z}(t)$, is easily computed from the samples of the phase, θ(t):

$$\hat{z}(t)=(\cos[\theta(t)],\sin[\theta(t)]).$$

The complex envelope representation is used for narrow band communications signals in order to avoid simulation of the center frequency, f_c. The real signal, z(t), can be obtained from the complex envelope as follows:

$$z(t)=Re\{\hat{z}(t)\cdot\exp(j2\pi f_c t)\}.$$

The spectrum of the real signal is the same as the spectrum of its complex envelope except that the center frequency is translated to the origin for the complex envelope.[1]

B.4 Fast Fourier Transform

The FFT algorithm is often used to estimate signal spectra digitally. The FFT itself is simply an algorithm for computing spectrum samples for a set of evenly spaced frequencies. Generally, the number of samples is a power of two in order to get the most computational advantage from the algorithm. The actual FFT algorithm is available as Fortran source code in several texts, or as a feature of a software math package (MATLAB, MATHCAD, etc.), or as compiled subroutines (IMSL for Fortran, and Math Toolbox for Turbo Pascal). The algorithm used in this analysis was taken from the FORTRAN listing in a textbook.[2]

The even spacing of frequencies generally limits the frequency resolution for the FFT. For example, if the FFT was used to compute the spectrum for a real FM signal with a center frequency of ten times the FM bandwidth, 90% of the spectral estimates from the FFT will be outside of the bandwidth of interest. Also, the FFT computes the

spectrum for both positive and negative frequencies which, for real signals, are complex conjugates of each other and thus are redundant. However, the spectra of bandpass signals can be computed as the FFT of their complex envelopes. The resulting spectrum consists of samples of only the bandwidth of interest and represents only the positive frequencies of the original real signal.

The FFT is an efficient algorithm for computing a digital Fourier transform (for sampled data) which only approximates the continuous time Fourier transform. If the continuous time signal is low-pass (or band-pass) and the signal is sampled at least twice the highest frequency (Nyquist criterion), then the primary errors of the approximation from the FFT result from the fact that only a finite interval is sampled. There are two types of errors. For a finite interval, the energy of a certain frequency will spread into several discrete frequency bins. This type of error can be controlled to some extent by the choice of window used on the time domain signal. The second type of error results from the variance of each sample when a random signal is sampled. This variance is reduced by comparing several FFTs of independent signals and by smoothing the spectrum in the frequency domain.

The time-domain window function used in this analysis is the Hanning window. Compared to the rectangular window

(no window), the spreading of spectral energy will be more concentrated in adjacent frequency bins; however, the computed magnitudes will be reduced because the window function has the effect of reducing the signal power.[3] The Hanning window function is a raised cosine that is positive over the sampled interval and is zero at the endpoints of the interval. Multiplying the signal with the Hanning window has the effect of reducing high frequency and aliasing effects resulting from signal discontinuities at the ends of the interval.

For the spectra presented in chapter 4, the maximum frequency is 24000 Hz, the bit rate is 9600 baud, and thus the FM signal is sampled five times per bit interval. The FFT was run on 1024 samples (or 204 bits). The output of the FFT gives the power spectral density with a frequency resolution of 46.875 Hz.

B.5 Spectral Smoothing

The FFT has two limitations when used with random signals: the FFT gives a biased result (the mean of the FFT estimate is not exactly the spectrum) and the variance of the FFT estimate does not go to zero as the number of samples is increased. The bias results from the same kind

of spreading described above and thus the bias is controlled by the choice of window.

The variance problem is more difficult to overcome. The effect of the variance is to make the spectral estimate look noisy and jagged although the spectrum theoretically should be smooth. For the spectral estimates in this thesis, the spectral estimates for several independent data sequences were compared. The approach for comparison was to select for each frequency bin the largest magnitude sample from five independent FFTs. Comparing more FFTs did not improve the variance much more.

To further smooth the spectral estimates, the data was smoothed in the frequency domain by a moving average with a length of five samples: the value for each frequency bin is the average of that frequency bin and the two adjacent bins on either side.

The selected sample size, windowing technique, comparison of multiple FFTs, and moving average resulted in spectral estimates that were fairly smooth. For the particular case of an MSK spectrum for which an analytic solution exists,[4] the approach described above is reasonably accurate, particularly in locating and estimating the relative maxima of the spectrum.

References

1. S. Haykin, Communication Systems, New York: John Wiley and Sons, 1978, pp. 89-93.

2. R.A. Gabel and R.A. Roberts, Signals and Linear Systems, 2nd Edition, New York: John Wiley and Sons, Inc., 1980, pp. 480-481.

3. F.G. Stremler, Introduction to Communication Systems, 2nd ed., Reading, Mass: Addison-Wesley Publishing Company, 1982, pp. 134-135.

4. J.G. Proakis, Digital Communications, New York: McGraw Hill, 1983, eq. 5-23.

Appendix C

Eye Pattern Simulation

The simulation used to generate eye patterns was an extension on the work done to generate spectra. This simulation models the effect of tuning errors and filter distortion on the eye pattern that must be sampled to recover the digital data. A block diagram of this simulation is provided in Figure C-1. The component blocks are described in the following sections.

C.1 FM Generation

The generation of the FM signal is accomplished as described in appendix B except that a different sampling rate is used and the complex envelope includes the effect of mistuning. The sampling rate requirement will be described in the section on the discriminator. The effect of mistuning by f_d can be represented as the following complex envelope based on the original center frequency:

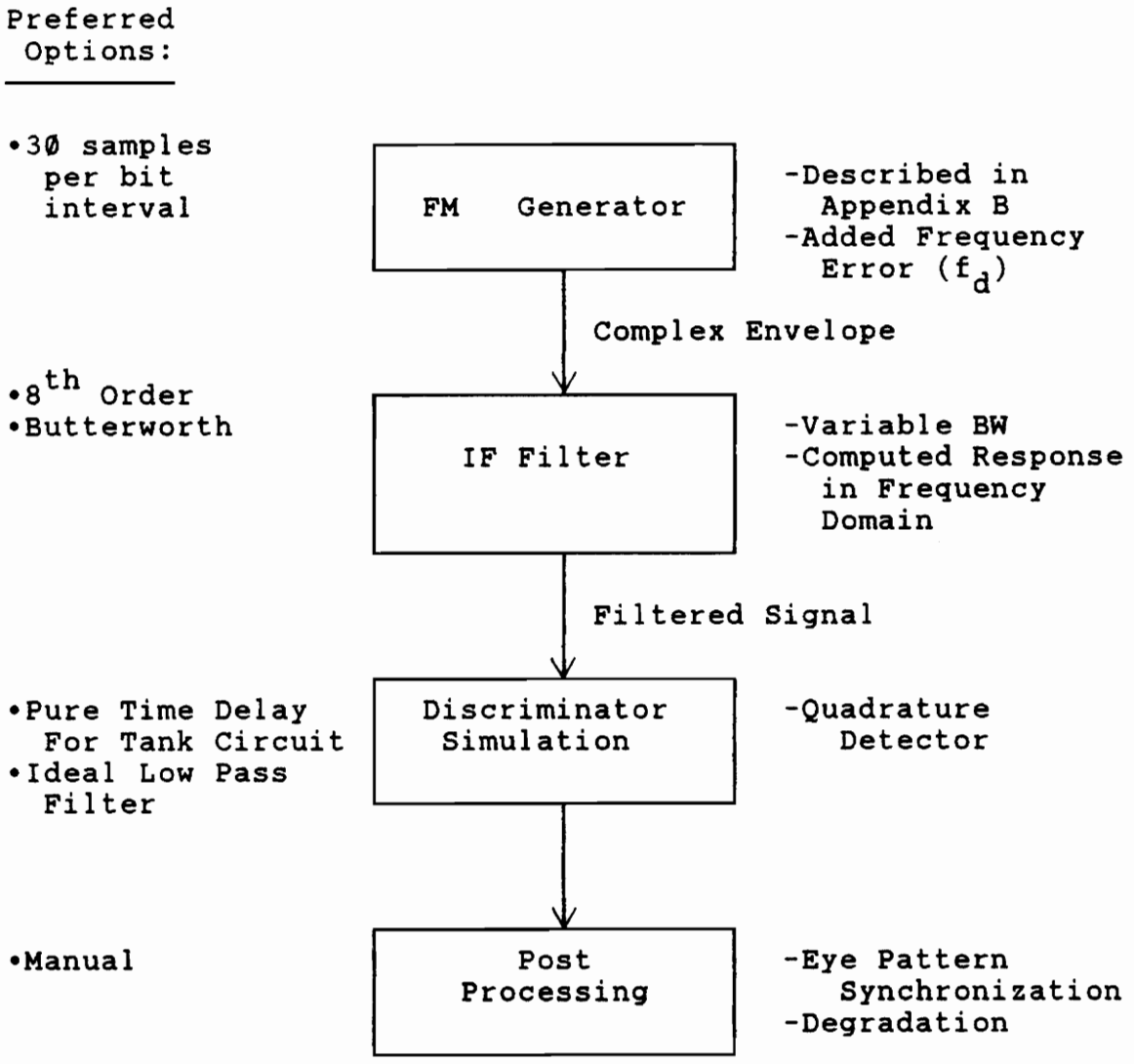

Figure C-1: Eye Pattern Generation Process

$$\hat{z}=(\cos(2\pi f_d t+\theta),\sin(2\pi f_d t+\theta)),$$

where θ is the continuous phase sample computed as in appendix B.

C.2 IF Filter

The IF filter will distort the FM digital signal if the signal is mistuned. In many transceivers, the IF filter is actually a set of crystal filters. Monolithic crystal filters are coupled resonators which can have some ripple in the pass-band and some unwanted resonances outside of the pass-band. However, in well-designed IF sections, the crystal filter response can approximate a Butterworth, maximally flat, response. A Butterworth filter model was used for this simulation in order to concentrate on the distortion cause by mistuning errors.

The Butterworth filter model in the frequency domain is simply the inverse of a polynomial. The characteristic polynomials of Butterworth filters are available in several sources.[1] For an eighth order Butterworth filter the characteristic polynomial consists of the following four quadratic factors:

$$s^2 + 0.3901806*S + 1$$

$$s^2 + 1.1111405*S + 1$$

$$s^2 + 1.6629392*S + 1$$

$$s^2 + 1.9615706*S + 1$$

The polynomials should be checked to see if the roots, p, are stable, distinct, and

$$p^{2n} = -1.$$

Although the IF filter is a bandpass filter, the simulation uses a complex envelope representation of the signal and thus the low-pass filter model is used in the simulation, i.e.,

$$s = j2\pi f/B,$$

where B is the baseband bandwidth (one half of the IF bandwidth).

The filtered signal is obtained from the inverse FFT of the product of the FFT of the FM signal and the above filter. The product must be done for both positive and negative frequencies since the complex envelope is an asymmetric spectrum.

C.3 Discriminator

The discriminator used in many transceivers is the integrated circuit based quadrature detector. The

quadrature detector is a phase detector that compares the response of a low-Q tank circuit with its input. The tank circuit behaves as a short delay so that the output of the phase detector is an estimate of the instantaneous frequency. The low pass part of the output is:

$$\sin(\theta(t))*\cos(\theta(t-dt)) = \tfrac{1}{2}\sin(\theta(t)-\theta(t-dt)),$$

$$\approx \tfrac{1}{2}(\theta(t)-\theta(t-dt)) \approx \tfrac{1}{2}\dot{\theta}(t)dt.$$

The approximation improves as the delay, dt, becomes shorter (i.e., as the Q of the tank circuit is reduced).

For the simulation, the tank circuit is modeled as a pure time delay. A more elaborate simulation would include a model of the actual tank circuit but, again, in a well-designed receiver, the distortion effects of the tank circuit itself is arbitrarily small.

The simulation modeled the entire discriminator as the product of a sample of the signal with the previous sample that includes the required quadrature phase shift. When multiplying the complex envelopes of signals, the low pass terms are easily separated from the high frequency terms. Therefore, the final baseband signal y(t) can be obtained from the IF complex envelope $\hat{x}(t)$ as follows:

$$y(t)=-j\hat{x}(t)\cdot\hat{x}^{*}(t).$$

C.4 Post Processing

To make an eye pattern, the signal coming from the discriminator is divided into bit intervals and then overlaid. Since the simulation was done with frequency domain techniques, one or two bit intervals at the ends may have to be deleted in order to avoid the end-effects caused by working with a finite interval.

To measure the distortion from the eye pattern, the width of the opening, w_o is compared to the width of the signal, w_s. The ratio of these widths give an indication of the additional signal power required to get back the performance that would have been achieved with an ideal eye pattern. The S/N degradation from the closing of the eye is:[2]

$$\text{Degradation} = 20 \log(w_o/w_s).$$

The eye patterns and degradations were selected manually by comparing different sample points. First, the eye pattern was visually inspected to find the best region to search. Second, two different techniques for computing the degradation were used: the selected degradation value was when the two results agreed. The first technique was as described above: compute the ratio of the inside width to the outside width. The second technique computed the inside of the eye as the distance from the computed mean

of the eye pattern. The second technique approximates the floating threshold that results from a DC blocking capacitor in the receiver.

References

1. D.G. Fink, Electronics Engineers' Handbook, Second Edition, New York: McGraw-Hill Book Company, 1982, p. 12-6.

2. F.G. Stremler, Introduction to Communication Systems, 2nd ed., Reading, Mass: Addison-Wesley Publishing Company, 1982, p. 526.

Vita

Ken Neumeister was born in Litchfield, Illinois on October 4, 196Ø. He graduated from the University of Illinois in 1983 with a bachelor's degree in Electrical Engineering. After spending over two years working on air traffic control products at Sperry Flight Systems in Phoenix, Arizona, he moved to Northern Virginia and joined Riverside Research Institute where he worked on system architecture development for the Stategic Defense Initiative. His primary interests are in engineering related to solving problems concerning large-scale systems related to business and government. He is interested in further research in systems with commercial applications of low earth orbits.